Universiteit Utrecht

Potential of a Suppletion Ditch for Restoration of Bog Woodland in De Wieden

A Modelling Study of the Effects of a Suppletion Ditch on the Hydrological System of a Peatland

UTRECHT UNIVERSITY

Master's Thesis – Master Water Science and Management

Name: Marijke Roos Ronduite
Email: m.r.ronduite@uu.nl
Student nr.: 4108159

Utrecht University Supervisor: Paul Schot

Date: 05/11/2020

Abstract

Currently there is a rapid decline in the expanse and biodiversity of wetlands, such as mire systems, due to human impacts. A leading cause for degradation of mires is desiccation, which through lowering water tables, affects the plant communities and biodiversity of mires. One mire system impacted by desiccation is the infiltration area of De Wieden in the Netherlands. Specifically, the bog woodland vegetation in this area is severely affected due to the high susceptibility of this vegetation to desiccation. Since bog woodland has a high national priority conservation of this habitat is important. For this reason, the scope of this thesis was a modelling study in the possibility of a suppletion ditch in providing adequate hydrological conditions. Hydrological conditions were regarded as adequate when rainwater occurred in the root-zone, soil moisture content was high and suitably high phreatic levels occurred in summer. The following research question was used to guide the modelling study: *to what extent will a suppletion ditch create suitable hydrological conditions for the restoration of bog woodland based on hydrological modelling of De Wieden?*

Using HYDRUS-2D a model domain of a transect in De Wieden that covered 210 by 4.4 m deep was created. The material distribution of this domain was based fieldwork borehole logs, which indicated the presence of a highly permeable, water-rich slurry layer along the transect. The model was further supplemented with literature data. Calibration of the model was done based upon theoretical data sources through the change of the hydraulic conductivity of the different peat layers in the model. The model was validated using field data of Electrical Conductivity (EC) in monitoring wells along the transect and indications of vertical groundwater flow direction found in the field at the end of September 2020. Based on both the calibration and validation the model was found to represent the study area to a sufficient degree.

With the developed model several scenarios runs were undertaken to indicate the potential effect of a suppletion ditch on the hydrological conditions. Each scenario implemented a different geometrical shape for the suppletion ditch. The simulation of the different scenarios indicated that drainage by the suppletion ditch lead to lower phreatic levels in the winter, although the decrease was minimal (max. 2.4 cm). In contrast to previous studies the simulations from this thesis indicate that a suppletion ditch leads to an increase up to 20 cm in phreatic level in summer. This positive effect is attributed to the high surface water level in De Wieden which provides a suitable hydraulic gradient for lateral inflow of water in summer. The suppletion ditch did lead to decreases in rainwater in the root-zone as surface water flows laterally into the root-zone. However, the extent to which rainwater is layered above surface water does increase with the implementation of a suppletion ditch which might indicate the formation of a rainwater lens. Furthermore, in the scenario where the suppletion ditch was in direct contact with the slurry layer more optimal results were found. This is attributed to the high permeability of this slurry layer which increases inflow of surface water into the system in summer.

Throughout the modelling several assumptions and simplifications were made that could affect the results. Although optimal use of available data was during the calibration both the calibration and validation process could be extended to obtain a more accurate representation of the field conditions. However, the results of this modelling study may still give a good indication of the effect of a suppletion ditch on a general peatland with high water levels and a slurry layer. From this modelling study the implementation of a suppletion ditch in vicinity or within the water-rich layer in De Wieden is recommended to obtain rapid inflow of water. For the winter it recommended to limit drainage of the suppletion ditch, for example by damming, to obtain more optimal phreatic levels. Overall, the results indicate that a suppletion ditch holds potential in the restoration of bog woodland vegetation by providing more suitable hydrological conditions.

Table of Contents

1. Introduction

1.1. Problem Description

Despite wetlands being regarded as valuable landscapes, due to their provisioning of ecosystem services, there unfortunately is a rapid decline in their expanse and associated biodiversity value due to human impacts (Maltby & Dugan, 1994; Mitsch & Gosselink, 2000). The importance of wetland ecosystems has been recognized by scientist, (inter)national conservation agencies, governmental organizations, and diverse sectors in the general public (Maltby & Dugan, 1994). However, even with increased recognition of the adverse impacts loss of wetland habitat causes, and large public support for conservation, degradation of wetlands still continues (Maltby & Dugan, 1994). One particular wetland type that shows degradation is mires.

Mires are categorized as peat-forming systems recognized by an excess of water (Casparie & Streefkerk, 1992; Goudie, 2013). These systems often consist of a great variety in plant communities, leading to a rich biodiversity, giving them a high priority for conservation (Lamers et al., 2002). A leading cause for mire degradation is known to be desiccation (Kooijman et al., 2018; Lamers et al., 2018).

The concept of desiccation describes the deterioration of habitat conditions due to human activities affecting the hydrological processes naturally occuring in the wet ecosystem (Mars, 1996). Desiccation influences natural systems through a complex web of physical, chemical, and biological pathways (Streefkerk & Casparie, 1989). By lowering of the groundwater table desiccation leads to a decrease in wetness and moisture availability (Lamers et al., 2002; Streefkerk & Casparie, 1989). Other associated impacts are acidification, nitrification, decomposition of peat, and eutrophication (Runhaar et al., 2013; Schot et al., 2004; Streefkerk & Casparie, 1989; Verhoeven, 1992). Through these processes desiccation changes vegetation patterns, often reflecting negatively on the biodiversity (Streefkerk & Casparie, 1989).

An example of a mire system impacted by desiccation is the Natura2000 area of De Wieden, located in the province of Overijssel in the Netherlands (Figure 1). To sustain agricultural practices in, and just outside, De Wieden extensive drainage systems have been established which have led to rapid removal of water out of nature area and the occurrence of desiccation (Cusell & Mandemakers, 2017; Dotinga & Bodde, 2018; Provincie Overijssel, 2017). Because De Wieden contains valuable and protected Natura2000 habitat communities deterioration of vegetation due to desiccation is undesirable (Cusell et al., 2018; Lamers et al., 2018). Specifically the Natura 2000 habitat *bog woodland* is considered the main priority for conservation in De Wieden since limited surface area of this habitat occurs in the Netherlands (Natuurmonumenten, 2019).

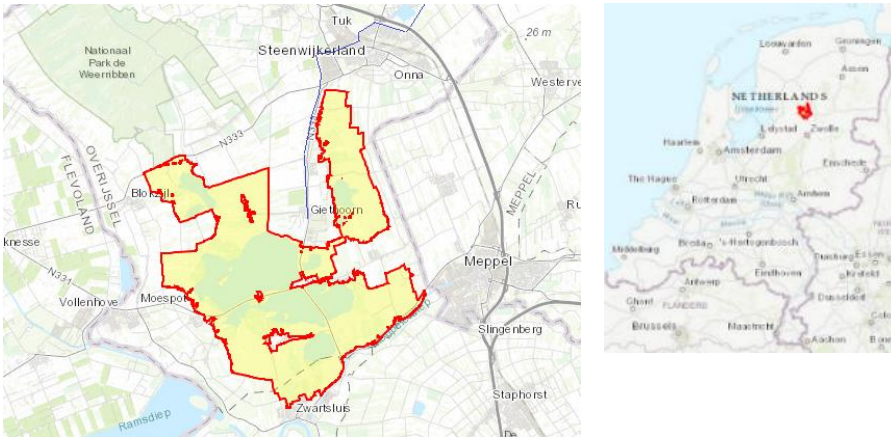

Figure 1: Left: Location of De Wieden as defined by the Natura2000 guidelines visualized by the colored area (European Environment Agency, 2019). Right: Location of De Wieden area in the Netherlands.

Desiccation forms a crucial issue for bog woodland vegetation owning to its high susceptibility to this process. (Provincie Overijssel, 2017; van der Kooij, 1997). Desiccation brings forth two main problems: 1) insufficient new high-quality bog woodland establishes and, 2) existing bog woodland vegetation disappears rapidly (Natuurmonumenten, 2019). Limiting desiccation can therefore be seen as a primary requirement in the conservation of bog woodland (Thomassen et al., 2008). To regenerate desiccated habitat the restoration of the hydrology, by limiting drainage or improving groundwater inflow, is considered essential (Runhaar et al., 2013; Thomassen et al., 2008). However, such thorough measures are not always feasible due to stakeholder interests at regional scales. Therefore, mitigation measures are often employed.

1.2. Conservation Project in De Wieden

One mitigation measure considered to have potential in limiting the effects of desiccation is the construction of a *suppletion ditch* (Natuurmonumenten, 2019). Although previous studies have indicated otherwise (Bootsma et al., 2002; Van Loon et al., 2017) for De Wieden this measure is expected to show positive impacts. The high surface water levels in the region combined with downwards seepage is anticipated to incite inflow of water through the suppletion ditch in summer (Natuurmonumenten, 2019). Therefore, the nature manager of De Wieden, Natuurmonumenten, is intending to implement a suppletion ditch to overcome desiccation issues. To determine the potential of a suppletion ditch in bog woodland conservation Natuurmonumenten and the 'Vereniging van Bos- en Natuureigenaren'[1] developed a research project. The execution of this research project lies with the consultancy firm RoyalHaskoningDHV (RHKDHV) and the Copernicus Institute of Utrecht University. The aim of the project is to identify the steering factors of intact and desiccated bog woodland vegetation and to determine whether a suppletion ditch can support the conservation and restoration of bog woodland vegetation (Natuurmonumenten, 2019).

As mentioned a suppletion ditch is expected to provide a positive effect on the inflow of water in De Wieden (Natuurmonumenten, 2019). To anticipate whether a positive effect would indeed occur a hydrological model can be utilized. With a hydrological model insight can be gained into the quantitative (ground-)water flows and water regime of the peat system in De Wieden. Specifically, predictive modelling to evaluate the effect of a suppletion ditch on water flows can be undertaken. Such a modelling evaluation should take place before the implementation of the suppletion ditch to determine factors, e.g. geometry of the ditch, essential for construction. Since an modelling analysis o can provide valuable information in regards to the implementation of a suppletion ditch this thesis support the overarching study by RHKDHV and Utrecht University by conducting such a modelling analysis.

1.3. Research Aim and Questions

The research aim of this thesis is to *simulate the effects of a suppletion ditch on the hydrological situation in De Wieden area using a model approach to determine whether this mitigation measure may improve the water supply for its bog woodlands*. To achieve this aim the following research question will be used:

TO WHAT EXTENT WILL A SUPPLETION DITCH CREATE SUITABLE HYDROLOGICAL CONDITIONS FOR THE RESTORATION OF BOG WOODLAND BASED ON HYDROLOGICAL MODELLING OF DE WIEDEN?

The sub-questions below were formulated to guide the study in answering the main question:

- SQI: How would a basic model representation of De Wieden be set-up?
- SQII: How can the basic model be modified to resemble field conditions in De Wieden sufficiently?
- SQIII: What are the effects of a suppletion ditch on the modelled hydrological system?

[1] Association of forest- and nature owners

2. Background Information

2.1. Study Area

De Wieden

De Wieden is a nature area with a surface height between -0.8 and 0 m below the Amsterdam Ordnance Datum (NAP) (Waterschap Reest en Wieden, 2007). The landscape of De Wieden consists of characteristic long, narrow ponds separated by thin baulks created by peat dredging and large lakes formed by erosion of these baulks (Cusell et al., 2018; Lamers et al., 2018; see Figure 2). Because De Wieden is located relatively high compared to the surrounding low-lying polders the region functions as an infiltration area (Hoogendoorn & Vernes, 1994; Provincie Overijssel, 2017).

Figure 2: Characteristic landscape of De Wieden. Left: Pattern of long narrow ponds with baulks (Provincie Overijssel, 2017). Right: Large lakes formed by the erosion of baulks between turf ponds (Natuurmonumenten, n.d.).

De Wieden is located between the highland area of the Drents plateau (250 m NAP) and the Noordoostpolder (-3 to -5 m NAP) (Waterschap Reest en Wieden, 2007; see Figure 3). The geohydrological basis of the area, at a depth of -250 m NAP, is a thick sea clay formation (Provincie Overijssel, 2017). No further impermeable deposits are present above this formation and the subsoil consist mostly of a large sequence of sandy deposits, with the exception of the Holocene top layer (Dotinga & Bodde, 2018). The Holocene formation is comprised of peat decreasing in thickness from 3-4 m in the west to 1-2 m in the east (Dotinga & Bodde, 2018). Locally clay or sandy ridges occur in the Holocene layer.

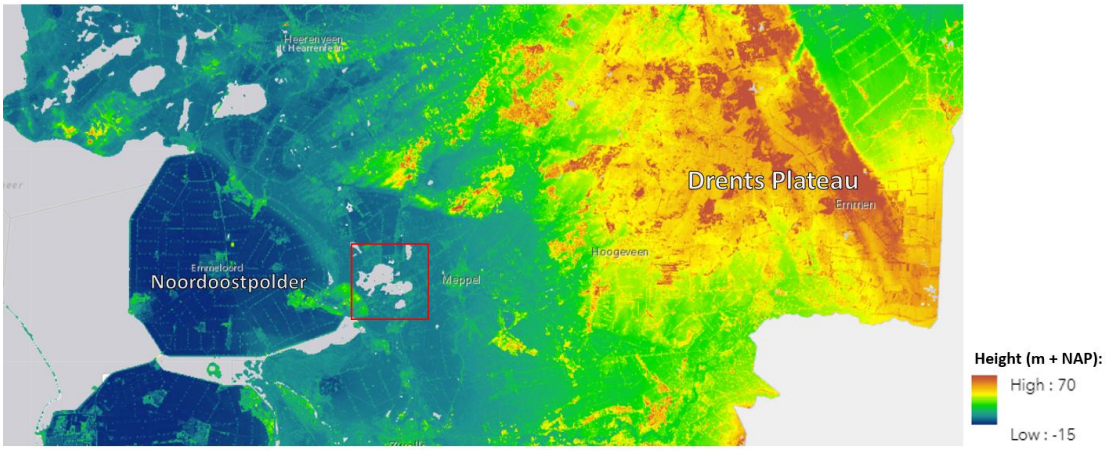

Figure 3: Surface Height map of the area around De Wieden, on the right the regions Noordoostpolder and on the left the Drents Plateau are indicated (Obtained from the AHN-3). The red square indicates the location of De Wieden.

Regional groundwater flow is directed from North-east towards South-west, following the decrease in elevation (Dotinga & Bodde, 2018). The hydraulic head contours from Figure 4 show this regional flow direction. Across De Wieden area the hydraulic head displays a gradual gradient in hydraulic head of roughly -5cm/1km, indicating horizontal flow is limited.

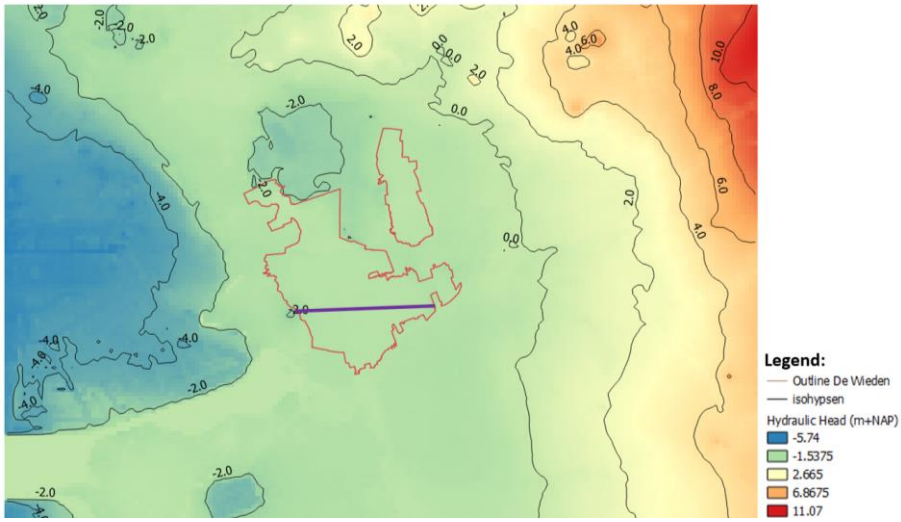

Figure 4: Map with simulated hydraulic head for the first aquifer, the hydraulic head is based on hydraulic head time series from DINOLoket and the Landelijk Nederlands Hydrologisch Model 3.0 (TNO Geologische Dienst Nederland, 2020a). The purple line indicates a distance of 7 km over which the Hydraulic head decreases from -0.8 m to -1.1 m.

2.2. Bog Woodland Vegetation

Bog woodland[2] vegetation is formed by the natural transition of mires from minerotrophic, groundwater-fed fen communities towards ombrotrophic, rainwater-fed bog systems (Lamers et al., 2002; Wiegers, 1985). More specifically, bog woodland vegetation is the climax community of the *mesotrophic succession* scheme (Kooijman et al., 2018; see Figure 5). Only the final stages of succession are discussed here, as bog woodland is the focus of the research. For a more extensive overview of the complete succession reference is made to Mettrop (2015), van Vliet et al. (2017), and Wiegers (1985).

The succession is characterized by the process of *terrestrialisation*, in which floating root mats expand horizontally from peat baulks into the open water surface (Stofberg et al., 2016). These floating mats, i.e. kragge, remain in constant contact with surface water (Ministerie van LNV, 2006; Verhoeven, 1992). As the kragge grows and peat accumulation increases floating characteristics are gradually lost, reducing contact with ground- and surface water (Mettrop, 2015; Provincie Overijssel, 2017; Thomassen et al., 2008). Once peat becomes isolated from minerotrophic waters a rainwater lens develops, which generates acidic conditions at the soil surface (Ministerie van LNV, 2006; Pons, 1992). With the accumulation of peat the groundwater table rarely rises above the soil surface in later successional stages (Goudie, 2013). In the drier and more acidic conditions peat bog vegetation starts to form, giving rise to bog woodland (Mettrop, 2015). When contact with groundwater is completely lost and only rainwater influences are present the required nutrient-poor conditions for bog woodland vegetation species, e.g. birches, to emerge occur (van der Sluijs & Tigchelaar, 2012).

[2] Dutch: Hoogveenbossen/Veenbossen

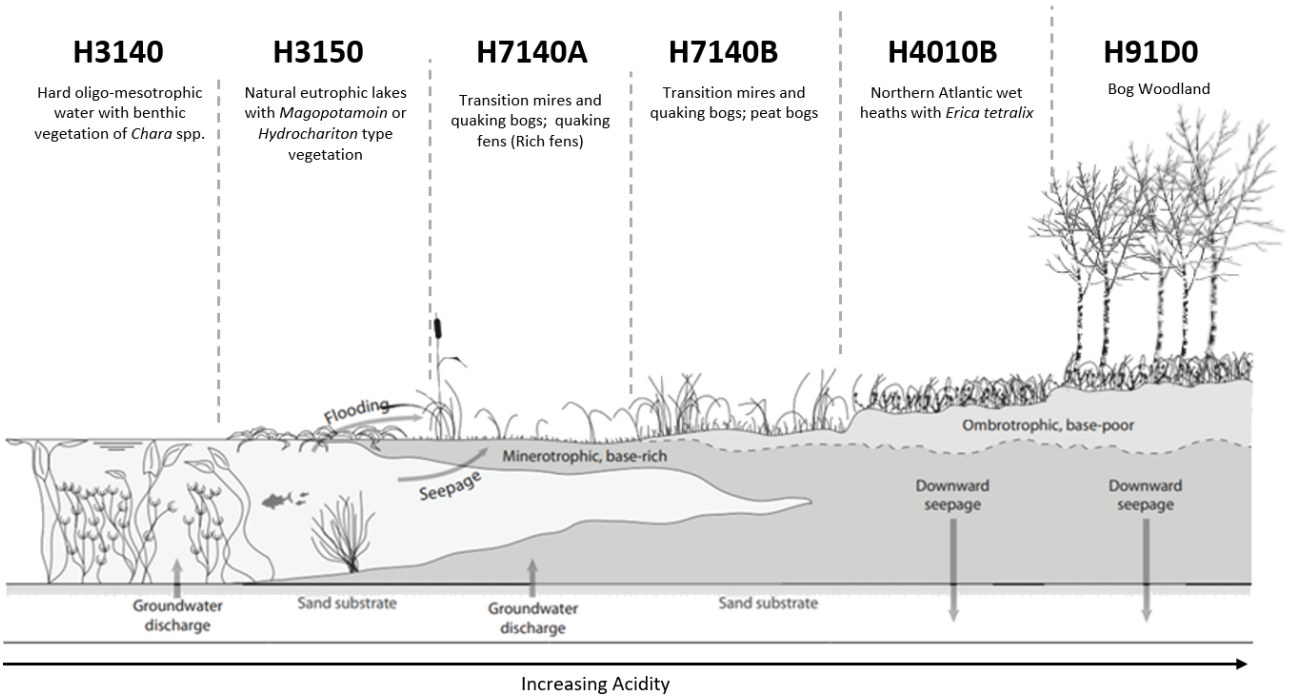

Figure 5: Schematic overview of the mesotrophic successional stages, from open water towards bog woodland vegetation (Adapted from Mettrop, 2015). The code references to the Natura2000 habitat codes.

2.3 Required Hydrological Conditions for Bog Woodland

For De Wieden the target vegetation is the sub-association '*Sedge-Birch Woodlands*'[3] as this is considered a high-quality variation of bog woodland (H. de Mars, personal communication, 18th March 2020). The required criteria used to determine suitable hydrological conditions for this sub-association are discussed below. These criteria should be fulfilled for successful bog woodland restoration.

The first criteria pertains to the *phreatic groundwater levels* required for bog woodland vegetation. Table 1 shows that phreatic levels should be between 10-60 cm below surface level in summer and 0-20 cm in winter, these ranges will be used as criteria. However, because high summer phreatic levels are considered more optimal for bog woodland the aim is to increase the phreatic level to the largest extent possible using a suppletion ditch (Ministerie van LNV, 2006). High-quality bog woodland is further recognized by limited fluctuations in phreatic levels (Diek et al., 2014; Provincie Overijssel, 2017). Therefore, *stable phreatic levels* are considered as a criteria.

For high-quality birch woodland the influence of rainwater should be maximized (Provincie Overijssel, 2017; Thomassen et al., 2008; van 't Veer et al., 2000). Influence of base rich waters, i.e. surface and groundwater, is undesirable for bog woodland vegetation (Jalink et al., 2003; Provincie Overijssel, 2017). The *presence of rainwater in the root-zone*, where it is available for plants, is therefore seen as a required hydrological condition. Specifically, for high-quality sedge-birch woodlands the layering of rainwater atop base-rich waters, in the shape of a (thin) rainwater lens, is considered essential (Ministerie van LNV, 2006; Provincie Overijssel, 2017). The formation of a rainwater lens is therefore a preferred condition.

[3] Dutch: Zompzegge-Berkebroekbos; Latin: *Carici curtae-Betuletum pubescentis*; ; Natura-2000 Code: H91D0-40Aa2

Finally, *soil moisture content* is considered as criteria since this indicates the available moisture for plant. The soil moisture content should be as high as possible since birch woodlands are recognized by wet, saturated conditions (Runhaar et al., 2013).

Table 1: Required water levels for Bog Woodland vegetation

Source	Specified Vegetation Type	Winter Phreatic Level below soil surface*	Summer Phreatic Level below soil surface **
Ministerie van LNV, 2006	Bog Woodland		20 < to < 40
de Waal & Hommel, 2005	Birch-Woodland	0-20 cm	
Provincie Overijssel, 2017	Bog Woodland		
Blokland & Kleiberg, 1997	Birch-Woodland	0 cm + inundation	10 cm
Bal, 2001	Bog Woodland		20-60
Range		0-20 cm -surface level l (+ inundation)	0 – 60 cm – surface level

* As based on the required average highest groundwater levels (Dutch: *'Gemiddeld Hoogste Grondwaterstand'*)
** As based on the required average lowest groundwater levels (Dutch: *'Gemmideld Laagste Grondwaterstand'*)

3. Methods

To determine the extent to which a suppletion ditch affects the hydrological system of De Wieden a model of the study area was constructed. The modelling study can be divided into three main sections, as based on the sub-questions: set-up of the base model, calibration of the model, and simulation of the suppletion ditch. This chapter will give an overview of the data sources and approach for each modelling section.

3.1. Base Model

To develop a model of De Wieden the Hydrus-2D (henceforth: Hydrus) software package was used. This is a numerical two-dimensional unsaturated-saturated groundwater flow and transport package that uses the partial differential equation of the Richard's equation (Šimůnek et al., 2012b). Hydrus was selected because it can consider both saturated and unsaturated processes, which is vital for modelling wetland environments. Inclusion of the unsaturated zone is essential because vegetation, through evapotranspiration, plays a crucial role in determining flow patterns (Dekker et al., 2005). Additionally, Hydrus can explicitly consider root-zone processes through using potential evapotranspiration as input and calculating the actual evaporation by considering prevailing moisture conditions and vegetation uptake (Joris & Feyen, 2003). Root-zone hydrological processes are essential to incorporate in a model of a wetland to be able to sufficiently evaluate restoration measures (Dekker et al., 2005). Hydrus can handle unsaturated conditions and root-zone processes, making it suitable for this study (Šejna et al., 2014). Furthermore, Hydrus has previously been successfully applied to study the effect of hydrological management in a floating fen system (Dekker et al., 2005). The software has also been used to study the impacts of drainage ditches on hydrological systems in earlier research (Błażejewski et al., 2018; Kacimov et al., 2020; Naghedifar et al., 2019; Youngs & al Jabri, 2018). Hydrus is therefore well suited for modelling the effect of a suppletion ditch in De Wieden.

In answer to SQI a base model of De Wieden was set-up. In this section the data sources for the set-up of the base model are given. In 4. Base Model the application of this data to the model is entailed.

Study Area and Model Location

In De Wieden two locations, Gezensloot and Klaverkooi, were selected by Natuurmonumenten as suitable locations for the placement of a suppletion ditch because moderately to well-developed birch woodland can be found in these areas. At each of the two locations two transects were established, one perpendicular to the suppletion ditch and one in parallel to the first transect (see Figure 6). The parallel transect were established to have a control transect, not impacted by a suppletion ditch, for future measurements. The locations of the transects are considered as the study area for this research.

The Hydrus model was developed for one transect in 2-D as limited differences in material distribution and water level were found between the different transect. Due to these large similarities modelling results were not expected to differ sharply between the transect. The modelled transect, W4, was chosen because one of the suppletion ditches is being placed across this transect and data was availability was greater for this transect at the start of the modelling compared to the other transects.

Figure 6: Location of the Transects W1-4 in De Wieden. Right*: The transects as indicated by the green line and the proposed location ditch indicated by the blue dotted line. The red dots represent measurement locations used during fieldwork.* Left: *Indication of the transect location within De Wieden by the yellow squares. The blue highlighted area indicate the location of DINOLoket data analyzed.*

Model Domain & Material Distribution

The model domain extends from the Belterwijde until a secondary ditch at the end of the transect (denoted by 'ditch' in Figure 6). The 'Actueel Hoogtebestand Nederland 3'[4] (AHN3)' was used to determine the surface elevation of the transect.

To create the material distribution for the model data on the composition and stratification of the peat along the transect was obtained during field work on 9-10 March 2020. The data was obtained at 4 to 9 locations along each transect using an Auger drill. The type of peat and level of humification was identified in the field based on colour and touch.

To determine to what degree fieldwork data was comparable to available data the 'Data en Informatie van de Nederlandse Ondergrond[5] (DINOLoket)' database of the 'TNO Geologische Dienst Nederland' was used (TNO Geologische Dienst Nederland, 2020b). Drilling logs from fieldwork were compared to drilling logs and soil composition found in the DINOLoket. A total of 165drill logs from DINLoket were analyzed, located approximately 2.5 km away from transect W4 in the blue area from Figure 6.

Boundary Conditions

The Boundary Conditions of the developed model were determined based on piezometric head data from DINOloket, climate input from the 'Koninklijk Nederlands Meteorologisch Instituut'[6] (KNMI) and literature on the surface water level in De Wieden.

[4] EN: Current Surface Elevation Map Netherlands 3 – Surface Level

[5] EN: Data and Information of the Dutch substrate

[6] EN: National Institute for Meteorological Data

Water Flow Parameters

Based on approaches in comparable studies the van Genuchten-Mualem soil hydraulic model was applied (Brunetti et al., 2018; Dekker et al., 2005; Joris & Feyen, 2003; Schot et al., 2004; Stofberg et al., 2016). For this soil hydraulic model six material properties per soil type are required: saturated hydraulic conductivity (K_s), residual soil water content (θ_r), saturated soil water content (θ_s), two empirical parameters affecting the hydraulic function alpha (α) and n, and the tortuosity parameter in the conductivity function (I) (Šimůnek et al., 2012b). The values for each parameter was established based upon literature analysis.

Throughout the modelling process it became clear that the K_s of the upper peat layer was an important factor determining the moisture conditions in the model. Therefore, it was considered beneficial to go back to the field to extend available knowledge on the K_s using the Auger-Hole Method (AM). Five measurements were made spread relatively evenly along transect W4 on the 1st of October 2020. AM was chosen based on expert advice (M. Hendriks, personal communication, 19th of September 2020). With this method the K_s of the 30 cm of soil surrounding a borehole is measured (Amoozegar & Warrick, 1986; Oosterbaan & Nijland, 1994).

For the application of AM a new borehole is created until approximately 30-70 cm below the groundwater level (Amoozegar & Warrick, 1986; van Beers, 1983). For De Wieden the boreholes were dug up to 70-80 cm as the groundwater level was expected at approximately 30 cm below the surface based on piezometric data from DINOLoket (see Table 2). The borehole was subsequently emptied multiple times to prime the hole (Amoozegar & Warrick, 1986). After priming the water is left to equilibrate with the groundwater. To measure the K_s the water level in the borehole is lowered as fast as possible using a handpump (Amoozegar & Warrick, 1986; Massop et al., 2005). After lowering the water level the rate of rise of the water is measured using a set time interval until 25% of the removed water has returned (Massop et al., 2005; van Beers, 1983). The aim should be to take at least 5 measurements when 25% of water has returned (van Beers, 1983). After the first measurement a duplicate measurement was taken to verify the consistency of the measurements (Amoozegar & Warrick, 1986). The K_s is then calculated using the following formula, based on the measured parameters detailed in Figure 7 (van Beers, 1983):

$$K_s = \frac{4000r^2}{(H + 20r)\left(2 - \frac{y}{H}\right)y}\frac{\Delta y}{\Delta t}$$

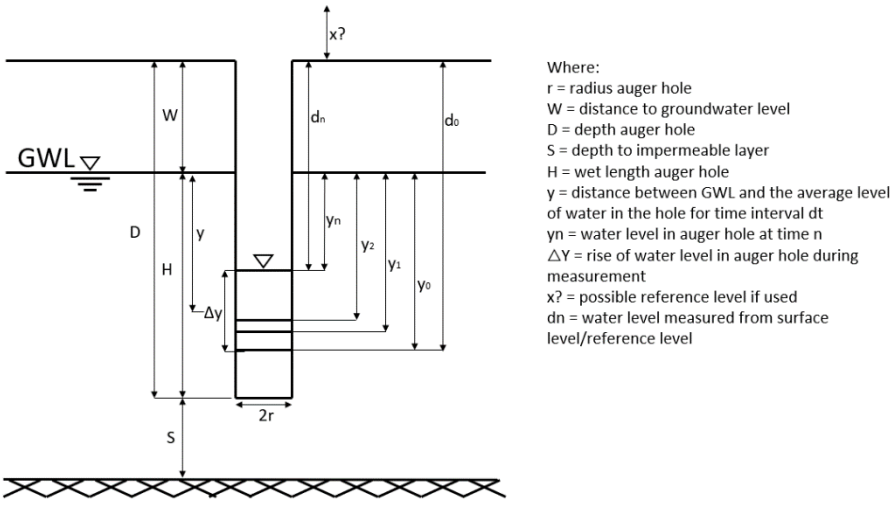

Figure 7: Schematic overview of the parameters measured at each borehole for the Auger-Hole method (Adapted from van Beers, 1983).

3.2. Calibration

For the model to be used for predictive simulations of the impacts of a suppletion ditch the model needed to be calibrated to field conditions in De Wieden (SQII). Model calibration is the process of adjusting a model to a particular problem by manipulating model specifications within reasonable ranges (Šimůnek et al., 2012a). This manipulation is undertaken until the simulated results from the model accurately represent observations.

Calibration of Hydrus models can be done using a large variety of the van Genuchten-Mualem parameters (Šimůnek et al., 2012a). One option is to calibrate the model using only hydraulic conductivity of the soil types incorporated into the model, as was done by Dekker et al. (2005), Stofberg et al. (2016) and Šimůnek & de Vos (1999). As limited field data was available for calibration this approach is taken for the modelling study of De Wieden. Considering all Van Genuchten-Mualem parameters for the multiple soil layers would give a large number of parameters to be estimated. Estimating such large amounts of parameter, based on the available data sources, would likely lead to the problem becoming non-unique or ill-posed (FAQ PC-Progress, 2019). Therefore, only the K_s values of the peat layers incorporated into the model were adjusted during calibration, these parameters were assumed to have the largest influence on water flow within the domain.

Quantitative calibration, using numerical parameters optimization or statistical means, was avoided. Undertaken such calibration steps based on limited amounts of data points could lead to the model containing unphysical parameters values and high predictive uncertainty (Brunetti et al., 2019). Therefore, the calibration took a more qualitative approach, in which simulated patterns were visually compared to available data. The used data was mostly *theoretical* in nature since limited field observations were available. This theoretical data was based on literature data from the surrounding area and expected patterns extrapolated from the characteristics of De Wieden.

The calibration process took place in three phases, each focussing on a resolving an objective:

1. Refinement of hydraulic head pattern
    - objective: obtain a vertical gradient in hydraulic head
2. Refinement of the gyttja layer
    - objective: resolve static phreatic level occuring in the model
3. Final K_s refinement of the peat layers
    - objective: optimize the model for representation of the phreatic level

Following these steps, a final validation step took place in which the simulated results were checked against available field data on piezometric data and Electrical Conductivity (EC). This was performed to confirm whether the model represented the study area well.

The used theoretical and observation data will be expanded upon in this section. In chapter 5 an extensive overview of each calibration phase is given, with further descriptions on the exact steps taken during each phase.

a) Hydraulic Head Pattern

Piezometric head data from DINOLoket shows that the hydraulic head in the peat layer approximates -0.8 m NAP while piezometric head in the deeper sand approximates -1.1 m NAP (see Figure A.2 for further detail). Based on these observations, and the knowledge that De Wieden is an infiltration area, a vertical decrease in the hydraulic head is theorized to occur in the study area (see Figure 8). Since no field data on the hydraulic head was available the sketched pattern was used as theoretical data for calibration.

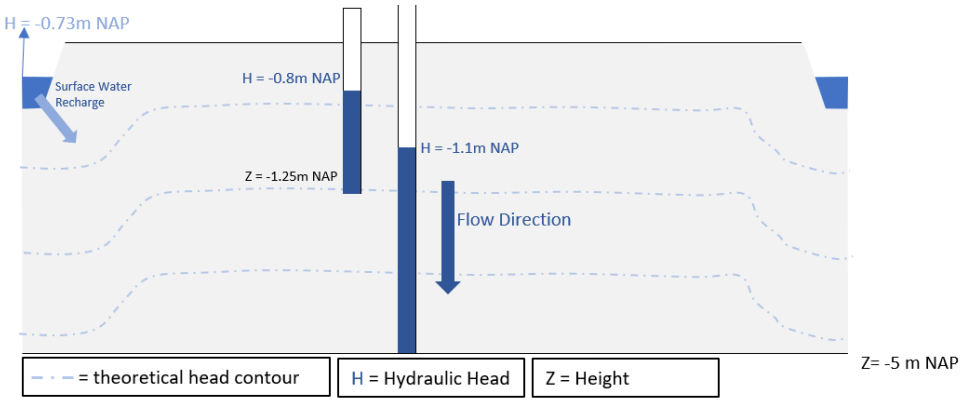

Figure 8: Indicative sketch of theorized vertical decrease in hydraulic head with depth along the transect as determined by piezometric data from DINOLoket, the used data is indicated by two monitoring wells. A situation of net recharge was assumed. The sketch is not to scale.

b) Phreatic Level

From three piezometers in the vicinity of the study area data on the average highest groundwater level (Dutch: GHG) and average lowest groundwater level (Dutch: GLG) were obtained through DINOLoket (see Table 2). The average GLG and GHG over the three piezometers were used as indicators of suitable phreatic levels in the model for, respectively, the summer and winter phreatic surface in the model. The data was supplemented with the GHG and GLG as based on the 'grondwatertrap'[7] coupled to the used piezometers by DINOLoket, which provided a maximum phreatic level for both winter and summer.

Table 2: Reference Phreatic Levels

Piezometer number ^	Phreatic Level (cm below surface level)	
	Winter *	Summer **
DINO Piezometer 1	11.3	35.4
DINO Piezometer 5	10.3	23.9
DINO Piezometer 8o	13.7	44.3
Average of Piezometers	11.8	34.5
Grondwatertap I	<20	<50

* As based on the required average highest groundwater levels (Dutch: *'Gemiddeld Hoogste Grondwaterstand'*)
** As based on the required average lowest groundwater levels (Dutch: *'Gemmideld Laagste Grondwaterstand'*)
^ References to the numbers applied to piezometers as in Appendix A**: DINOLoket Data**

c) Vertical Flow Direction

Several monitoring wells were installed along transect W1-4 on the 30th of June and the 1st of July 2020. On every transect five well locations were created perpendicular to the proposed ditch, as visible in Figure 9 For W2 two supplementary well nests were placed opposite of the ditch. Two piezometers with a filter length of 20 cm were installed at each point, one at 0.5m and one at 1.25m deep. The deeper wells were embedded within the sandy layer underneath the peat. The shallow pipes were placed in the upper peat layer. At the first and last piezometer nest for transect W2 and W4 deeper monitoring wells with the filters in the sandy layer, depth 2-2.5 m, were placed. These deeper wells were placed to gain insights into the direction of flow between the sand and peat layer.

[7] Dutch indication measure for visualizing the yearly fluctuation in groundwater level

The water level in the wells were manually measured on the 30th of September 2020 so that the piezometers had sufficient time to equilibrate (Baird et al., 2004). For well the two deeper wells at W2.1 electronic diver measurements were taken every six hours from the 30th of June to the 30th of September. Because the height of the monitoring wells were not measured in relation to a fixed reference the measured data could not be used directly for calibration. Instead with the data from the monitoring wells insights were gained into the direction of flow at the well locations by analyzing the difference in head between the deep and shallow filters.

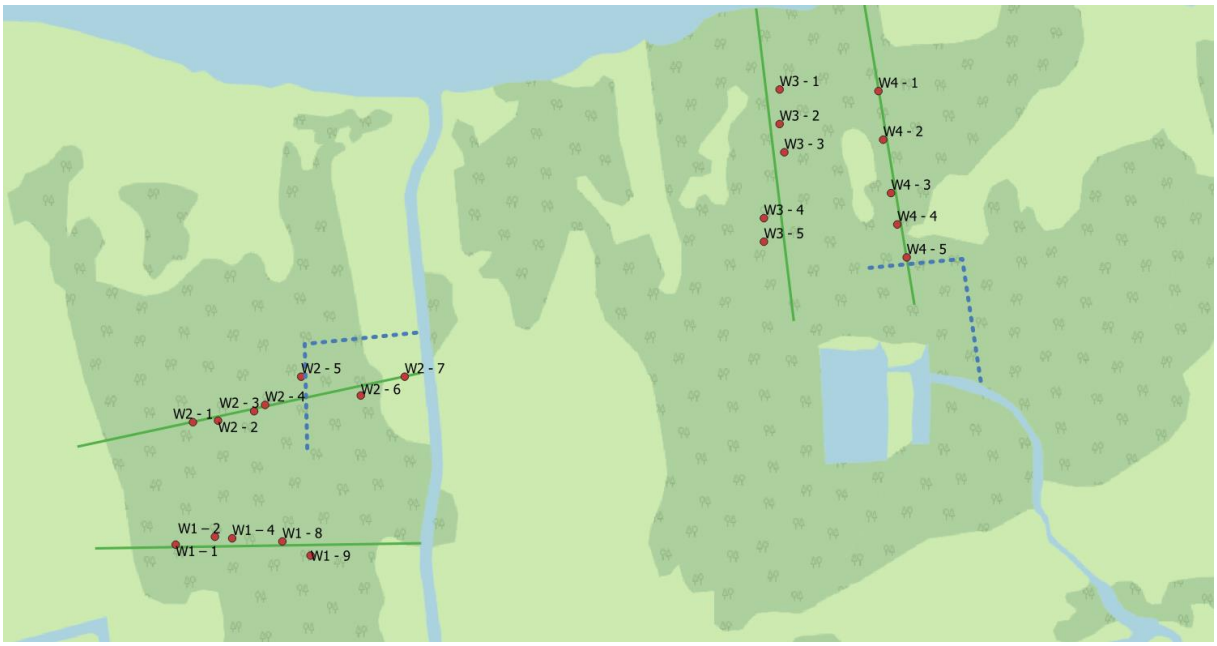

Figure 9: Locations of the placed monitoring wells along the four transects in De Wieden. At W2 and W4 the fifth well was located directly next to the suppletion ditch. The other wells at W2 were located at intervals of 20 m. For W4 the other wells were located at 10, 30, 60 and 100 m in distance. The monitoring wells in W1 and W3 were set up to mirror the neighboring transect.

d) EC Pattern

Groundwater in the transect is fed by two main sources of water: rain and surface water. These two water sources are associated with different magnitudes of ion concentrations, and consequently Electrical Conductivities (EC). Through the analysis of the EC it is thus theoretically possible to determine the source of water at a certain point, when only conservative transport is considered. To gain insights into the bog woodland vegetation criteria of rainwater influence in the root-zone the EC is incorporated as a solute in the Hydrus model. Additionally, the simulated solute pattern is compared to field measurements of EC to evaluate to what extend simulated waterflow sufficiently represents the field conditions.

EC measurements were made on the 1st of October by pumping the water out of the placed monitoring wells piezometers and subsequently measuring the EC using a WTW handheld EC meter. The EC of the surface waters near the transects were also measured during the fieldwork in October. The obtained data was interpolated along the transect using Inverse Distance Weighting interpolation with the standard distance coefficient of 2 in QuantumGIS.

e) Expert Guidance

Throughout the modelling process recommendations from several experts were acquired. Their suggestions and comments with regards to HYDRUS-2D and the model is referenced to in the text. The experts, including their profession and manner of contact, are:

- Stefan Dekker, Professor Global EcoHydrology and Sustainability at Utrecht University. Extensive experience with hydrological modelling. Contact through Skype on the 3rd of March 2020.
- Darell Tang, PhD student at Wageningen University & Research. Expertise in hydrological modelling, including Hydrus. Email contact from May to August 2020.
- Jirka Šimůnek, Professor and Hydrologist at University of California Riverside. Developer of the HYDRUS program code. Contact through the PC Progress discussion forum March to October 2020.
- Martin Hendriks, Emeritus Associate Professor Physical Geography and Hydrology at Utrecht University. Contact through email in September 2020.
- Ron Stroet, Senior Advisor Geohydrology at RHKDHV. Expert in groundwater modelling. Meeting on the 11th of September 2020.

3.3. Suppletion Ditch

After calibration the model was used to analyze the effect of a suppletion ditch on the phreatic level, soil moisture content and root-zone EC in De Wieden. A ditch with the same surface water level as the existing ditches was incorporated into the model. Several different scenarios, using different characteristics for the ditch, were used to determine which particular design would lead to favourable changes in the system. The location for the suppletion ditch itself has already been determined by Natuurmonumenten at a distance of 172 m from the Belterwijde and as such will not be changed. The ditch is planned to be small, hence the width and depth of the ditch were only varied between 0.5 and 1 m (see Table 3). This variation was done to see whether a larger ditch would show more favourable results. In one scenario the suppletion ditch was placed into the water-rich slurry layer by extending the present slurry layer 15 m to the right (see Figure B.1). This scenario was included to determine whether the slurry layer could have a large influence on the results.

For the scenario analysis the results from the calibrated model were applied as initial condition, for both pressure head and concentration. Climate data for 2015-2019 was used as input.

Table 3: Used scenarios for the implementation of a suppletion ditch

Scenario	Width Ditch	Depth Ditch	Slurry underneath the Ditch?
1	1m	1m	No
2	1m	0.5m	No
3	0.5m	1m	No
4	0.5m	0.5m	No
5	1m	1m	Yes

4. Base Model

In answer to SQI this chapter expands upon the design of the base model from De Wieden.

4.1 Model Domain

The length of the model domain was set to 210 m at the top. The top surface of the model was palced at a constant -0.6 m NAP based on the average soil surface height along the transect in the AHN-3. Surface height variations were disregarded to simplify the modelling process. The bottom of the domain was fixed at -5 m NAP following from the availability of observation data for the boundary condition at this approximate height.

On the left and right of the domain the Belterwijde and the secondary ditch were incorporated as 'ditches' of 1.2 m and 1 m deep respectively. (H. de Mars, personal communication, 12th of May 2020). The ditch representing the Belterwijde lake was established as 5 m wide, while the secondary ditch on the left was 1 m wide. Based on the approach by Dekker et al. (2005) the boundary of both ditches gradually lowered from the soil surface to the maximum surface water level over a distance of 15 cm before lowering to the bottom of the ditch sharply over a distance of 10 cm.

4.2 Material Distribution

The material distribution in the model was based on the borehole logs taken during fieldwork in March. These borehole logs tend to follow the same general sequence of layers (see Figure 10 and Figure D.2-3):

1. a discontinuous ***non-humified sphagnum peat*** layer of 0-40cm thick;
2. ***reed-sedge peat*** varying in degree of humification and thickness (0-100 cm). In transect W1, W2 and W4 this layer can extend to 300 cm deep;
3. a ***slurry layer***, defined as water rich (>90% water) with dissolved organic compounds and recognizable plant rests, starting at 60 cm depth and continuing up to 200 cm. In W3 and W4 this layer is 50-100 cm thicker;
4. sometimes a thin ***reed-sedge peat*** layer occurs underneath the slurry layer;
5. a ***smearing, gyttja-type peat layer*** of 20-50 cm thick at the transition of peat to sand, defined as a peat layer with gyttja characteristics;
6. the start of a ***sandy layer*** at approximately 250 to 300cm deep. Likely part of the thick sandy aquifer present in the study area as found in DINOLoket.

This sequence seems in accordance with the borehole logs available DINOLoket as compiled in Appendix A: DINOLoket Data. For both log sets the thickness of the peat layer is approximately 2.5-3 m after which the sandy layer starts. Deeper drilling logs in DINOLoket illustrate that this sandy layer can continue up to 70 m deep and is only sporadically interrupted by clay or peat layers.

A major difference between the DINOLoket and fieldwork logs is the presence of the slurry layer. However, as DINOLoket only distinguish 'peat' and no other notable features it could be that slurry layers were also present in DINOLoket borehole logs in the surrounding Wieden area but not classified as such. In relation to the good fit between the fieldwork and the DINOLoket borehole logs it was decided that the sequence of layers found during fieldwork gives a suitable representation of the material distribution in the study area.

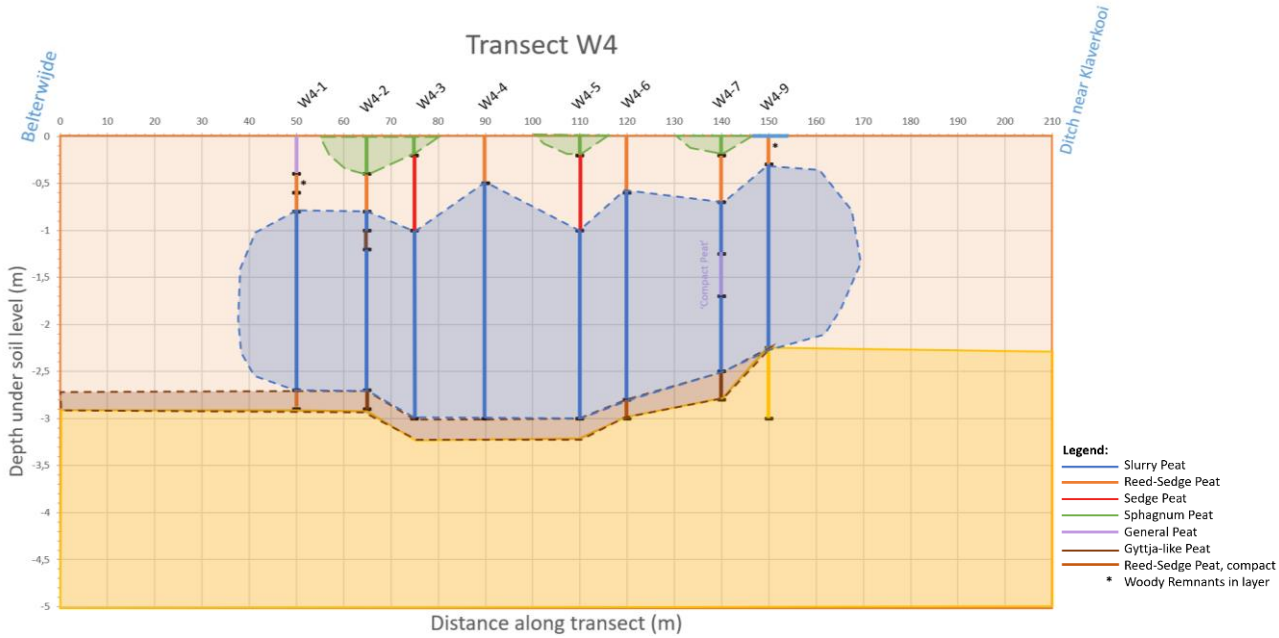

Figure 10: Profile of the soil along transect W4 as based on the borehole logs from fieldwork. The Slurry peat and Gyttja-like peat presence is estimated.. The location of the drill samples along the transect are indicated at the top, the numbers reference to the locations given in Figure D.1.

To reduce the amount of Van Genuchten-Mualem parameters required for the model the variety of peat found during fieldwork was simplified to the four major types found most commonly: Sphagnum, Reed-Sedge, Slurry, and the gyttja-type peat mixture (henceforth: Gyttja/Peat). The parameters required for the soil hydraulic function were reduced in order to restrict the model complexity and the limit inclusion of large amount of values with high uncertainty. The established material distribution in the model, Figure 10, was derived from the material distribution extrapolated from borehole logs in W4.

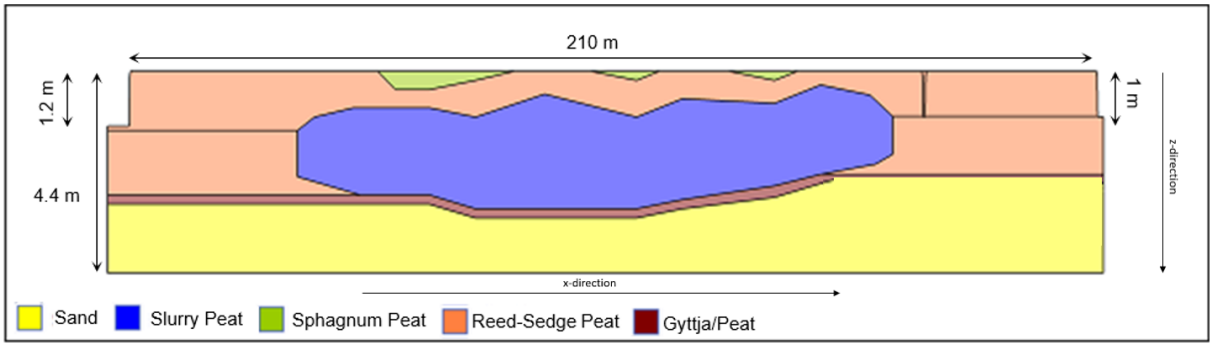

Figure 11: Model domain in HYDRUS-2D with the applied material distribution as based on fieldwork data. The model domain was created on the x,z-plane. This figure shows the domain with a stretch factor of 10 in the z-direction.

4.3 FE-Mesh

The established finite-element mesh (FE-mesh) in Hydrus reduced in nodal density downwards. The higher nodal density at the soil surface was incorporated because larger gradients and more variable fluxes are expected in the unsaturated zone (Joris & Feyen, 2003). Anisotropy, with larger horizontal elements, was included since vertical flow was expected to play a more significant role based on the limited horizontal flow processes incorporated into the model. For the computation of the FE-mesh a smoothing factor of 2.5 was applied (Šimůnek & Šejna, 2009).

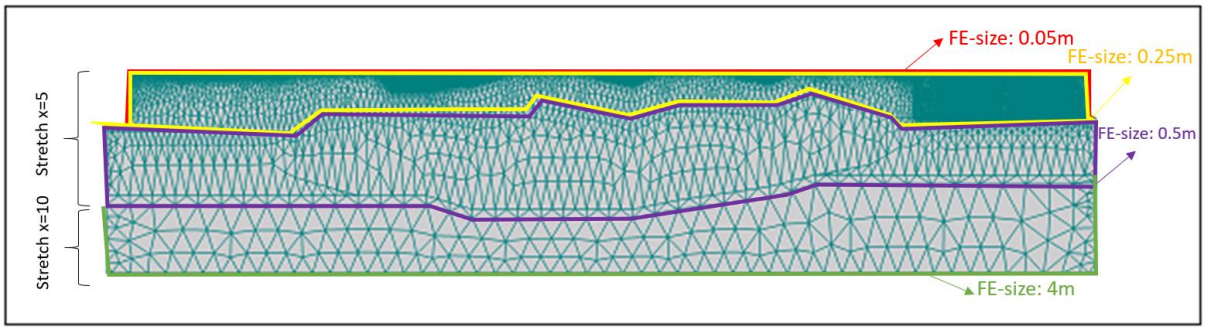

Figure 12: The established FE-Mesh with applied mesh sizing and stretching for each sector. The higher nodal density at the soil surface is visible in this figure. The figure shows the model domain stretched in the z-direction with a factor 10.

4.4 Boundary & Initial Conditions

Table 4 provides an overview of the applied boundary conditions (BCs), and their data sources. At the atmospheric boundary monthly climate input, precipitation and potential Makkink evapotranspiration, was applied (KNMI, n.d.-b). The potential Makkink evapotranspiration for grassland from the KNMI was adjusted using a crop factor of 1.04 and incorporated into the model as transpiration based on recommendations by R. Stroet (personal communication, 11th of September). The increase of evapotranspiration with the crop factor was implemented because woody vegetation is highly evaporative in comparison to smaller vegetation (Spieksma & Schouwenaars, 1997; Streefkerk & Casparie, 1989). The assumption that evapotranspiration can be incorporated as transpiration is made in relation to the relatively small contribution of evaporation to evapotranspiration (Sutanto et al., 2012).

Table 4: **Applied Boundary Conditions**

Boundary		Applied Boundary Condition	Location / Value
Upper Boundary		Atmospheric boundary	Precipitation and Evapotranspiration from KNMI station Hoogeveen
Left and Right Ditches	From the bottom of the ditch until the maximum water level	Variable Head	Hydrostatic equilibrium with winter or summer water level (-0.83/-0.73 m NAP). A seepage face is applied when negative pressures occur.
	From maximum water levels to transect surface	Seepage face	
Left and Right Boundary		No Flux	-
Bottom Boundary		Constant Head	Specified at -1.1 m NAP based on piezometric head DINOLoket

To achieve steady conditions a spin-up period of three years was used in which 'long-year averages' calculated over 1981-2010 by the KNMI were applied as atmospheric conditions (Figure 13a). Only three years of spin-up were employed since the model showed steady conditions, without large in- or outfluxes, after approximately two years. For the model simulations monthly climate data from 2015-2019 was applied (Figure 13b). This period was selected as it pertains the most recent available climate data for full years.

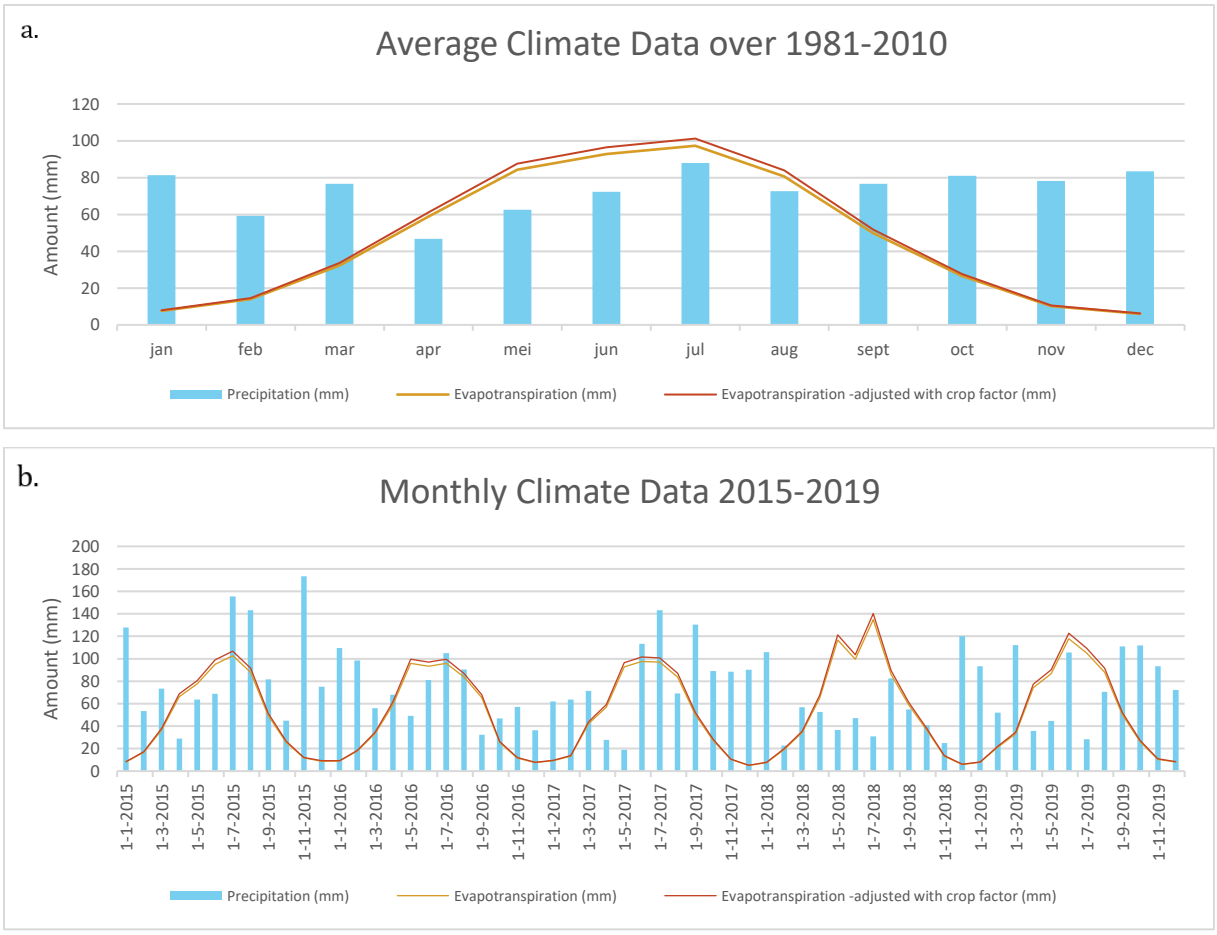

Figure 13: Applied climate data for spin-up (a) and simulation runs (b) in the model as obtained through the KNMI (KNMI, n.d.-a, n.d.-b)*. Monthly climate data was used for both spin-up and simulations.*

On the left and right side of the domain from the bottom of the ditches downwards a no flux boundary. Even though such a simplification can be considered as physically unrealistic (Joris & Feyen, 2003), this approach is often used across literature (Brunetti et al., 2018; Dekker et al., 2005; Naghedifar et al., 2019). For this modelling study the simplification was considered acceptable because horizontal flow across the transect is expected to be small based on the hydraulic head gradient of -5cm/1km calculated from the head contours.

Along the perimeter of the ditches a variable head BCs was applied. In summer, April to October, surface water level was set to -0.73 m NAP while in winter, November to March, surface water level was fixed at -0.83 m NAP (Waterschap Drents Overijsselse Delta, 2020). For October summer water level was applied as this month is a transitional month in which the water level can gradually lower from summer to winter level. Since the gradual lowering leads to water levels being higher than -0.83 m NAP for at least parts of October the surface water level of -0.73 m NAP was applied. Located above the highest water level is a seepage face (Dekker et al., 2005).

To establish the bottom BC a detailed examination of four possible options was undertaken. From this analysis it was concluded that two options, a *constant flux* or *no flux,* would be physically unrealistic boundaries (D. Tang, personal communications, 25th of May 2020). The application of a no flux would generate irreversible accumulation of water and hydrostatic conditions, which is unsuitable for the infiltrating nature of De Wieden. A constant flux is considered unrealistic as it is unlikely that a certain amount of seepage always occurs at the bottom, irresponsive of prevailing soil moisture conditions or head gradients. The third option, a *deep drainage* BC, would give accurate representations of field conditions as this boundary creates a flux based on the position of the groundwater table (Hopmans & Stricker, 1989). However, large quantities of field data are

required to successfully apply a deep drainage BC. Therefore, the bottom boundary was simplified to a *constant head* BC (D. Tang, personal communication, 28th of May 2020).

A constant head BC is regarded as more physically realistic as it can be determined based on piezometric head data. By using piezometric data of the sandy layer the regional environment is well represented in the model since the hydraulic head in the sandy layer is determined by regional influences on the system and not merely atmospheric variability (R. Stroet, personal communication, 11th of September). The use of this boundary condition was also recommended by all experts (M. Hendriks, personal communication, 25th august 2020; R. Stroet, personal communication, 11th of September 2020; Šimůnek, 2020b). The value for bottom BC was approximated from DINOLoket data to be -1.1 m NAP (See Appendix A.II: Hydraulic head).

4.5 Root Water Uptake

Root water uptake is included using the Feddes water uptake model, adjusted for water uptake during both saturated and unsaturated conditions by peat mosses (Dekker et al., 2005). The root water uptake was considered for the upper 20cm of the domain (Dekker et al., 2005; Schot et al., 2004).

4.7 Water Flow Parameters

A literature review was used to obtain the values for the required van Genuchten-Mualem parameters. This review indicated large variabilities in the K_s of peat occur across studies, with values ranging between 0.001-100 m/d (Table C.1). The K_s of peat has been negatively correlated to both depth and grade of humification, this relationship is ascribed to decreasing pore sizes with decomposition (Morris et al., 2011; Quinton et al., 2008; Rycroft et al., 1975). Because of the significant variability in the K_s of peat in time and space this parameter may be regarded as highly uncertain. With respect to this uncertainty a range of potential K_s values for the various types of peat was selected, visible in Table 5, and the most suitable value was determined during the calibration runs.

For Sphagnum peat a range of 1-100 m/d was founded on values found by Branham (2013) and used by Dekker et al. (2005) for Hydrus modelling. Only data from Schwärzel et al. (2006) was available for Reed-Sedge peat, who found K_s values of 0.01-1 m/d. However, because Reed-Sedge is present above the slurry layer, as a (semi-)floating raft, the saturated hydraulic conductivity might be higher as shown by values of 0.001-75 m/d for floating rafts (Table C.1). Taking this aspect into account the Reed-Sedge peat was given a range of 0.01-25 m/d. The range was kept lower compared to Sphagnum peat since Reed-Sedge peat was considered more humified during fieldwork. The slurry layer was given higher permeabilities of 500-1500 m/d (van Wirdum, 1990). For the Gyttja/Peat the range of 0.0001-1 m/d was selected based on Table C.1.

The other soil hydraulic parameters were based on a variety of sources. The parameter I was kept at 0.5 for all materials (Mualem, 1976). To all layers a θ_r of 0.045 was applied (Schot et al., 2004). The other parameters for Reed-Sedge peat were based on 'weakly humified reed-sedge peat' since the K_s of this peat fit best with the selected range (Schwärzel et al., 2006). No soil hydraulic parameters for Gyttja/Peat were available, therefore parameters for 'humified reed-sedge peat' were applied as this peat showed the most comparable K_s value to the selected range for Gyttja/Peat (Schwärzel et al., 2006; Table C.1). For Sphagnum peat the same α and n as Reed-Sedge peat were applied because preliminary modelling indicated that applying values α and n found for Sphagnum peat resulted in the model not converging (Figure C.1). The θ_s for Sphagnum was based on Dorland et al. (2015). The used soil hydraulic parameters for sand were obtained from (Carsel & Parrish (1988). These parameters were also applied for the slurry layer as data on the soil hydraulic parameters for this layer were not available, although the θ_s was changed to 0.9 in line with the water-rich characteristic of this layer.

Table 5: Initial Determined Parameters

Soil Type	θ_r (-)	θ_s (-)	α (1/m)	n (-)	K_s (m/d)	I (-)
Sand	0.045	0.43	14.5	2.68	50	0.5
Slurry	0.045	0.9	14.5	2.68	500-1500 (initial: 500)	0.5
Sphagnum Peat	0.045	0.88	0.3	1.16	1-100 (initial: 25)	0.5
Reed-Sedge Peat	0.045	0.891	0.3	1.16	0.01-25 (initial: 5)	0.5
Gyttja/Peat	0.045	0.741	0.5	1.15	0.001-0.01 (initial: 0.01)	0.5

4.8 Solute Transport

As indicator for rainwater influence in the root-zone, a formulated hydrological condition, EC was incorporated into the model as a solute. This simulated EC could additionally be used for validation of the model through comparison with fieldwork measurement.

For solute transport default Hydrus settings with Crank-Nicholsen time weighting scheme, Galerkin finite element space weighting scheme and Millington and Quirk tortuosity formulation were applied. The longitudinal dispersivity of EC was set to 5 cm and transversal dispersivity was set to 1 cm (Stofberg et al., 2016). Conservative transport of the solute was assumed. A diffusion coefficient of 1.2 cm^2/d with free water was used while gaseous diffusion was not considered (Stofberg et al., 2016). Rainwater EC was set at 50 µS/cm (Rijksdients voor Ondernemend Nederland, 2015). Surface water was set to 450 µS/cm based on field measurements on the 1st of October in the Belterwijde and Gezensloot. Initial conditions were set to 200 µS/cm.

At all water flow boundaries third-type, Cauchy, boundaries were applied (Batu & van Genuchten, 1990; Šimůnek & Šejna, 2018). The third-type boundary condition considers the input value for the solute on the boundary node as the concentration of infiltrating water (Šimůnek & Šejna, 2018). This boundary type is considered more physically realistic and mass conservative compared to, also available, Dirichlet boundary.

5. Calibration Process

In answer to SQII this chapter discusses the calibration process in which the model was adjusted to field conditions in De Wieden.

5.1 Initial Model Refinement

The first simulations using the base model showed limited variations in hydraulic head along the transect (see Figure 14). This was not as anticipated based on the theoretical hydraulic head pattern from Figure 8, which indicates a vertical decrease in hydraulic head. In order to obtain some degree of vertical variation in hydraulic head the K_s values for the Sphagnum, Reed-Sedge, and Gyttja/Peat layer needed to be lowered with a factor 5-100 to respectively 2, 0.05, and 0.002 m/d. The use of these K_s values leads to the occurrence of a vertical gradient on the left and right side of the slurry (Figure 15).

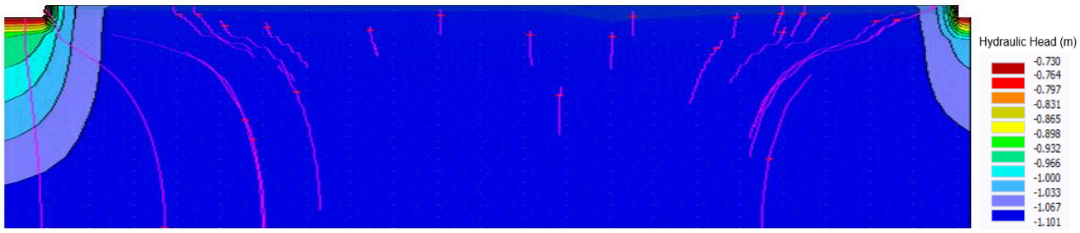

Figure 14: Hydraulic head across the base model in December when applying long-year average climate input for three years. This pattern is visible for all months of the simulations and shows no variation in time. The red dots are particles incorporated into the model which flow through conservative transport. The pink lines represent the flow trajectories of these particles. The domain is stretched in the z-direction with a factor 10.

From Figure 14 and 15 it became evident that the initially expected theoretical hydraulic head pattern might be inaccurate because the influence of the highly permeable slurry layer was not considered. A purely vertical decrease in hydraulic head is improbable as the highly permeable slurry pulls water towards the middle of the transect. This effect is visible through the high hydraulic head region in Figure 15. Since the pattern used as theoretical data may be incorrect, and no other data is available, the hydraulic head of Figure 14 and 15 could both be deemed reasonable. The results of this calibration phase are therefore inconclusive. The adjusted K_s values were however kept during the second phase of calibration.

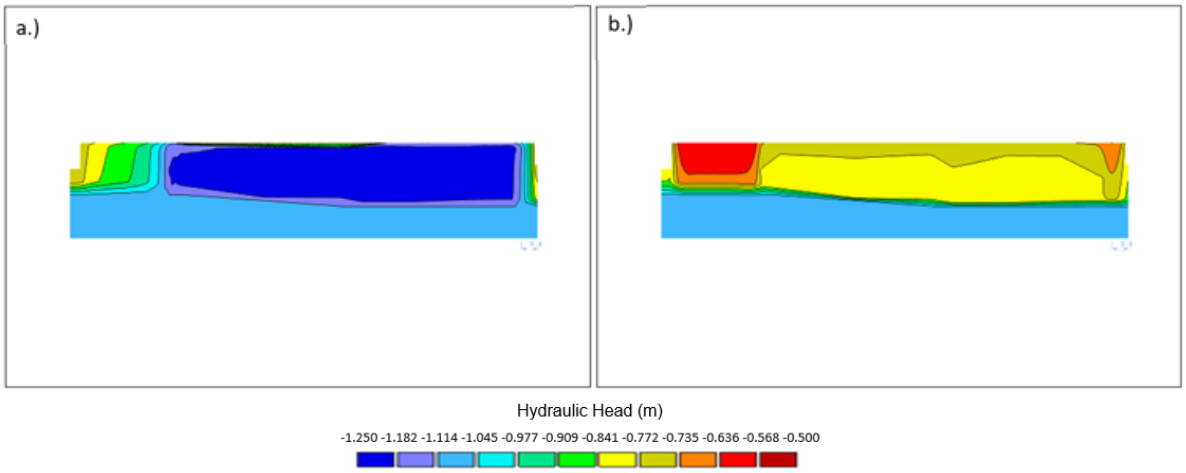

Figure 15: Hydraulic head pattern for the base model with smaller K_s values for the peat layers. a.) represents July in the third year of spin-up b.) December in the third year of spin-up. The model is stretched in the z-direction with a factor 10.

5.2 Gyttja layer refinement

Exploratory modelling with the developed base model exposed that the phreatic level simulated in the model was irresponsive to changes in climate input or saturated hydraulic conductivities of peat layers. As this seemed improbable the second calibration phase focussed on resolving this concern.

It became clear that the constant phreatic level could be attributed to the properties of the Gyttja/Peat layer. On account of the low permeability ascribed to this layer a sharp hydraulic gradient should occur over the Gyttja/Peat layer (R. Stroet, personal communication, 11th of September; see Figure 16). In this layer the hydraulic head should reduce from the value occuring in the upper peat layers to the hydraulic head of the sandy layer, established at -1.1 m NAP. Two adjustments to the model were required to establish a gradient across the Gyttja/Peat.

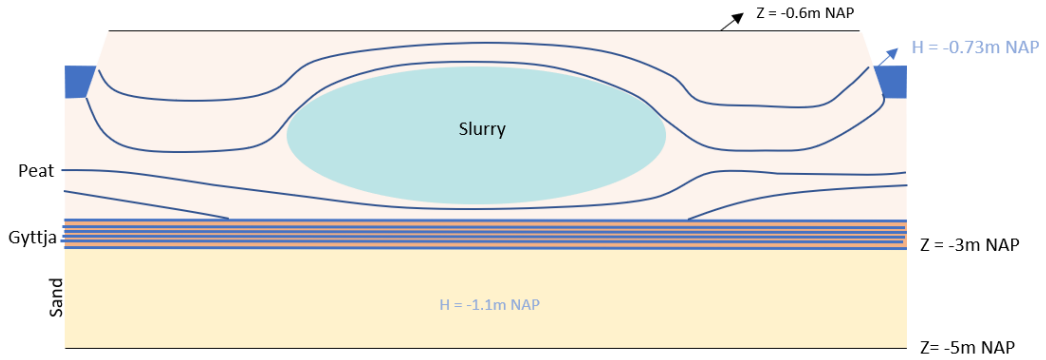

Figure 16: Expected hydraulic head contours across the transect due to the influence of the highly permeable slurry and sand, and the low conductivity of the gyttja. The blue lines represent probable head contours. The figure is not to scale.

Firstly, the Gyttja/Peat layer was extended to the end of the transect to be able to realize a sharp hydraulic gradient along the full model domain (R. Stroet, personal communication, 11th of September). Initially the Gyttja/Peat layer was only present up to 175 m into the transect, based on borehole logs from fieldwork. As a territorialised peatland often lies on top of a gyttja soil the extension of the Gyttja/Peat layer can be regarded as acceptable (Dorland et al., 2015; Kellner, 2007).

Secondly, to obtain a suitable hydraulic gradient the K_s of the Gyttja/Peat layer ($K_{s\text{-gyttja}}$) was calculated based on the following formula (Heij, 1984):

$$q = \frac{\Delta\varphi}{c} = \frac{\Delta\varphi}{\sum c}$$

Where q is the discharge (m/d), Δφ the difference in hydraulic head across a distance (m) and c is the hydraulic resistance (day). The sum of the hydraulic resistance over multiple layers given by (Heij, 1984):

$$\sum c = \sum^{n} \frac{d_n}{K_n}$$

With d_n as the thickness of soil layer n (m) and K_n the hydraulic conductivity for soil layer n (m/day). Using a simplified representation of the transect (Figure 17) and both formulas the optimal $K_{s\text{-gyttja}}$ was calculated based on three assumptions:

1. The hydraulic head in the peat (φ_{peat}) is equal to the winter surface water level, i.e. -0.83 m. This assumption is supported by the limited hydraulic head surplus occuring in kragge systems in winter, indicating the hydraulic head approaches surface water levels (van Wirdum, 1990).
2. An input flux (q) of 2 mm/day is used based on an average precipitation excess of 363 mm in winter for the long-year average climate data (figure 11a).

3. The lowered value for the K_s of the Reed-Sedge peat in the first calibration phase, 0.05 m/d, is a reasonable estimate.

On grounds of these assumption the $K_{s\text{-gyttja}}$ was calculated:

$$\sum c = \frac{\Delta\varphi}{q} = \frac{\varphi_{zand} - \varphi_{peat}}{q} = \frac{-0.830 - -1.1}{0.002} = \frac{0.270}{0.002} = 135\ days$$

$$c_{gyttja} = \sum c - -c_{slurry} - c_{carex} = 135 - \frac{1}{500} - \frac{1}{0.05} = 114.9\ days$$

$$K_{s-\ gyttja} = \frac{c_{gyttja}}{d_{gyttja}} = \frac{114.99}{0.2} = \mathbf{0.0017\ m/d}$$

Integrating the extended Gyttja/Peat and new $K_{s\text{-gyttja}}$ into the model provided fluctuations in phreatic level. Presumably the extension of the layer has been a deciding factor in the model showing phreatic level fluctuations as the change in $K_{s\text{-gyttja}}$ is relatively small compared to the initial estimate (0.01) and estimate used in the first calibration phase (0.002).

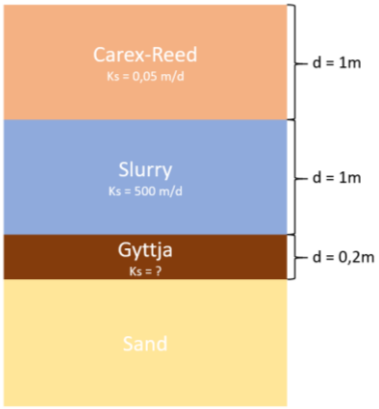

Figure 17: Simplified middle part of the transect used for calculations. For the calculation the thickness of the peat layers was of main importance

5.3 K_s Refinement of Peat Layers

The phreatic level in the model with the extended Gyttja/Peat layer demonstrated significant sensitivity to the K_s of the Reed-Sedge peat ($K_{s\text{-reed}}$). The third calibration phase therefore focussed on fitting simulated phreatic levels to expected levels to obtain a model that represented the De Wieden sufficiently by varying the $K_{s\text{-reed}}$. The K_s of the Reed-Sedge layer was the focus of the calibration as the model showed limited sensitivity for the K_s of the Sphagnum and Slurry peat. The limited response in phreatic level to changes in the K_s of Sphagnum is ascribed to the limited occurrence of Sphagnum peat in the model domain. While the limited influence of the K_s of Slurry on the phreatic level is attributed to the comparatively large K_s of this layer. Changing the K_s of Slurry within the determined range presumably leads to limited changes in hydraulic head gradients and subsequently water flow along the transect. In relations to this irresponsiveness the calibration was centred around $K_{s\text{-reed}}$.

The fieldwork measurements of K_s along the transect provided a guideline for possible reasonable values of $K_{s\text{-reed}}$. Throughout the execution of the Auger-Hole measurements it became apparent that the soil in De Wieden might be highly permeable since it was difficult to lower the water table in the borehole. With constant inflow of water into the boreholes it was only possible to lower the water level with 1-3 cm. One borehole (near W4-1) even showed such rapid recharge that measurements of rise were not possible. Possibly the boreholes perforated the more solid peat at the top until the slurry, providing the possibility for rapid flow of water from the slurry towards the borehole. The K_s obtained from fieldwork might therefore be an overestimation.

Table 6 provides the K_s for the upper peat layer based on the calculations provided in Appendix D.IV: Hydraulic Conductivity. The K_s the peat, assumed to be Reed-Sedge peat, ranged between 0.95-8.55 m/d. From this range it was established that the $K_{s\text{-reed}}$ ought to be higher than the applied value from the first calibration phase (0.05).

Table 6: Ks parameters as found during fieldwork in October for different points along transect W4

Point	W4-2		W4-3		W4-5		W4-6			W4-7		Average
Measurement	1	2	1	2	1	2	1	2	3	1	2	
K_s (m/d)	4.76	7.95	2.31	8.55	2.10	2.68	-1.52*	-35.90*	0.95	2.15	3.26	3.86

*These measurements likely contain large errors and where not taken account in the calculation of the average

To fit the model to the field conditions in De Wieden several calibration runs with $K_{s\text{-reed}}$ values between 0.5-10 m/d, as based on the field measurements, were undertaken. This range was however adjusted to 0.5-50 m/d after initial calibration indicated that higher K_s values provided phreatic levels in better accordance with the theoretical data.

All calibration runs, summarized in Table 7, were in accordance with the phreatic level for winter (<20 cm). Lower K_s produced more optimal results with phreatic levels nearer to criteria of 11.8 cm. The runs with K_s above 10 m/d were in better accordance with the summer phreatic level limit of <50 cm and the average of 34.5 cm. The K_s of run 6 is applied in the model as this calibration run is in accordance with both summer and winter phreatic levels while the K_s is also comparable to the K_s found during fieldwork.

Using $K_{s\text{-reed}}$=15 m/d three calibration runs with different variations of $K_{s\text{-slurry}}$ were carried out. From these runs the value of 500 m/d, as previously applied throughout the study, was determined as most suitable since it provided the most optimal summer and winter phreatic levels in relation to the theoretical data. Applying both a $K_{s\text{-reed}}$ of 15 m/d and $K_{s\text{-slurry}}$ of 500 m/d lead to the development of the final model which proposed to represent the phreatic levels in de Wieden sufficiently.

Table 7: Summary of the calibration runs taken

Calibration Run	K_s Reed-Sedge (m/d)	K_s Slurry (m/d)	Phreatic Level at the midpoint of the transect (cm below surface level)	
			Winter*	Summer**
1	1.5	500	16.0	69.5
2	2.5	500	17.9	65.1
3	5	500	17.7	59.8
4	7.5	500	17.7	54.5
5	10	500	18.4	50.1
6	**15**	500	**18.5**	**43.5**
7	20	500	18.7	38.9
8	25	500	18.9	35.6
9	30	500	19.0	27.6
10	50	500	19.2	26.8
11	15	1000	18.6	43.5
12	15	15000	18.9	43.7

5.4 Validation: EC and Groundwater Flow Direction

The final model was validated to determine to what extent the De Wieden was represented sufficiently. The validation was performed using data on EC patterns and groundwater flow direction.

EC Pattern

For validation field measurements, visible in Figure 18, were used to check whether the simulated EC would be considered acceptable. In general, the model simulation represents the field conditions to a reasonable degree (Figure 19). Comparable to most measurements points the EC increases with depth in the model, especially in the top 40 cm of soil. The model reflects the increase in measured EC near the secondary ditch on the right. This increase in measured EC on the right is attributed to surface water influence. The higher simulated EC near the ditches is also of similar magnitude (>300 µS/cm) compared to the field data.

In the measurements surface water influence is visible up to W4.2 as compared to location W4.4 in the model .This discrepancy is likely due to the model not taking into account chemical processes, such as dissolvement of organic substances, which could give an underestimation of the simulated EC. Additionally, at middle of the transect the simulated data indicates only low EC concentrations (<250 µS/cm). These lower values are due to limited horizontal flow incorporated in the modelled domain (Šimůnek, 2020a).

Even with the discrepancies the model is determined to simulate the EC in a sufficient manner as the model does give a good indication where rainwater or surface water influences predominantly occur. This way the simulated results may be used to give an indication the suppletion ditch might affect water flow.

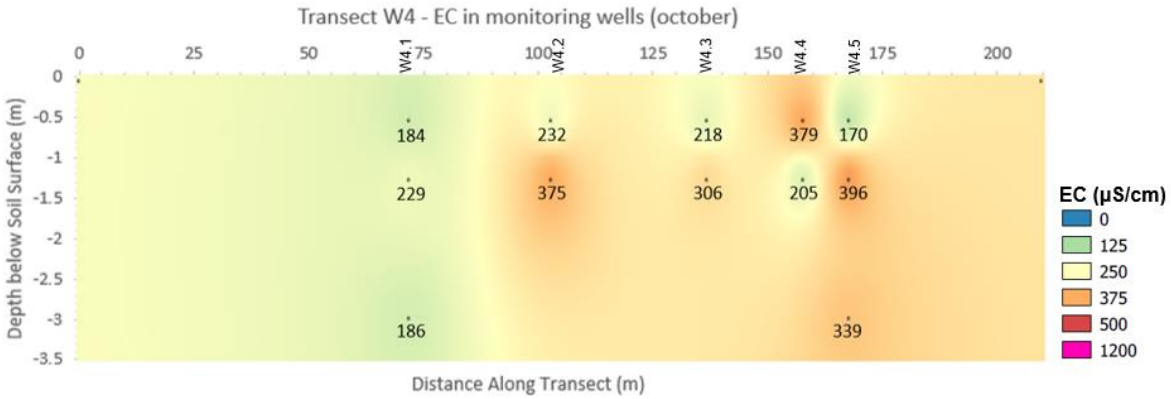

Figure 18: Interpolated Electrical Conductivity of the water in the monitoring wells along transect W4 on the 1st of October. The black dots represent the location of the filters of the monitoring wells. The black values underneath the dots show the measured values.

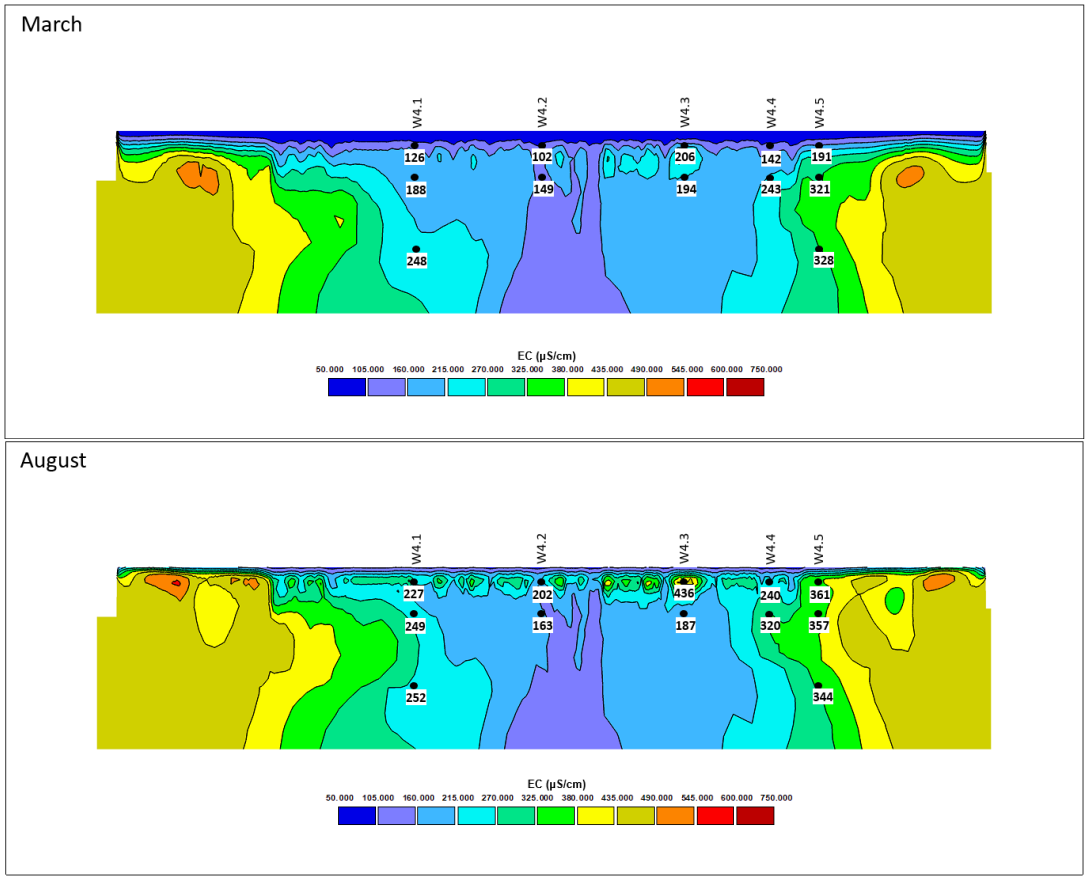

Figure 19: Simulated EC along the transect for March and August 2019. The black dots represent the location of the monitoring well filters marked above the soil. The numbers in the white squares are the values simulated at the location of the filters.

Groundwater Flow Direction

From the simulated Darcian velocity vectors in Figure 20 it is evident that during months of precipitation deficit upward seepage can occur in the model. Predominantly from the Slurry towards the soil surface upwards water flow occurs. The simulated upward seepage fits with hydraulic head measurements from the monitoring wells along transect W4 (Figure 21). The measured head at the shallow standpipes at W4.2-W4.5 were lower compared to the deeper filters, indicating upwards flow occurs along the transect. The simulated upwards flow in the peat layer is therefore considered to represent water flow in De Wieden sufficiently.

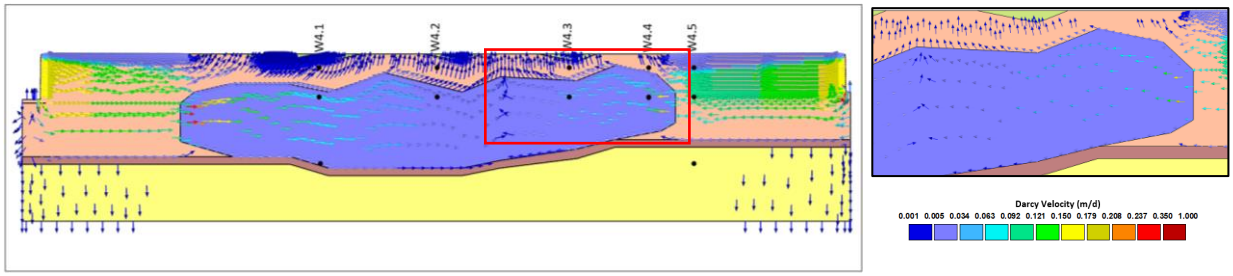

Figure 20: Darcy Velocity (m/d) in July of 2019 illustrating upwards flow in the peat layer. July is presented as the high precipitation deficit for this month leads to clear upwards flow. Left: Overview of the transect. The location of the monitoring well nests are indicate above the transect and the well filters by black dots. The red square inset in marks the location of the detailed overview. Right: Detailed overview of the upward flow at the soil surface.

In the model infiltration prevails in the sandy layer for all months. Diver data along transect W2 indicates that water flows from the sand to the peat in August 2020 (Figure D. 8). This upwards seepage seems at odds with the infiltrating nature of De Wieden but could be explained by the precipitation deficit in August 2020 (KNMI, n.d.-b). Evapotranspiration at the soil surface presumably lead to more water being transported upwards from the sandy layer, specifically with the presence of highly permeable slurry water can be transported rapidly upwards to resupply evapotranspiration losses. While the model does not represent upwards water flow in the sandy layer the velocity vectors do indicate downwards flows becomes markedly less in summer. This was assumed to represent the changing water flow between the sand and peat to a satisfactory degree.

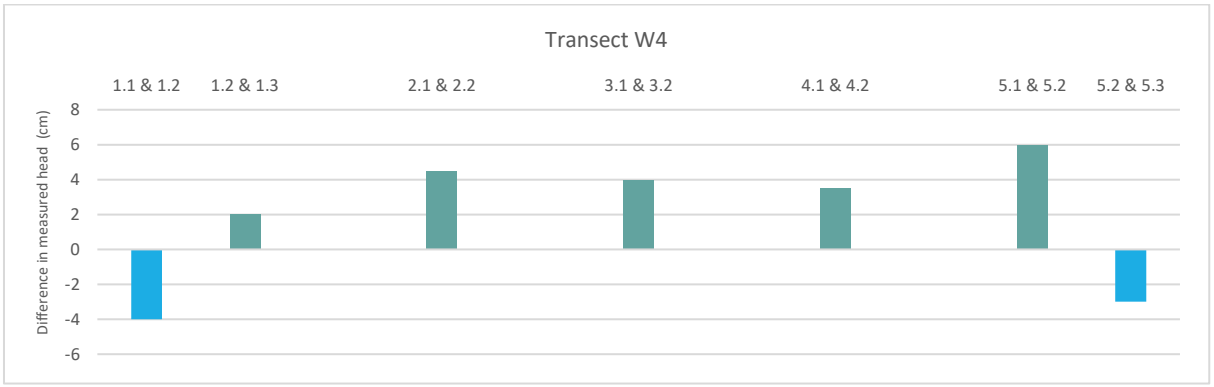

Figure 21: Difference in hydraulic head between two monitoring wells illustrating the direction of water flow. Negative value (blue) indicates infiltration while a positive value (green) indicates upwards seepage. The hydraulic heads were adjusted using as reference the monitoring well extending the furthest above the surface. The wells filters are located at x.1 = -0.5 m below the surface, x.2 = -1.25 m below the surface and x.3 = -3 m below the surface (in sand). Numbers reference to location along transect.

6. Simulation Suppletion Ditch

To answer SQIII this chapter examines the main findings from five variations of a suppletion ditch incorporated in the model. To analyse the results two months in 2019 will be discussed. March represents winter conditions since it is the final month in a hydrological year. For summer August is considered since it is the final summer month in 2019 with a precipitation deficit. The results are examined for two locations: the middle of the transect (x=105 m) and in the middle in between the suppletion ditch and the existing boundary ditch on the right (x=192 m). Both locations are considered since they show markedly different results.

Table 8 summarizes the main findings of the suppletion ditch simulations. This table shows that the phreatic level decreases in winter and increases in summer for all five ditch scenarios. The change of phreatic level is visible along the full transect (see Figure E.1-2). All scenarios maintain high soil moisture contents throughout both seasons. An increase in root-zone EC is visible for all scenarios. Scenario 5, in which the suppletion ditch is connected to the slurry, displays the largest changes in phreatic level & soil moisture content and smallest change in EC.

Table 8: Summary of the main results of the suppletion Ditch Scenarios

		Phreatic Water Level (cm below surface level)				Soil Moisture Content at Soil Surface (-)				Average EC root zone (µS/cm)	
		Middle of the Transect		Between suppletion and boundary ditch		Middle of the Transect		Between suppletion and boundary ditch			
Code	Scenario	March	August	March	August	March	August	March	August	March	August
B	Baseline	21.9	36.8	22.3	24.2	0.886	0.882	0.886	0.885	81.7	223.2
S1	Scenario 1	22.5	23.5	22.8	15.2	0.886	0.886	0.886	0.888	85.7	250.9
S2	Scenario 2	22.5	23.7	22.9	15.4	0.886	0.886	0.886	0.888	86.5	256.9
S3	Scenario 3	22.4	23.5	22.9	15.3	0.886	0.886	0.886	0.888	86.6	257.9
S4	Scenario 4	22.5	23.7	22.9	15.4	0.886	0.886	0.886	0.888	86.2	255.1
S5	Scenario 5	22.7	17	22.8	15.2	0.886	0.887	0.886	0.888	82.2	231.9

6.1 Phreatic Water Level

Between Scenario 1-4 minimal differences occur, with a decrease of approximately 0.6 cm for all scenarios. For the middle of the transect Scenario 5 shows a slightly larger drop in phreatic level of around 0.8 cm. The decrease in phreatic level for all scenarios is attributed to a drainage effect of the suppletion ditch. Winter surface water level is below the simulated phreatic level, namely at -0.83 m NAP i.e. 23 cm below soil surface. The formed hydraulic gradient generates lateral flow towards the suppletion ditch (Schlotzhauer & Price, 1999). This lateral flow is visible by the Darcian velocity vectors which (Figure 22). The found lower phreatic level for S5 is attributed to the direct connection of the suppletion ditch to the Slurry. Through this connection drainage can occur more rapidly, as indicated by the higher velocities compared to other scenarios.

In August an increase phreatic level increases with 13 cm for S1-4 and 19.8 cm for S5 at the middle of the transect. In summer the surface water level of -0.73 m NAP, i.e. 13 cm below surface level, is higher compared to the found phreatic levels. Here the hydraulic gradient produces inflow of water from the ditches, which is visible in the velocity vectors (

Figure 23). The suppletion ditch provides the possibility for increased influx of water, generating higher phreatic levels compared to the baseline. For S5 the direct connection to the Slurry produces rapid flow (>0.350 m/d) of water from the suppletion ditch directly into the Slurry. This rapid inflow results in the higher phreatic level increase for S5 compared to S1-4.

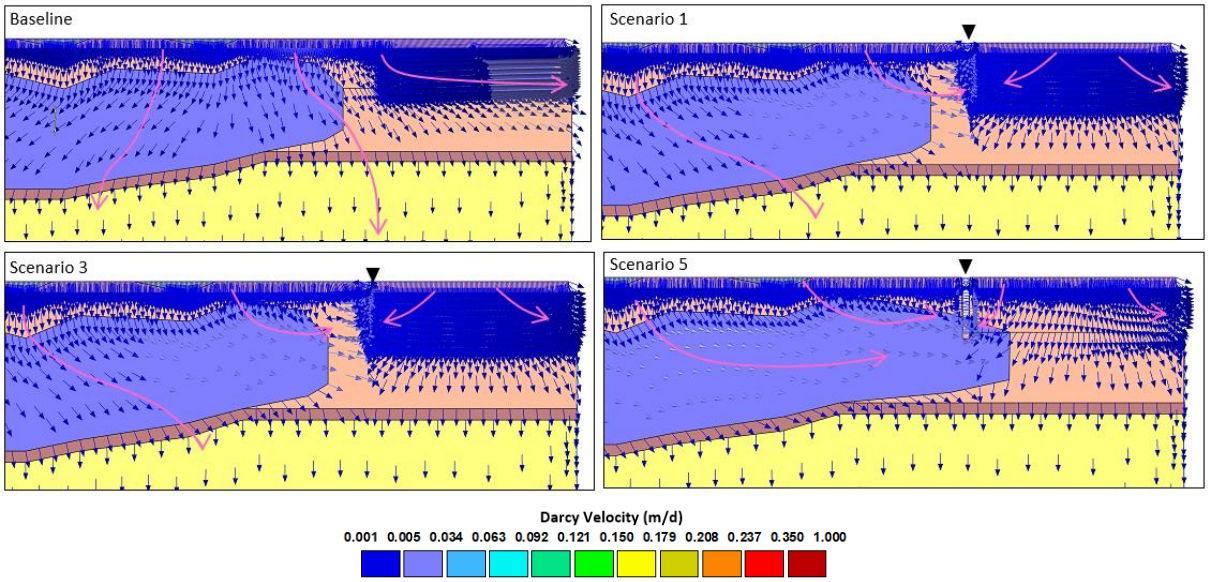

Figure 22: Velocity vectors surrounding the suppletion ditch (black triangle) for March 2019 indicating the drainage effect of incorporated ditches through the lateral orientation of the vectors. The pink arrows indicate main flow directions. Velocity vectors for the full transect and other scenarios are in Figure E.7.

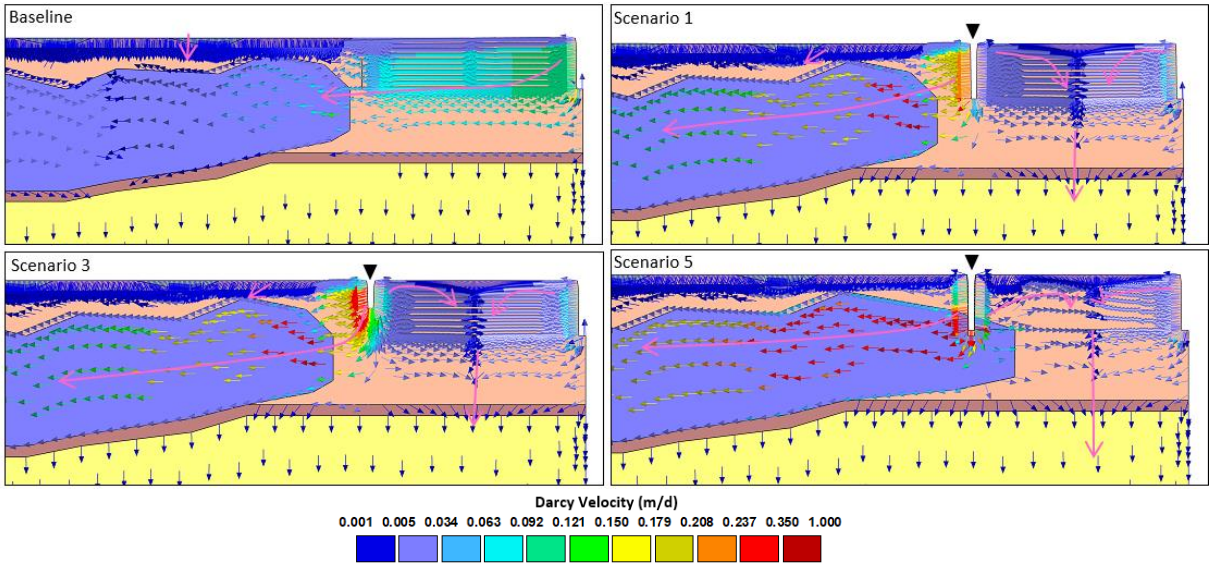

Figure 23: Velocity vectors surrounding the suppletion ditch (black triangle) for August 2019 illustrating the influx of water from the suppletion ditch to the peat and slurry. The pink arrows indicate main flow directions. Velocity vectors for the full transect and other scenarios are in Figure E.8.

On the right side of the suppletion ditch a large influx of water, from two ditches, occurs over a small (>40 m wide) of the transect compared to the left side (Figure 23). Water flow from both ditches converges and infiltrates towards the sand. Infiltration towards the sandy layer is however limited by the permeability of the Gyttja/Peat layer. The low K_s of this layer leads to water accumulating in the reed-sedge peat, generating the higher phreatic levels on this side of the transect visible for all scenarios.

The implementation of a suppletion ditch generates more stable phreatic levels over time as fluctuations in level are dampened (Figure 24). For S5 the phreatic level follows the changes in surface water level, indicating a direct link between the surface water and the peat system. This link is attributed to the direct connection to the slurry layer. On the right side of the suppletion ditch a similar link is visible for S1-4. On this side the slurry is not present and instead the fluctuations are attributed to the influence of surface water influx from two ditches across a small surface area.

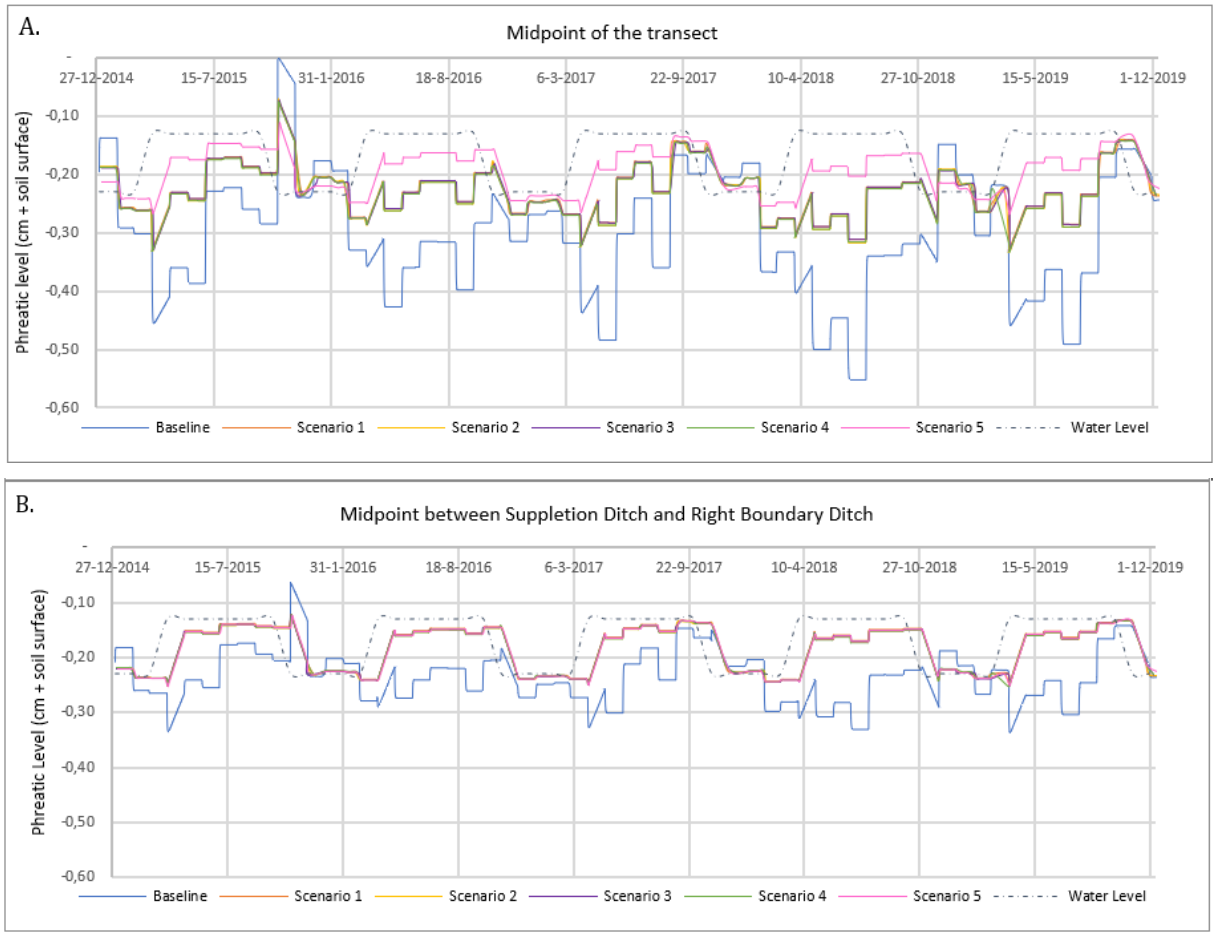

Figure 24: Time-series of the Phreatic Level for all Scenarios for January 2014 to December 2019 illustrating the more stable levels for suppletion ditch scenarios. A. Phreatic level at the midpoint of the transect. B: Phreatic level at the midpoint between the suppletion ditch and right boundary ditch.

6.2 Soil Moisture Content

The soil moisture content at the soil surface is near saturation (0.891) for all scenarios. In summer S1-4 the soil moisture increased with 0.004 at the middle of the transect and 0.003 between the two ditches. For S5 the increase in the middle of the transect was 0.005. The increase in soil moisture content follows from the higher phreatic levels compared to the baseline in summer. In winter, despite the phreatic level decreasing, the soil moisture content remains the same. Precipitation excess presumably keeps the moisture content high even while ditches drain water out of the transect.

6.3 EC in Root-Zone

Because of surface water inflow through the suppletion ditch the root-zone EC increases for all scenarios. Specifically, in the direct vicinity, 10 m, of the suppletion ditch the root-zone EC increases in summer (Figure 25). Further away from the ditch an increase in root-zone EC is less prevalent (Figure E.4). The higher EC in the root-zone are attributed to these zones of surface water inflow near the ditch. For S5 the increase in root-zone EC is of a smaller magnitude, 0.5-8.7 µS/cm compared to 5-35 µS/cm for S1-4. This is ascribed to surface water flowing more rapidly into the Slurry layer instead of the upper peat layer as indicated by orientation of the velocity vectors (Figure 23).

The thickness of rainwater influence (<160 µS/cm) remains the same for all scenarios compared to the baseline, 40 cm in March and 10 cm in August (Figure E.3-4). However, in comparison to the baseline the length over which rainwater layers above high EC surface water extends from 40 m away from the ditches to 70 m away from the suppletion ditch (Figure E.4). This region extends due to inflow of surface water into the Slurry layer, providing rapid transport of surface water laterally. The lateral spread of surface water EC might be an indication that a thin rainwater lens could take shape with the implementation of a suppletion ditch.

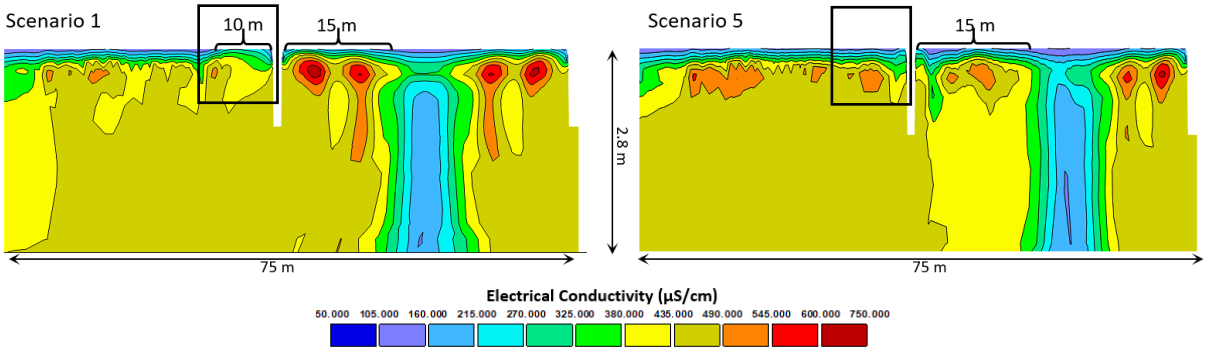

Figure 25: EC in the direct vicinity of the suppletion ditch for August for two Scenarios. Scenario 5, with direct connection between the slurry layer and the suppletion ditch, shows lesser surface water influence (high EC) on the left side of the suppletion ditch (indicated with square). Only the top right corner of the transect is visualized (black square in Figure E.4) the full EC for all transect can be found in Appendix E: Results Simulation Suppletion Ditch

7. Discussion

This chapter first discusses the implications of several limitations of the research in relation to the found results. Then the implications of the suppletion ditch simulations are considered in relation to literature.

7.1. Limitations

Boundary Conditions

Some notable simplifications were made regarding the boundary conditions. In the natural environment the hydraulic head in the sandy layer would fluctuate in response to seasonal or annual variations, as is also visible from the DINOLoket data (Figure A.3). The applied constant head BC does not fluctuate or vary over time and is independent of prevailing moisture conditions in the system. Consequently, the model represents the natural environment less accurately. However, the constant head is considered an acceptable rendition of field conditions because the bandwidth of fluctuation in the piezometric data is only 10 cm (R. Stroet, Personal Communication, 11th of September 2020).

To refine the model a variable head BC could be implemented to incorporate seasonal fluctuations of the hydraulic head in the sandy layer. Since there was no hydraulic head available from monitoring wells in the study area this approach was not taken for this study. A global average was considered a more optimal approach in relation to the distance between the study area and DINOLoket data used. Obtaining data on the hydraulic head in the sandy layer over time, in relation to a fixed reference point, would give the opportunity to reflect natural conditions more accurately in the model.

At the ditch boundaries constant water levels are applied for summer and winter whereas in reality the surface level can fluctuate. In De Wieden the surface water level is allowed to drop to -0.83 m NAP in summer when water shortage is high. The applied constant summer water level at -0.73 m NAP for the ditches consequently overestimates water levels during periods of high evapotranspiration compared to precipitation. Owning to the phreatic level and surface level being inherently linked (van Wirdum, 1990) the simulated phreatic levels could also be overestimated when precipitation deficit is high. This possible overestimation is important to consider when analysing the results.

Kragge System

In the developed model the implication of a moving and floating root mat is not explicitly considered. This while the root mat can move up to 30-90% of changes in surface water level (van Wirdum, 1990). This buoyancy of a root mat can affect water flow in the system by decreasing hydraulic gradients between the root mat and surface water level (Stofberg et al., 2016). To represent the natural environment floating characteristics are thus essential to consider. However, the simplification of steady root mat taken in this study could be regarded reasonable as Stofberg et al. (2016) found in their modelling study of the Nieuwkoopse Plassen that the phreatic levels relative to the surface remain relatively stable with buoyancy.

Calibration

In relation to the nature of the available data and limited unique data points quantitative calibration was not possible for this study. Model calibration using limited available measured data produces high parameters uncertainty (Brunetti et al., 2019). For future modelling the use of more comprehensive measured data sets is therefore recommended to obtain more certainty in the applied parameter values. Specifically, field scale data of hydraulic head, in relation to a fixed reference point, would be of interest to further calibrate the model more accurately to field conditions. A rigorous uncertainty assessment is also suggested to clarify which parameters affect the simulated patterns significantly. Such an assessment was not possible in this study due to time-limitations. As the model stands right now it might not represent the actual field conditions of De Wieden in detail. However, the main aspects of the hydrological conditions in De Wieden

region are likely incorporated sufficiently through the optimal use of available theoretical data points based on the wider region around the study area. The simulated results could therefore be used as an indicative representation of peatlands in De Wieden and as such give an indication on the whether the suppletion ditch would hold value.

Fieldwork Data

The material distribution of the model is based on nine drill logs mainly located in the middle of the transects. Due to the limited drill logs on the sides of the transect the material distribution at these locations was extrapolated. The slurry layer was not extended to the end of the transect as it was assumed that the slurry would gradually disappear near the edges of transect, similar to location W3-1 (Figure D.4). However, during fieldwork in October 2020 it became clear that the slurry might extend further than incorporated in the model, specifically on the right side of the domain. A longer slurry layer could influence the water flow of the system severely due to its high permeability. Currently, the model might underestimate the influence of the model. In regards to the suppletion ditch it could be that the similar conditions to Scenario 5, with direct connection to the slurry, would more readily occur with larger presence of the Slurry.

The calculated values for K_s based on the Auger-Hole measurements are influenced by measurements and calculation errors. As the rise of water was rapid it provided difficult to accurately measure the water level manually at small or constant intervals. This rapid rise is attributed to the presence of the Slurry layer of the slurry layer. Because the Slurry contributes to rapid flow of water towards the borehole the calculated K_s could be overestimated as based on the current measurements. Furthermore, the rapid inflow of water meant that the point after which 25% of removed water flowed back into the borehole was reached within 1-3 measurements. Consequently the calculated values might be unreliable. However, as the K_s found during fieldwork is used as a guideline and indicative value the effect of measurement errors on the suppletion ditch results presumably small.

7.2. Results

Phreatic Level

Literature indicates that the presence of ditches leads to lower phreatic levels (Bootsma et al., 2002; LaRose et al., 1997; Price et al., 2003; van Loon et al., 2009). For this study similar results are visible in the winter. However, in contrast to literature the model indicate a rise of phreatic level up to 19.8 cm in summer. Although these results seem at odds with previous studies it does fit with higher groundwater levels found when incorporating open-water reservoirs in peatlands (LaRose et al., 1997; Schlotzhauer & Price, 1999). Open-water reservoirs area areas of open water, such as a ditch, disconnected from surface water networks which limits their drainage effects (LaRose et al., 1997). Due to the high surface water level in the summer the suppletion ditch likely functions as an open-water reservoir, with limited drainage, in De Wieden. The found results from this study are attributed to the high surface water levels which generate a hydraulic gradient that incites lateral inflow of water towards the peat in summer. In peatland where the drainage effect of a suppletion ditch can be limited by high surface water levels a suppletion ditch thus has the potential to provide high phreatic surfaces in summer.

In relation to the possible overestimation of summer surface water levels the high phreatic levels are likely exacerbated in the results. For S1-4 on the left side of the suppletion ditch the phreatic levels remain below the lowest possible surface water level at all times in summer. Here a positive effect of the suppletion ditch is reasonable to expect even when considering a possible overestimation of surface water level in summer. For S5, and the location between the two ditches, surface water levels theoretically would only need to drop with 2.4 cm for drainage of water through the suppletion ditch to occur and the phreatic level to drop. The effect of a suppletion ditch at this location, and for S5, could thus be smaller than currently found for the summer.

Another reason for the positive effect of the suppletion ditch could be the relatively high permeability of the soil in the model. Other studies indicate intrusion of surface water from ditches to be limited to only 0.5-2 m away from the ditch (Beltman et al., 1996; Bootsma et al., 2002; van Loon et al., 2009). The limited intrusion is attributed to the low hydraulic permeability of peat (Bootsma et al., 2002; Price et al., 2003). For this study the influence of surface water is visible up to 10 m away from the suppletion ditch in the root-zone and up to 70 m in deeper layers. For the deeper layer the highly permeable Slurry layer provides rapid transport of water originating in the suppletion ditch into the domain. This is especially clear in the results of Scenario 5. The presence of a water-rich slurry layer could therefore be essential for the suppletion ditch to provide positive increases in phreatic level of a peatland.

However, similar positive effects for the application of a suppletion ditch in fen areas with a kragge system were not found in previous studies (Beltman et al., 1996; Bootsma et al., 2002). Instead the applied relatively high K_s for the Reed-Sedge peat could be a prominent factor in generating the positive effects of the suppletion ditch. Boelter (1972) found that in peats with higher permeabilities ditches showed a greater effect. The K_s of 15 m/d for Reed-Sedge allows water to enter the transect more easily, providing the possibility for more inflow of water from the suppletion ditch. The success of a potential ditch is thus not only related to the permeability of the Slurry layer but also the permeability of the surrounding peat. In peatlands with higher values for K_s, perhaps with lesser grades of humification, a suppletion ditch could provide the capacity to overcome desiccation issues.

Rainwater Presence

The lateral inflow of surface water into the transect leads to a diminished presence of rainwater in the root-zone for all scenarios, specifically in a region of 10 m around the ditch. A clear rainwater lens does not take shape, presumably because infiltration at the bottom boundary leads to overall downwards flow, giving shape to the funnel like pattern visible on the right of the suppletion ditch and to a lesser extent on the left side of the ditch. The implementation of a suppletion ditch does lead to an extension of the region for which rainwater is layered atop of base-rich surface water. As specifically the layering of rainwater and base-rich water is essential for high-quality bog woodland the suppletion ditch could be beneficial for bog woodland restoration.

Distance between ditches

The efficiency of drainage has been related to smaller distance between two ditches (Price et al., 2003). A similar effect of distance is visible in this study. On the right side of the suppletion ditch, where the distance between two ditches is 40 m, the phreatic level is higher in summer and lower in winter. Indicating that smaller distances between a suppletion ditch and existing ditch would be optimal.

Implications of bog woodland restoration

For the restoration of bog woodland vegetation in a suppletion ditch seems to have potential. Specifically for areas where high surface water levels and highly permeable layers occur, such as in De Wieden, a positive effect of a suppletion ditch is expected. All scenarios show higher summer phreatic levels within the required hydrological conditions of 0-60 cm below surface level. Additionally, the phreatic level becomes more stable in time which is more suitable for high-quality bog woodland vegetation. The soil moisture content at the soil surface also increases. Although a rainwater lens does not take shape layering of rainwater above surface water does become clearer along the transect, indicating suitable acidic conditions will prevail for bog woodland vegetation.

For the implementation the shape, width and depth, of the suppletion ditch has limited effects on the results. Rather, the implementation of the suppletion ditch in *direct* connection with the present slurry layer seems essential to obtain higher phreatic levels and soil moisture content along the full transect in summer. Construction of the suppletion in close vicinity of the Slurry

layer is thus recommended. This is further supported by the lower EC values found in the root-zone for this scenario.

The drainage effect of the ditch generates phreatic levels below the determined required hydrologic conditions, 0-20 cm, in winter. It is therefore proposed to block the suppletion ditch during periods of low surface water levels to limit loss of water from peat system. This would support the retention of water in the system and optimize the phreatic level to accomplish the required criteria.

8. Conclusion

The following answer to the question '*To what extent will a suppletion ditch create suitable hydrological conditions for the restoration of bog woodland based on hydrological modelling of De Wieden?*' was found: Based on the developed model the construction of a suppletion ditch will generate higher phreatic levels during summer within the required range for bog woodland vegetation. In winter the suppletion ditch leads to drainage of water, generating lower phreatic levels unsuitable for bog woodland vegetation. As such blocking of the suppletion ditch in winter is recommended. A rainwater lens, essential for high-quality birch woodland vegetation, does not take shape when constructing a suppletion ditch. Although the presence of a suppletion ditch does lead to a layering of rainwater atop surface water for at least part of the transect, indicating suitable acidic conditions would occur at the soil surface. However, in the vicinity of the suppletion ditch influence of surface water in the root-zone could have negative effects on vegetation patterns.

Overall, the findings of this report provide the insights that a suppletion ditch could have positive effects on the hydrological conditions of a peatlands. The positive effect is mostly attributed to the high surface water levels occuring in De Wieden in summer and the high permeability of the peat surrounding the suppletion ditch, including a water-rich slurry layer, and high surface water levels in summer. This implies that a suppletion ditch holds potential to support peatlands with a floating root mat and high surface water levels in overcoming the effects of desiccation.

9. References

Amoozegar, A., & Warrick, A. W. (1986). Hydraulic Conductivity of Saturated Soils: Field Methods. In *Hydraulic conductivity of saturated soils: field methods. Methods of Soil Analysis: Part 1 Physical and Mineralogical Methods* (2nd Editio, pp. 735–770). American Society of Agronomy - Soil Science Society of America. https://doi.org/10.2136/sssabookser5.1.2ed.c29

Bal. D (2001). *Handboek Natuurdoeltypen.* Expertisecentrum Ministerie van Landbouw, Natuurbeheer en Visserij, Wageningen.

Baird, A. J., Surridge, B. W. J., & Money, R. P. (2004). An assessment of the piezometer method for measuring the hydraulic conductivity of a Cladium mariscus - Phragmites australis root mat in a Norfolk (UK) fen. *Hydrological Processes*, *18*(2), 275–291. https://doi.org/10.1002/hyp.1375

Batu, V., & van Genuchten, M. Th. (1990). First- and Third-Type Boundary Conditions in Two-Dimensional Solute Transport Modeling. *Water Resources Research*, *26*(2), 339–350.

Beltman, B., van den Broek, T., Bloemen, S., & Witsel, C. (1996). Effects of restoration measures on nutrient availability in a formerly nutrient-poor floating fen after acidification and eutrophication. *Biological Conservation*, *78*(3), 271–277. https://doi.org/10.1016/S0006-3207(96)00052-3

Błażejewski, R., Nieć, J., Murat-Błażejewska, S., & Zawadzki, P. (2018). Comparison of infiltration models with regard to design of rectangular infiltration trenches. *Hydrological Sciences Journal*, *63*(11), 1707–1716. https://doi.org/10.1080/02626667.2018.1523616

Blokland, K. A., & Kleijberg, R. J. M. (1997). *De gewenste grondwatersituatie voor terrestrische natuurdoelen: holoceen Nederland*. STOWA.

Boelter, D. H. (1972). Water Table Drawdown Around an Open Ditch in Organic Soils. *Journal of Hydrology*, *15*(4), 329–340.

Bootsma, M. C., van den Broek, T., Barendregt, A., & Beltman, B. (2002). Rehabilitation of acidified floating fens by addition of buffered surface water. *Restoration Ecology*, *10*(1), 112–121. https://doi.org/10.1046/j.1526-100X.2002.10112.x

Branham, J. (2013). *Spatial variability of soil hydrophysical properties in Canadian Sphagnum dominated peatlands (Unpublished Master's Thesis)*. University of Calgary, Calgary, AB. https://doi.org/10.11575/PRISM/27846

Brunetti, G., Kodešová, R., & Simunek, J. (2019). Modeling the Translocation and Transformation of Chemicals in the Soil-Plant Continuum: A Dynamic Plant Uptake Module for the HYDRUS Model. *Water Resources Research*, *55*(11), 8967–8989. https://doi.org/10.1029/2019WR025432

Brunetti, G., Šimůnek, J., & Bautista, E. (2018). A hybrid finite volume-finite element model for the numerical analysis of furrow irrigation and fertigation. *Computers and Electronics in Agriculture*, *150*(May), 312–327. https://doi.org/10.1016/j.compag.2018.05.013

Carsel, R. F., & Parrish, R. S. (1988). Developing joint probability distributions of soil water retention characteristics. *Water Resources Research*, *24*(5), 755–769. https://doi.org/10.1029/WR024i005p00755

Casparie, W. A., & Streefkerk, J. G. (1992). Climatological, stratigraphic and palaeo-ecological aspects of mire development. In J. T. A. Verhoeven (Ed.), *Fens and Bogs in the Netherlands* (pp. 81–129). Kluwer Academic Publishers.

Cusell, C., de Haan, B., Kooijman, G., van Dijk, G., van Diggelen, J. M. H., & Kooijman, A. (2018). Roadmap voor herstel Weerribben-Wieden. *Landschap*, *35*(2), 111–117.

Cusell, C., & Mandemakers, J. (2017). *PAS-onderzoek M1 naar defosfatering in de Wieden en Weerribben*.

de Waal, R. W., & Hommel, P. W. F. M. (2005). *Abiotische typering van bostypen in Nederland*.

Dekker, S. C., Barendregt, A., Bootsma, M. C., & Schot, P. P. (2005). Modelling hydrological management for the restoration of acidified floating fens. *Hydrological Processes*, *19*(20), 3973–3984. https://doi.org/10.1002/hyp.5864

Diek, R., Schep, S., & Pelsma, T. (2014). Flexibeler peil Naardermeer beter voor hoogveenbossen. *H2O-Online*, *1410–11*(november), 1–11.

Dorland, E., Gijsbert, C., & Witte, J. P. M. (2015). *Verband tussen stijghoogte en grondwaterstand in schijnspiegelsystemen* (Issue April).

Dotinga, F., & Bodde, M. (2018). *Plan-Mer De Wieden*.

European Environment Agency (2019a, March 15th). *Natura 2000 – Standard Form: De Wieden.* http://natura2000.eea.europa.eu/Natura2000/SDF.aspx?site=NL2003064.

Goudie, A. (2013). *Encyclopedia of geomorphology* (Vol. 2). Routledge.

Heij, G. J. (1984). Schatting van de Hydraulische Weerstand van Slechtdoorlatende Lagen. *H2O*, *17*(14).

Hoogendoorn, J. H., & Vernes, R. W. (1994). *Hydrologische Systeemanalyse Noordwest Overijssel*.

Hopmans, J. W., & Stricker, J. N. M. (1989). Stochastic analysis of soil water regime in a watershed. *Journal of Hydrology*, *105*(1–2), 57–84. https://doi.org/10.1016/0022-1694(89)90096-6

Jalink, M. H., Grijpstra, J., & Zuidhoff, A. C. (2003). Hydro-ecologische systeemtypen met natte schraallanden in Pleistoceen Nederland. In *Rapport / EC-LNV;nr. 2003/225 O* (Issue september).

Joris, I., & Feyen, J. (2003). Modelling water flow and seasonal soil moisture dynamics in analluvial groundwater-fed wetland. *Hydrology and Earth System Sciences*, *7*(1), 57–66. https://doi.org/10.5194/hess-7-57-2003

Kacimov, A. R., Obnosov, Y. v., & Šimůnek, J. (2020). Seepage to ditches and topographic depressions in saturated and unsaturated soils. *Advances in Water Resources*, *145*(May). https://doi.org/10.1016/j.advwatres.2020.103732

Kellner, E. (2007). *Effect of Variations in Hydraulic Conductivity and Flow Conditions on Groundwater Flow and Solute Transport*.

KNMI. (n.d.-a). *Hoogeveen, langjarige gemiddelden, tijdvak 1981-2010*. http://www.klimaatatlas.nl/tabel/stationsdata/klimtab_8110_279.pdf

KNMI. (n.d.-b). *Meetstation Hoogeveen, Maandoverzicht Neerslag en Verdamping in Nederland 2015-2019*. Retrieved November 3, 2020, from https://www.knmi.nl/nederland-nu/klimatologie/gegevens/monv

Kooijman, A., Cusell, C., Loeb, R., & van Diggelen, J. M. H. (2018). Mesotrofe verlanding en behoud van trilvenen. *Landschap*, *35*(2), 83–91.

Lamers, L. P. M., Geurts, J. G. M., van Schie, J. M., van Dijk, G., Barendregt, A., Mettrop, I. (Ivan S.), Moria, L., Fritz, C., Roelofs, J. G. M., Smolders, A. J. P., & Rip, W. J. (2018). Waterkwaliteit en biodiversiteit in het laagveenlandschap. *Landschap*, *35*(2), 95–103.

Lamers, L. P. M., Smolders, A. J. P., & Roelofs, J. G. M. (2002). The restoration of fens in the Netherlands. *Hydrobiologia*, *478*, 107–130. https://doi.org/10.1023/A:1021022529475

LaRose, S., Price, J., & Rochefort, L. (1997). Rewetting of a cutover peatland: Hydrologic assessment. *Wetlands*, *17*(3), 416–423. https://doi.org/10.1007/BF03161431

Maltby, E., & Dugan, P. J. (1994). Wetland ecosystem protection, management, and restoration: an international perspective. In *Everglades: The ecosystem and its restoration* (pp. 29–46). CRC Press.

Mars, H. de. (1996). *Chemical and physical dynamics of fen hydro-ecology*. Koninklijk Nederlands Aardrijkskundig Genootschap.

Massop, H. Th. L., van der Gaast, J. W. J., & Kiestra, E. (2005). *De doorlatendheid van de bodem voor infiltratiedoeleinden*.

Mettrop, I. (Ivan S.). (2015). *Water level fluctuations in rich fens: an assessment of ecological benefits and drawbacks*. Universiteit van Amsterdam.

Ministerie van LNV. (2006). ** Veenbossen (H91D0)*.

Mitsch, W. J., & Gosselink, J. G. (2000). The value of wetlands: importance of scale and landscape setting. *Ecological Economics*, *35*, 25–33. www.elsevier.com/locate/ecolecon

Morris, P. J., Belyea, L. R., & Baird, A. J. (2011). Ecohydrological feedbacks in peatland development: A theoretical modelling study. *Journal of Ecology*, *99*(5), 1190–1201. https://doi.org/10.1111/j.1365-2745.2011.01842.x

Mualem, Y. (1976). A New Model for Predicting the Hydraulic Conductivity of Unsaturated Porous Media. *Water Resources Research*, *12*(3), 513–522.

Naghedifar, S. M., Ziaei, A. N., & Naghedifar, S. A. (2019). Optimization of Quadrilateral Infiltration Trench Using Numerical Modeling and Taguchi Approach. *Journal of Hydrologic Engineering*, *24*(3), 04018069. https://doi.org/10.1061/(asce)he.1943-5584.0001761

Natuurmonumenten. (n.d.). *Kanoroute Dwarsgracht in De Wieden*. Natuurmonumenten. Retrieved November 3, 2020, from https://www.natuurmonumenten.nl/natuurgebieden/nationaal-park-weerribben-wieden/route/kanoroute-dwarsgracht-in-de-wieden

Natuurmonumenten. (2019). *PAS maatregel in Natura-2000 gebied De Wieden - M2A Onderzoeksmaatregel Behoud Hoogveenbos*. Natuurmonumenten.

Oosterbaan, R. J., & Nijland, H. J. (1994). Determining the Saturated Hydraulic Conductivity. In H. P. Ritzema (Ed.), *Drainage Principles and Applications.* (2nd ed.). International Institute for Land Reclamation and Improvement (ILRI).

PC-Progress. (2019). *FAQ 21-30. 30. Maximum number of optimized parameters*. https://www.pc-progress.com/en/Default.aspx?h3d-faq-21-30

Pons, L. J. (1992). Holocene peat formation in the lower parts of the Netherlands. In J. T. A. Verhoeven (Ed.), *Fens and Bogs in the Netherlands* (pp. 7–79). Kluwer Academic Publishers.

Price, J. S., Heathwaite, A. L., & Baird, A. (2003). Hydrological processes in abandoned and restored peatlands. *Wetlands and Ecological Management*, *11*, 65–83.

Provincie Overijssel. (2017). *Natura 2000-beheerplan definitief: De Wieden en Weerribben*.

Quinton, W. L., Hayashi, M., & Carey, S. K. (2008). Peat hydraulic conductivity in cold regions and its relation to pore size and geometry. *Hydrological Processes*, *22*, 2829–2837. https://doi.org/10.1002/hyp.7027

Rijksdients voor Ondernemend Nederland. (2015). *Best Practice Proceswater*.

Runhaar, J., Lucassen, E. C. H. E. T., Smolders, A. J. P., Verdonschot, R. C. M., & Hommel, P. W. F. M. (2013). *Herstel broekbossen* (Issues 2013/OBN169-BE).

Rycroft, D. W., Williams, D. J. A., & Ingram, H. A. P. (1975). The Transmission of Water Through Peat : *Journal of Ecology*, *63*(2), 535–556.

Schlotzhauer, S. M., & Price, J. S. (1999). Soil Water Flow Dynamics in a Managed Cutover Peat Field, Quebec: Field and Laboratory Investigations. *Water Resources Research*, *35*(12), 3675–3683.

Schot, P. P., Dekker, S. C., & Poot, A. (2004). The dynamic form of rainwater lenses in drained fens. *Journal of Hydrology*, *293*(1–4), 74–84. https://doi.org/10.1016/j.jhydrol.2004.01.009

Schwärzel, K., Šimůnek, J., Stoffregen, H., Wessolek, G., & van Genuchten, M. Th. (2006). Estimation of the Unsaturated Hydraulic Conductivity of Peat Soils: Laboratory versus Field Data. *Vadose Zone Journal*, *5*(2), 628–640. https://doi.org/10.2136/vzj2005.0061

Šejna, M., Šimůnek, J., & van Genuchten, M. Th. (2014). *The HYDRUS Software Package for Simulating the Two- and Three-Dimensional Movement of Water, Heat, and Multiple Solutes in Variably-Saturated Porous Media*.

Šimůnek, J. [Jirka] (2020a). *Concentration Vertical Pattern* [Discussion Forum Post]. PC-Progress Discussion Forums. Obtained from: https://www.pc-progress.com/forum/viewtopic.php?f=3&t=3729&p=13738#p13738

Šimůnek, J. [Jirka] (2020b). *Constant Head BC Ditch & Fluctuating GWT* [Discussion Forum Post]. PC-Progress Discussion Forums. https://www.pc-progress.com/forum/viewtopic.php?f=3&t=3621&p=13371#p13371

Šimůnek, J., & de Vos, J. A. (1999). Inverse optimization, calibration and validation of simulation models at the field scale. In *Modelling transport processes in soils at various scales in time and space.* (pp. 431–445).

Šimůnek, J., & Šejna, M. (2009). Notes on Spatial and Temporal Discretization (when working with HYDRUS). In *PC-Progress* (pp. 1–18). http://www.pc-progress.com/Images/Pgm_Hydrus3D2/Notes_on_Spatial_and_Temporal_Discretization.pdf

Šimůnek, J., & Šejna, M. (2018). *Solute Transport Boundary Conditions*. PC-Progress.

Šimůnek, J., van Genuchten, M. Th., & Šejna, M. (2012a). Hydrus: Model use, calibration, and validation. *Transactions of the ASABE*, *55*(4), 1261–1274.

Šimůnek, J., van Genuchten, M. Th., & Šejna, M. (2012b). *The HYDRUS Software Package for Simulating the Two- and Three-Dimensional Movement of Water, Heat, and Multiple Solutes in Variably-Saturated Porous Media*.

Spieksma, J. F. M., & Schouwenaars, A. J. D. J. M. (1997). De verdamping van natuurterreinen. *Stromingen*, *0317*.

Stofberg, S. F., van Engelen, J., Witte, J. P. M., & van der Zee, S. E. A. T. M. (2016). Effects of root mat buoyancy and heterogeneity on floating fen hydrology. *Ecohydrology*, *9*(7), 1222–1234. https://doi.org/10.1002/eco.1720

Streefkerk, J. G., & Casparie, W. A. (1989). The Hydrology of Bog Ecosystems. *Guidlines for Management*. https://doi.org/10.1017/CBO9781107415324.004

Sutanto, S. J., Wenninger, J., Coenders-Gerrits, A. M. J., & Uhlenbrook, S. (2012). Partitioning of evaporation into transpiration, soil evaporation and interception: A comparison between isotope measurements and a HYDRUS-1D model. *Hydrology and Earth System Sciences*, *16*(8), 2605–2616. https://doi.org/10.5194/hess-16-2605-2012

Thomassen, E., Jaspers, D., van der Burg, R., & Weerksink, H. (2008). *Op weg naar Natuurbossen: Ontwikkelingsplan natuurbos in Noord-Brabant*.

TNO Geologische Dienst Nederland. (2020a). *Isohypsen & Grondwaterdynamiek*. Grondwatertools. https://www.grondwatertools.nl/grondwatertools-viewer

TNO Geologische Dienst Nederland. (2020b). *Ondergrondgegevens*. DINOLoket. Data En Informatie van de Nederlandse Ondergrond. https://www.dinoloket.nl/ondergrondgegevens

van Beers, W. (1983). The Auger Hole Method. A field measurement of the hydraulic conductivity of soil below the water table. *International Institute for Land Reclamation and Improvement*, 23.

van der Kooij, C. A. (1997). *Abiotiek in oude elzenbroekbossen*.

van der Sluijs, W. J., & Tigchelaar, D. (2012). *Hoogveenbos in de Wieden: Ontwikkeling van het Zompzegge-berkenbroekbos*.

van Loon, A. H., Schot, P. P., Bierkens, M. F. P., Griffioen, J., & Wassen, M. J. (2009). Local and regional impact of anthropogenic drainage on fen contiguity. *Hydrology and Earth System Sciences*, *13*(10), 1837–1848. https://doi.org/10.5194/hess-13-1837-2009

van 't Veer, R., Geel, B. van, Pals, J. P., & Smeerdijk, D. (2000). Fossiele plantengemeenschappen als referentiekader voor moderne moerasontwikkeling. In J. H. J. Schamineé & R. van 't Veer (Eds.), *De geschiedenis van de plantensociologie in Nederland* (Issue September 2019, pp. 174–188). Opules Press Nederland.

van Vliet, C. J. M., Bos, F., & van Duinhoven, G. (2017). *De kennis van het lage land*. OBN/VBNE.

van Wirdum, G. (1990). *Vegetation and hydrology of floating rich-fens*. Datawyse.

Verhoeven, J. T. A. (1992). Fens and Bogs in the Netherlands. In *Fens and Bogs in the Netherlands*. Springer Netherlands. https://doi.org/10.1007/978-94-015-7997-1

Waterschap Drents Overijsselse Delta. (2020). *Toelichting herziening Peilbesluit Boezem van Noordwest Overijssel*.

Waterschap Reest en Wieden. (2007). *Watergebiedsplan boezem NWO (ontwerp)*.

Wiegers, Jaap. (1985). *Succession in fen woodland ecosystems in the Dutch Haf District : with special reference to Betula pubescens Ehrh*. J. Cramer.

Youngs, E. G., & al Jabri, S. A. (2018). Transient Water-Table Recession in Drained Lands Modeled Using HYDRUS and Compared with Theoretical Analyses Assuming a Succession of Momentarily Steady States . *Journal of Irrigation and Drainage Engineering*, *144*(1), 04017054. https://doi.org/10.1061/(asce)ir.1943-4774.0001263

Appendix

Appendix A: DINOLoket Data

Through the DINOLoket of the TNO Geologische Dienst Nederland several drill logs on the lithostratigraphy and lithology were obtained for monitoring wells in the vicinity of the study area (Figure A. 1). Additionally, data on the hydraulic head was obtained for several of these monitoring wells. The wells were at a minimal distance of approximately 2 km away from the study areas. The 15 selected wells were picked because they are located within the N2000 protected area of De Wieden. Each well was ascribed a number, as visible in Figure A. 1, for easy reference.

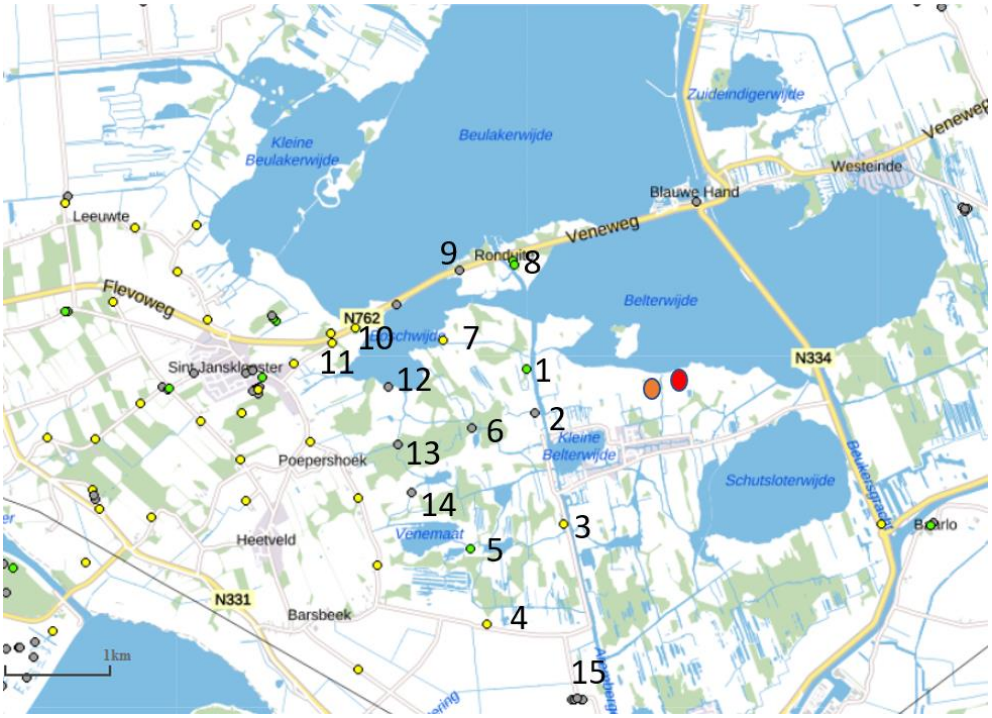

Figure A. 1: Location of the data obtained from DINOLoket (Adapted from TNO Geologische Dienst Nederland, 2020b*). The two circles indicate the location of the study areas, the orange circle is the Gezensloot location and the red circle the Klaverkooi.*

A.I: Drill Logs

The depth of the drill logs is in meters in reference to NAP. For the drill logs the following two keys are used:

Lithology:

- Clay
- Sand, fine
- Sand, medium
- Sand, coarse
- Gravel
- Peat
- Unkown
- Plants

Lithostratigraphy:

- Anthropogenic
- Formation of Nieuwkoop
- Formation of Naaldwijk
- Formation of Boxtel
- Formation of Kreftenheye
- Formation of Urk

Point 1
B21B0776

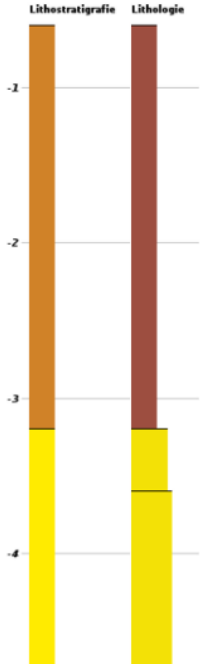

B21B04050

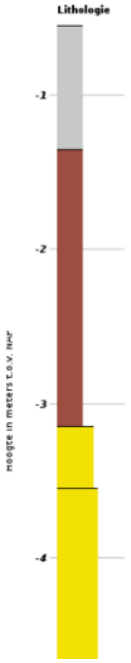

Point 2
B21B0746

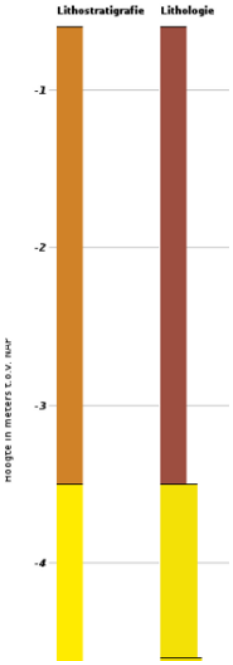

B21B0453

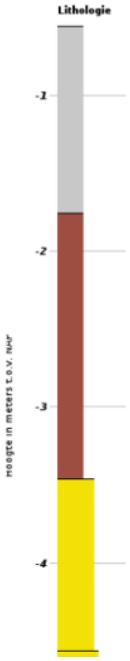

Point 3
B21E0396

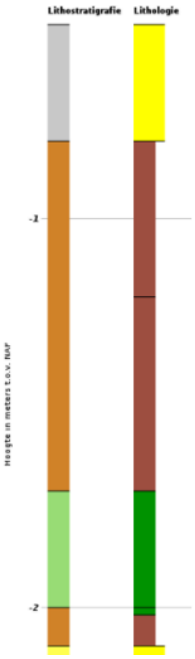

Point 4
B21B0694

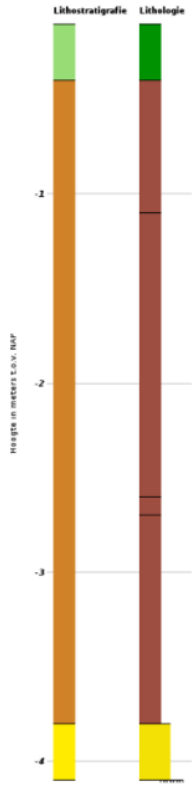

Point 5
B21B0458

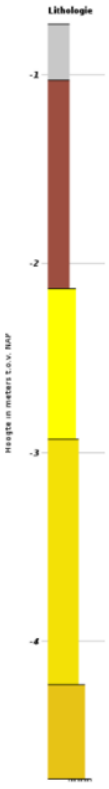

B21B0734

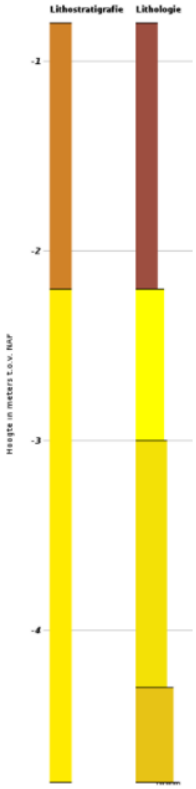

Point 6
B21B0454

B21B0744

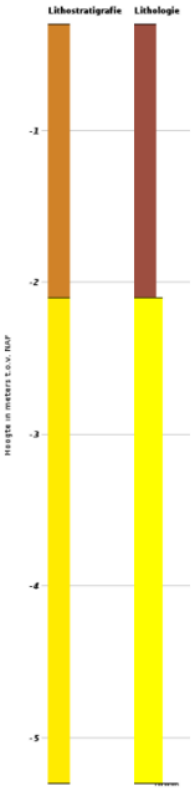

Point 7
B21B0774

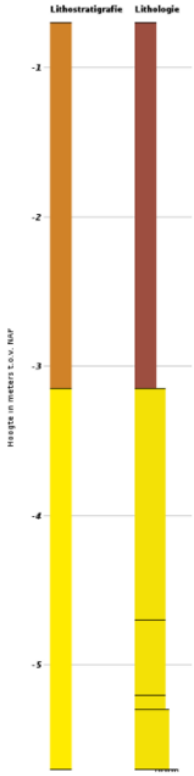

B21B0451

Point 8o
B21B0447

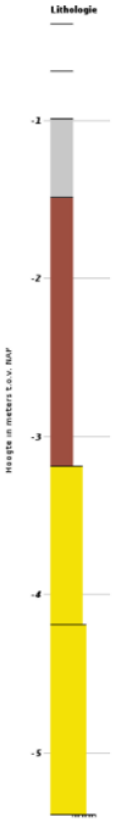

B21B0799

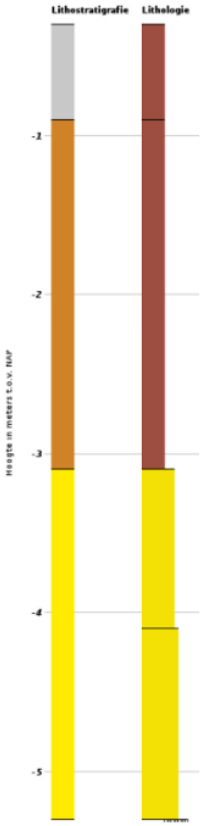

Point 9
B21B0798

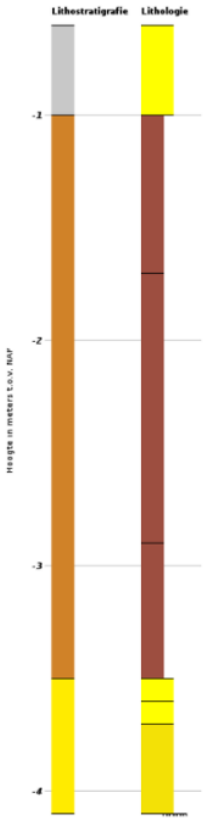

Point 12
B21B0773

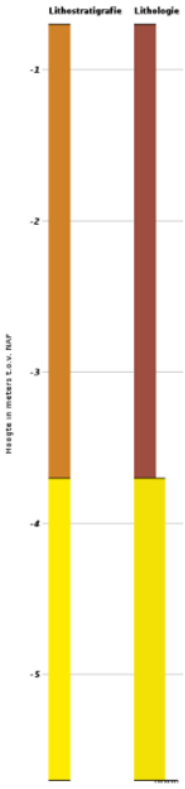

B21B0452

Point 13
B21B0455

Point 14
B21B0456

Point 15
B21E0252

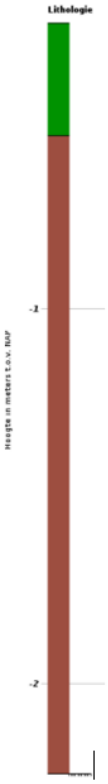

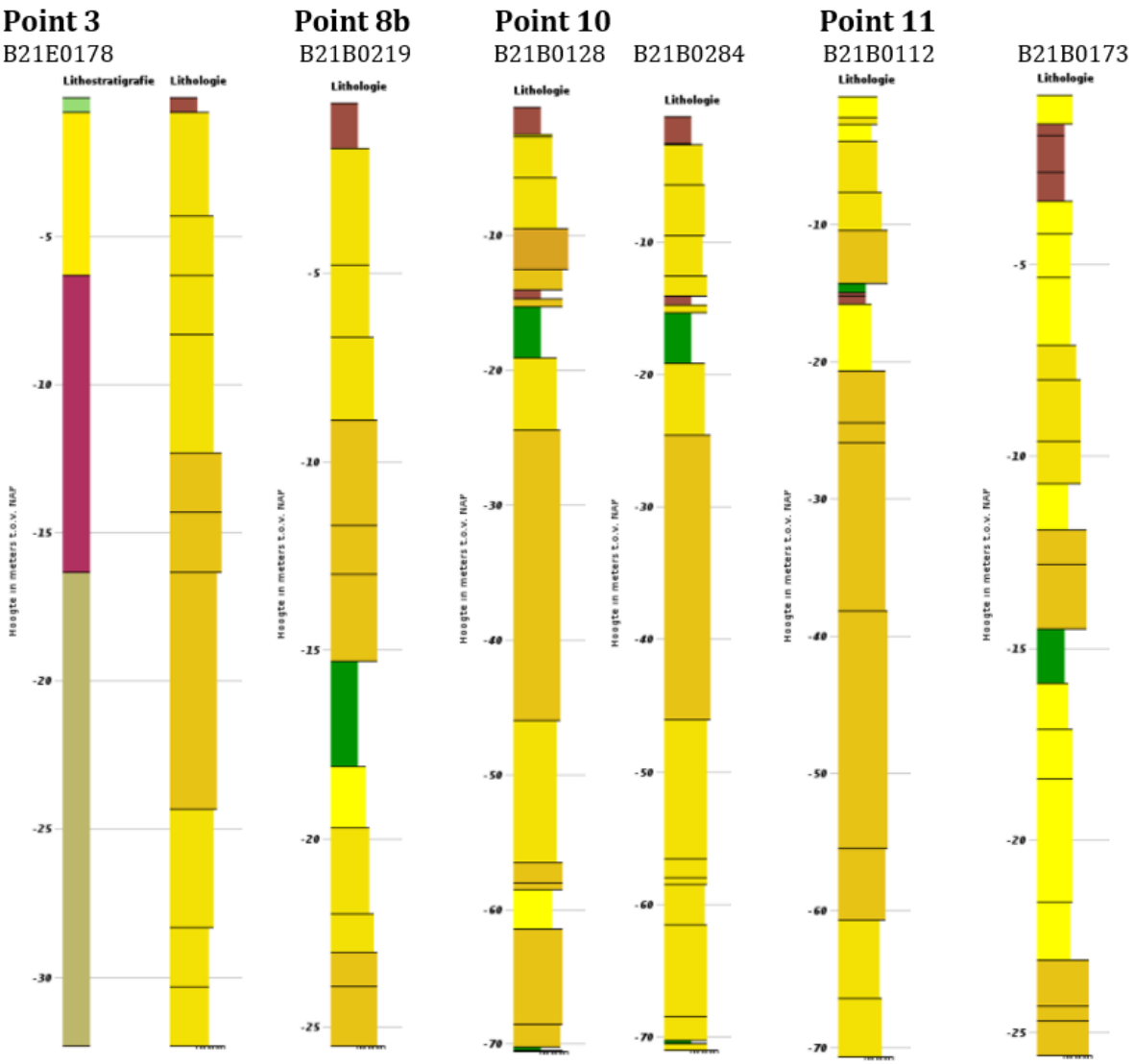

A.II: Hydraulic head

The median hydraulic head, as available through TNO Geologische Dienst Nederland (2020a), for all monitoring wells from Figure A. 1 is visualized in Figure A.2. Based on this graph the hydraulic head at the *constant head boundary condition* in the HYDRUS-2D model was set at -1.1 m NAP. This decision was based on the cluster of median heads in the vicinity of -5 m NAP.

For two points, 1 and 2, the hydraulic head can be found in Figure A.3. These two points were selected as they are closest to the study areas and their soil profile is similar to the profile found during fieldwork in De Wieden. For point 1 the filter depths are, respectively, -1.38 m and -4.7 m below NAP for filter 001 and 002. Filter 001 and 002 for point 2 are located at -1.24 and -4.53 m NAP. The selected hydraulic head for the model, at a depth of -4.4 m NAP was set at -1.10 m NAP. The graph indicates infiltration from the upper layers towards the lower monitoring wells occurs. Additionally, the hydraulic head of the deeper filters fluctuates at depths of -1.0 to -1.1 m NAP, indicating the selected constant head is a suitable approximation.

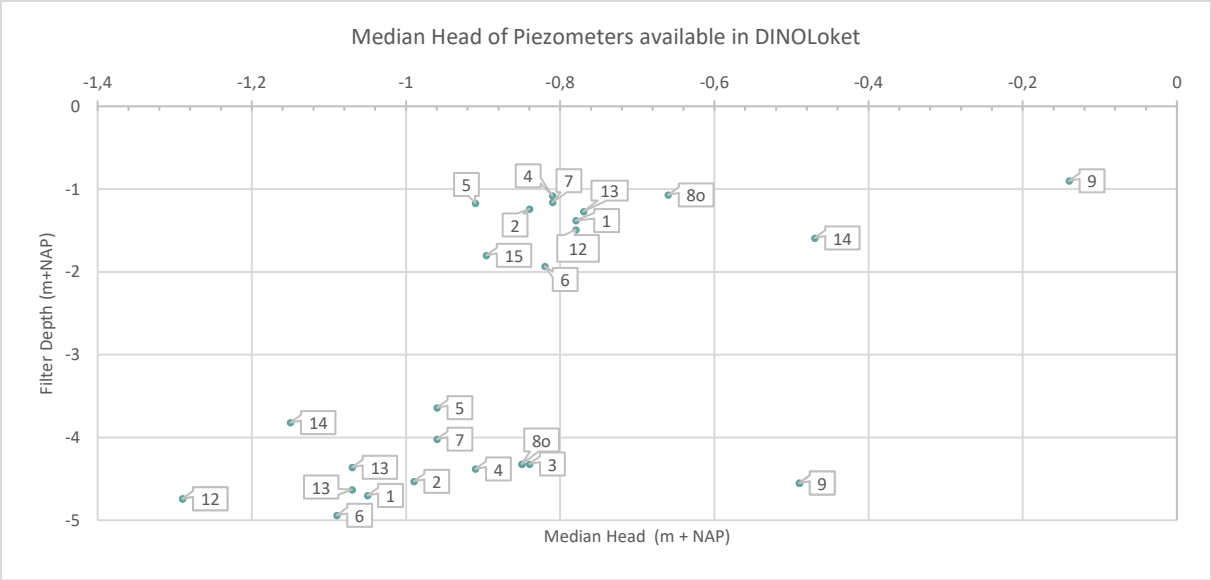

Figure A.2: Median Hydraulic Head provided for the monitoring wells studied from DINOLoket. The numbers in the labels indicate the monitoring well location. At -5 m NAP a hydraulic head approximation of -1.1 m NAP was applied since of the expected hydraulic head at this location in relation to the cluster of measured hydraulic head in this region.

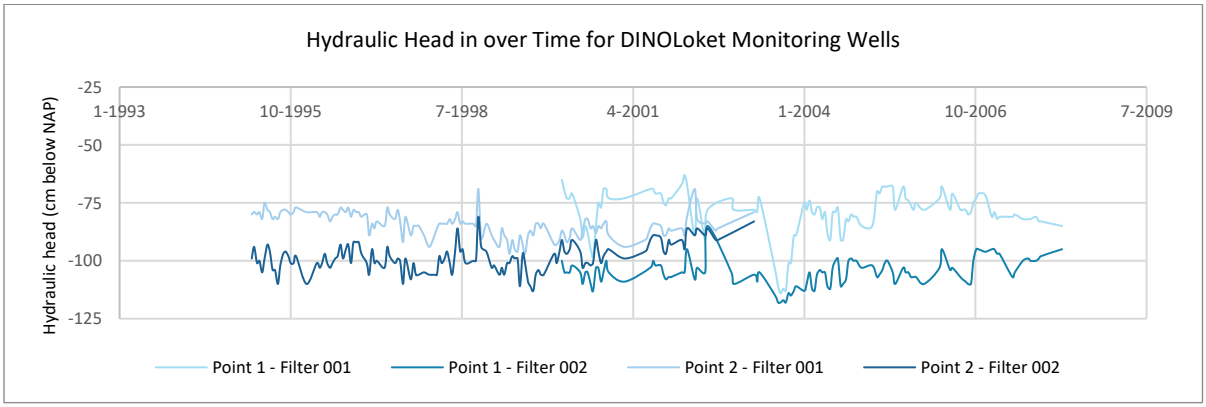

Figure A.3: Hydraulic head for two piezometer nests from the monitoring wells nearest to the study areas. For Point 1 the filter depths are -1.38 m NAP for 001 and -4.70 m NAP for 002. For Point 1 the filter depths are -1.24 m NAP for 001 and -4.53 m NAP for 002. The figure indicates the hydraulic head in the shallower filters, in the peat, is higher compared to the deeper filters in the sand, indicating infiltration.

Appendix B. Model Detail

B.I: Constructed Suppletion Ditches

In Figure B.1 the extension of the Slurry layer for the implementation of a suppletion ditch into the Slurry layer for Scenario 5 can be seen. On all sides of the suppletion Ditch a small Reed-Sedge layer of 10 cm was incorporated in order to obtain model convergence.

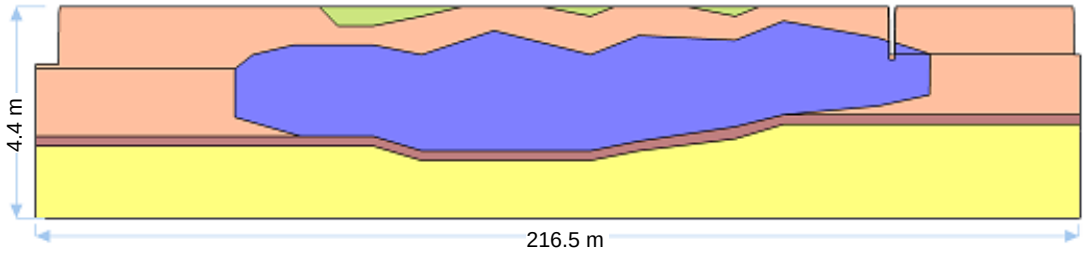

Figure B.1: Overview of the model domain with an extended slurry layer for Scenario 5 of the suppletion ditch, in which the slurry is direct contact with the suppletion ditch. The domain is stretched in the z-direction with a factor 10.

Appendix C: Soil Hydraulic Parameters Data

Through a literature analysis values for all van Genuchten-Mualem parameters for each soil type were obtained. In the collection of the data no differentiation in regard to manner of data collection of the study, e.g. fieldwork or laboratory data, nor location of the studied peatland were made. The obtained data is summarized in Table C.1, used parameters are in bold face.

Figure C.1 shows the soil moisture content curves for the different layers incorporated in the model. For model convergence the curve of the Sphagnum was adjusted to fit with the reference curve (C.1c) by changing the soil hydraulic parameters to the same values as applied for the Reed-Sedge Peat. Although the curves do not fit entirely with the general curve of peat it is estimated that the curves from C.1b fit to a reasonable degree.

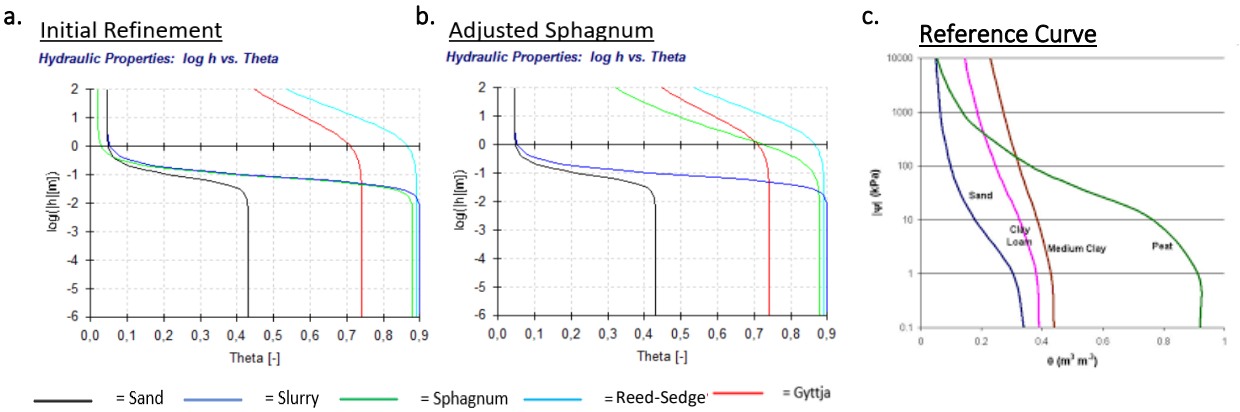

Figure C.1: Soil Moisture Content curve for a. the model using the initial parameters as determined by Dorland et al. (2015), b. adjusted sphagnum parameters to obtain a soil moisture content curve more in line with c. a general peat curve (obtained from Choler, 2013).

Table C.1: Soil Hydraulic parameters for Sand

Source	Soil Type	Soil Description	Parameter				
			Ks (m/d)	θr (-)	θs (-)	n	α (1/m)
Van Wirdum, 1990	Peat	Firm peat, mineral soil	1				
Van Wirdum, 1990	Peat	Floating raft	>75				
Van Wirdum, 1990	Peat	Just underneath kragge	>400				
Van Wirdum, 1990	Peat	Peat mud	1-10				
"doorlatendheid k.", 2020	Peat		0.001-0.1				
"doorlatendheid k.", 2020	Peat	clayey	0.005				
Schot et al., 2014	Peat		0.5-5	**0.045**		2.68	14.5
Stofberg et al., 2016	Peat	Floating Raft	0.001-10				
Baird et al., 2014	Peat	Floating Raft	*1.2 – 25.9*				
Koerselman et al., 1989	Peat	Floating Raft	*60-65*				
Kellner, 2007	Peat	Organic Layer	*Variable*	0.078	0.5	3.6	1.56
Branham, 2013	Sphagnum		0.001-100				
Dekker et al., 2005	Sphagnum	Floating Raft	1-100		0.7		
Da Silva et al., 1993	Sphagnum		70				
Dorland et al., 2015	Sphagnum	Non-humified	10	0.02	**0.88**	**2.82**	**47**
Dorland et al., 2015	Sphagnum	Humified	1	0.02	0.92	2.82	10
Dorland et al., 2015	Sphagnum	Strongly humified	0.02	0.07	0.93	1.38	1.59
Schwärzel et al., 2006	Reed-Sedge	Humified peat, compacted	*0.01*		**0.741**	**1.15**	**0.5**
Schwärzel et al., 2006	Reed-Sedge	Very humified, compacted	*0.07*		0.73	1.12	1.2
Schwärzel et al., 2006	Reed-Sedge	Very humified	*0.14*		0.797	1.23	2
Schwärzel et al., 2006	Reed-Sedge	Weakly humified	*1.04*		**0.891**	**1.16**	**0.3**
Doll & Schneider, 1995	Gyttja		*0.0004- 0.0009*				
Malloy & Price, 2017	Gyttja		*0.0001-0.041*				
Malloy & Price, 2017	Peat/Gyttja		*0.001*				
Ferone & Devito, 2004	Gyttja		*0,000864-0.00864*				
Kishel & Gerla, 2002	Gyttja		*0.086-8.6*				
"doorlatendheid k.", 2020	Sand	Fine	1-10				
Dorland et al., 2015	Sand	Medium fine	*0.67*	0.02	0.36	2.29	2.24
"doorlatendheid k.", 2020	Sand	Very Coarse	80				
"doorlatendheid k.", 2020	Sand	Extremely Coarse	200				
"doorlatendheid k.", 2020	Sand	Coarse	30				
Carsel and Parrish, 1988	Sand	USDA Sand	7.12	0.045	**0.43**	**2.68**	**0.145**
Schaap et al., 2001	Sand		6.43	0.053	0.375	3.18	0.035
Smedema & Rycroft, 1983	Sand	Coarse	10-50				
Smedema & Rycroft, 1983	Sand	Medium	1-5				

References:

Choler, P. (2013). 3. The Soil Water Balance [powerpoint]. Retrieved from: http://www.philippe-choler.com/resources/Choler_Ecohydrology_Part3.pdf

Doll, P., & Schneider, W. (1995). Lab and field measurements of the hydraulic conductivity of clayey stilts. *Ground Water*, *33*(6), 884-892.

doorlatendheid k. (2020). Retrieved June 5, 2020, from http://www.grondwaterformules.nl/index.php/vuistregels/ondergrond/doorlatendheid-per-grondsoort

Dorland, E., Gijsbert, C., & Witte, J. P. M. (2015). *Verband tussen stijghoogte en grondwaterstand in schijnspiegelsystemen*. Nieuwegein, The Netherlands.

Baird, A. J., Surridge, B. W. J., & Money, R. P. (2004). An assessment of the piezometer method for measuring the hydraulic conductivity of a Cladium mariscus - Phragmites australis root mat in a Norfolk (UK) fen. *Hydrological Processes*, *18*(2), 275–291. https://doi.org/10.1002/hyp.1375

Koerselman, W., Caluwe, H. de & Kieskamp, W.M. (1989). Denitrification and dinitrogen fixation in two quacking fens in the Vechtplassen area, the Netherlands. *Biogeochemistry, 8,* 153-165.

Ferone, J. M., & Devito, K. J. (2004). Shallow groundwater–surface water interactions in pond–peatland complexes along a Boreal Plains topographic gradient. *Journal of Hydrology*, *292*(1-4), 75-95.

Kellner, E. (2007). *Effects of variations in hydraulic conductivity and flow conditions on groundwater flow and solute transport in peatlands* (No. SKB-R--07-41). Swedish Nuclear Fuel and Waste Management Co..

Kishel, H. F., & Gerla, P. J. (2002). Characteristics of preferential flow and groundwater discharge to Shingobee Lake, Minnesota, USA. *Hydrological Processes*, *16*(10), 1921-1934.

Malloy, S., & Price, J. S. (2017). Consolidation of gyttja in a rewetted fen peatland: Potential implications for restoration. *Mires & Peat*, *19*.

Schot, P. P., Dekker, S. C., & Poot, A. (2004). The dynamic form of rainwater lenses in drained fens. *Journal of Hydrology*, *293*(1–4), 74–84. https://doi.org/10.1016/j.jhydrol.2004.01.009

Schwärzel, K., Šimůnek, J., Stoffregen, H., Wessolek, G., & van Genuchten, M. T. (2006). Estimation of the Unsaturated Hydraulic Conductivity of Peat Soils: Laboratory versus Field Data. *Vadose Zone Journal*, *5*(2), 628–640.

Smedema, L. K., & Rycroft, D. W. (1983). *Land drainage: planning and design of agricultural systems.* Batsford Academic and Educational Ltd.

van Wirdum, G. (1990). *Vegetation and hydrology of floating rich-fens*. Maastricht: Datawyse.

Malloy, S., & Price, J. S. (2017). Consolidation of gyttja in a rewetted fen peatland: Potential implications for restoration. *Mires & Peat*, *19*.

da Silva, F. F., Wallach, R., & Chen, Y. (1993). Hydraulic properties of sphagnum peat moss and tuff (scoria) and their potential effects on water availability. *Plant and Soil*, *154*(1), 119–126. https://doi.org/10.1007/BF00011080

Branham, J. (2013). *Spatial variability of soil hydrophysical properties in Canadian Sphagnum dominated peatlands* (Unpublished master's thesis). University of Calgary, Calgary, AB. https://doi.org/10.11575/PRISM/27846

Dekker, S. C., Barendregt, A., Bootsma, M. C., & Schot, P. P. (2005). Modelling hydrological management for the restoration of acidified floating fens. *Hydrological Processes*, *19*(20), 3973–3984. https://doi.org/10.1002/hyp.5864

Stofberg, S. F., van Engelen, J., Witte, J. P. M., & van der Zee, S. E. A. T. M. (2016). Effects of root mat buoyancy and heterogeneity on floating fen hydrology. *Ecohydrology*, *9*(7), 1222–1234. https://doi.org/10.1002/eco.1720

Appendix D: Fieldwork Results

D.I: Fieldwork Drill Logs

The borehole logs were taken from 9-10 March 2020 at locations in Figure D.1.

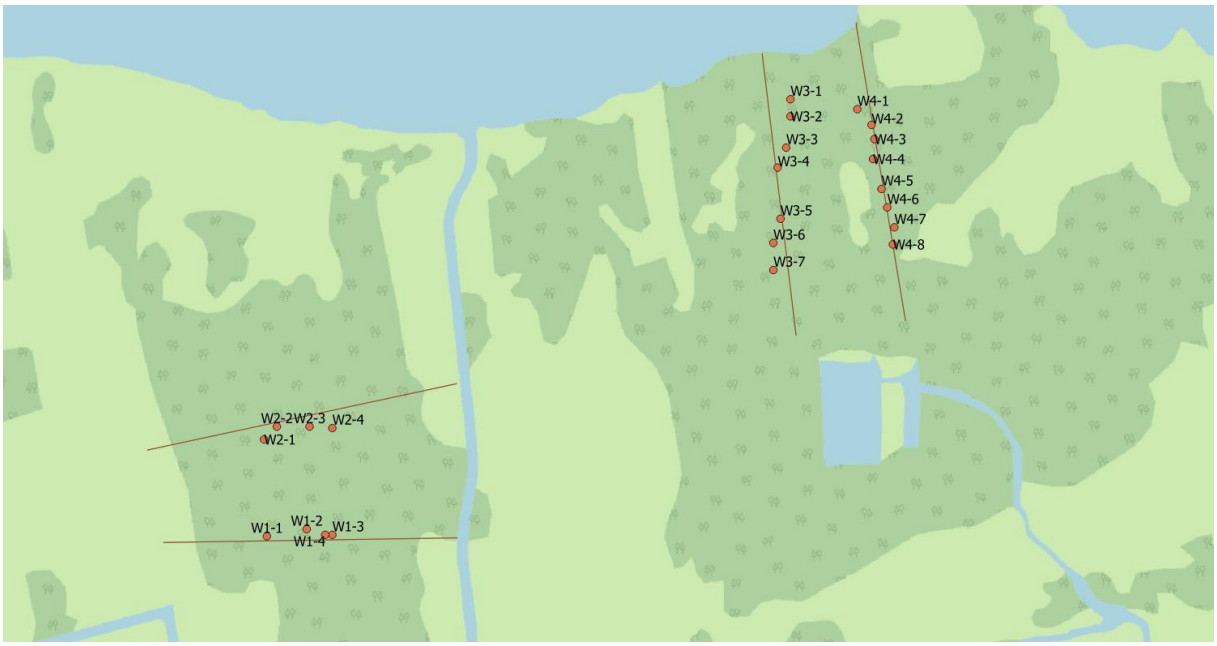

Figure D.1: Indication of the location of the borehole logs taken during fieldwork in March. The red line indicates the transects as presented throughout this study.

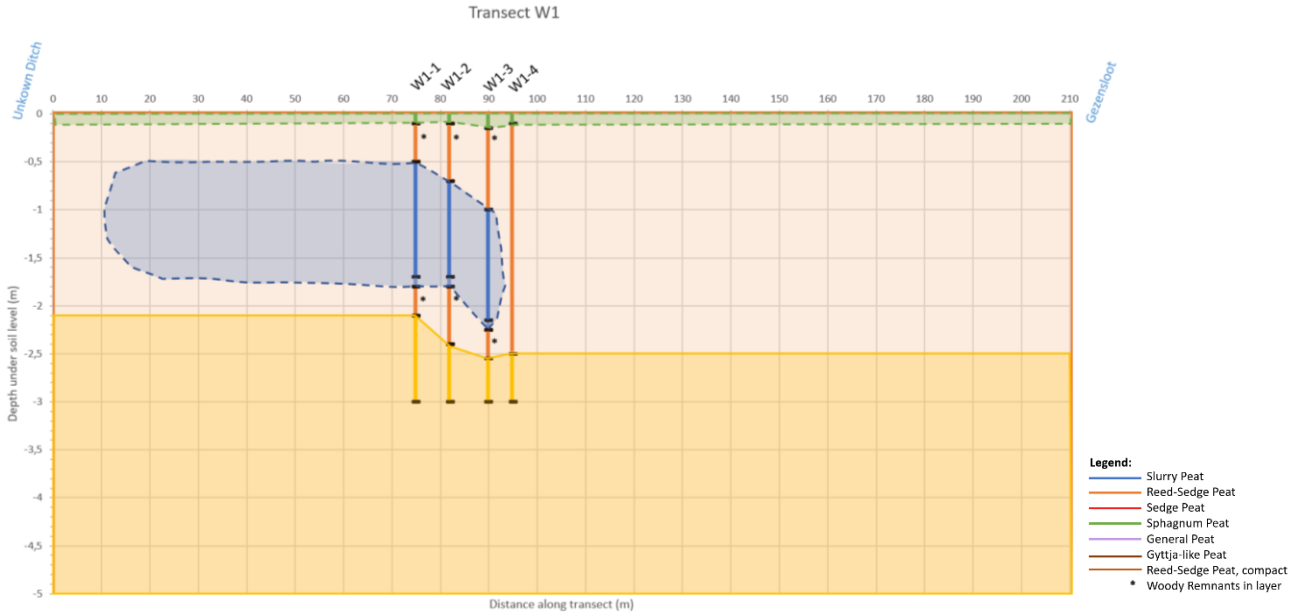

Figure D.2: Borehole logs and estimation soil profile across transect W1.

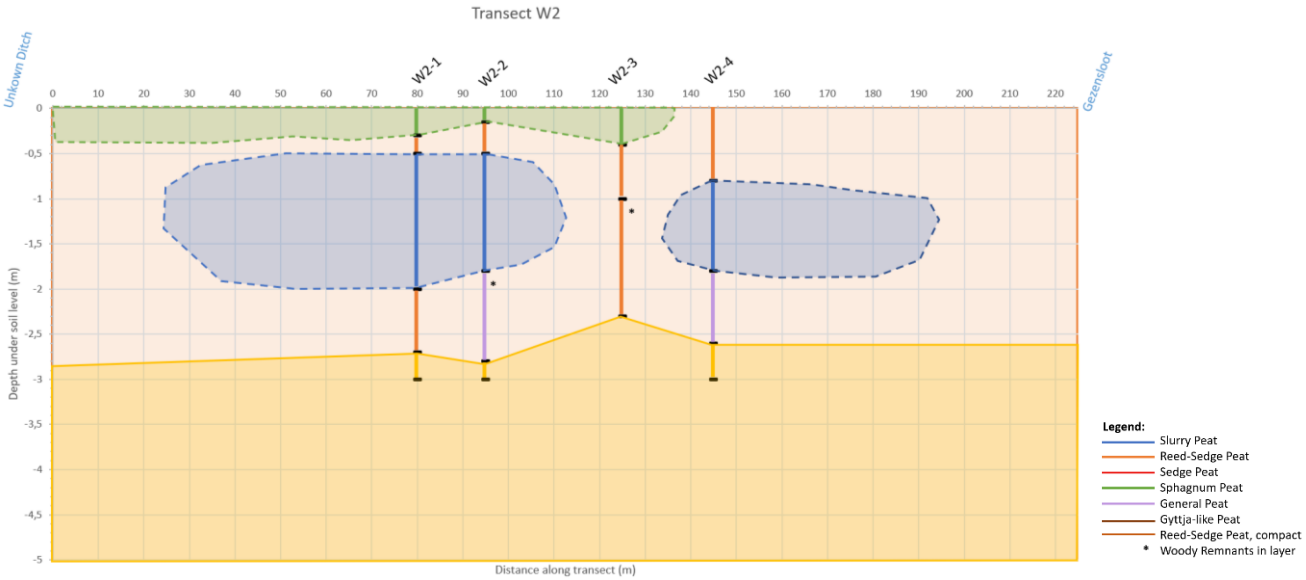

Figure D.3: Borehole logs and estimation soil profile across transect W2

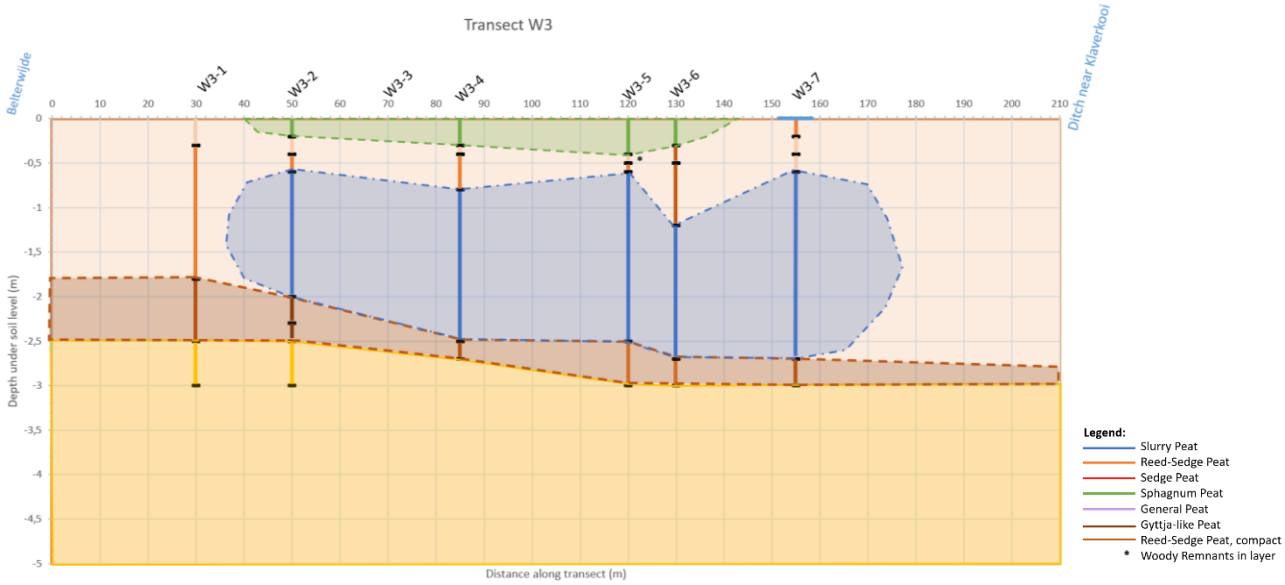

Figure D.4: Borehole logs and estimation soil profile across transect W3.

D.II: Electrical Conductivity

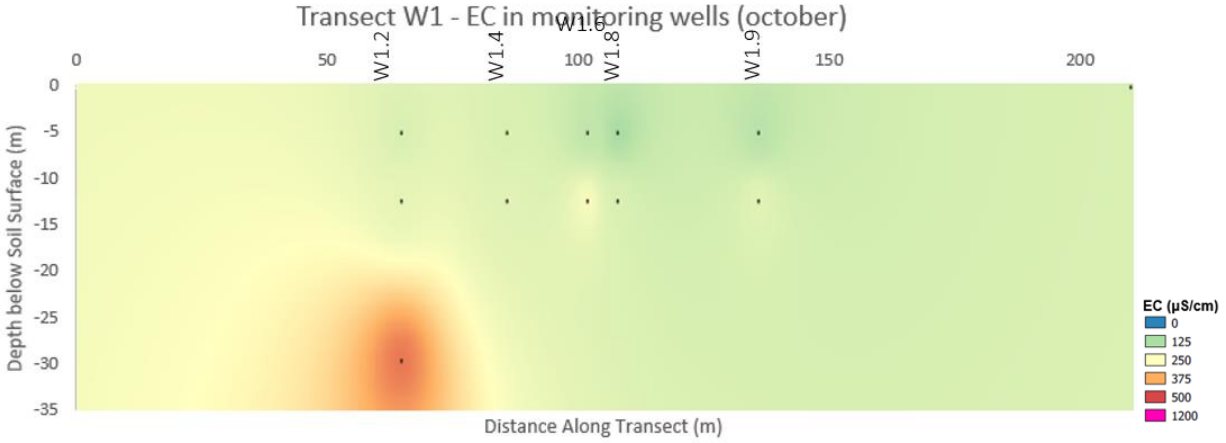

Figure D.5: Electrical Conductivity interpolated from measurements in the monitoring wells along transect W1 in October. The black dots represent the location of the well filters.

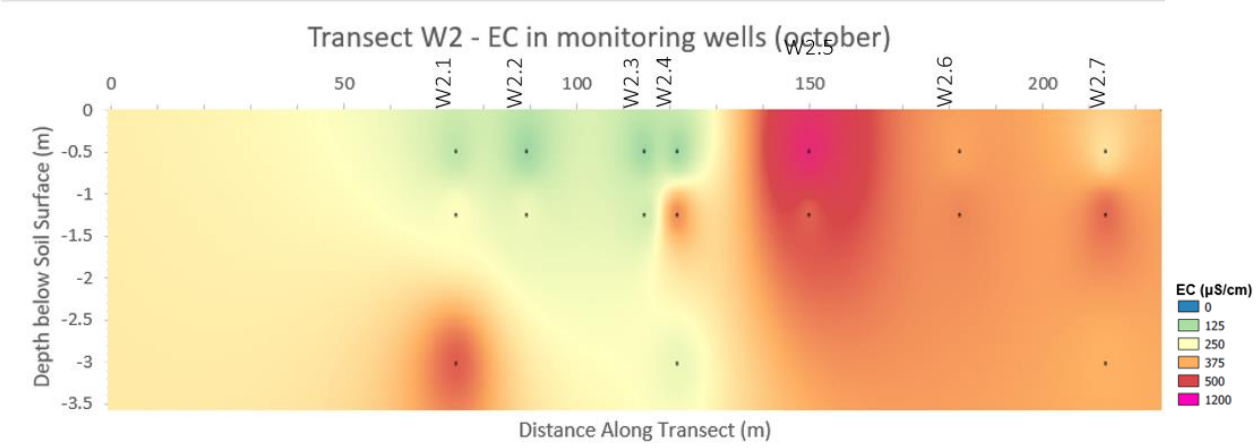

Figure D.6: Electrical Conductivity interpolated from measurements in the monitoring wells along transect W2 in October. The black dots represent the location of the well filters.

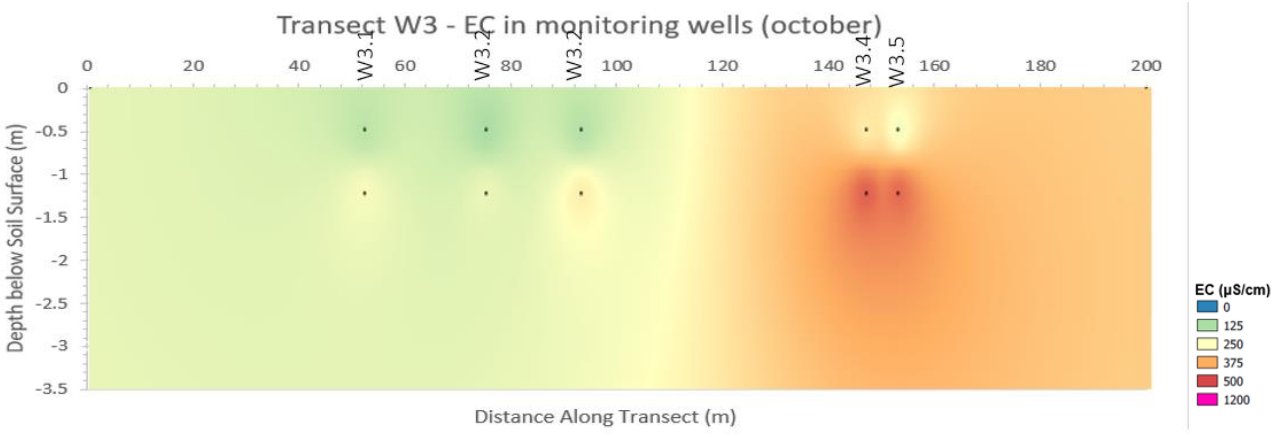

Figure D.7: Electrical Conductivity interpolated from measurements in the monitoring wells along transect W3 in October. The black dots represent the location of the well filters.

D.III: Monitoring Wells – Groundwater flow Direction

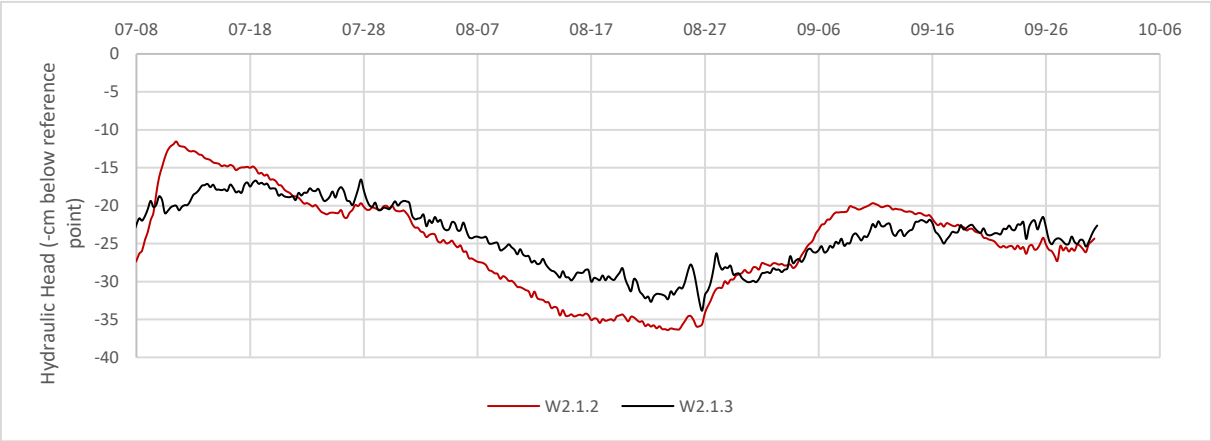

Figure D. 8: Piezometric head data from two divers located along transect W2 illustrating the occurrence of infiltration of upward seepage. The hydraulic heads measurements of the divers were adjusted to the height of monitoring well W2 – 1.3 above the surface and as such can be compared. The wells filters are located at 1.2 = -1.25 m below the surface and 1.3 = -3 m below the surface (in sand).

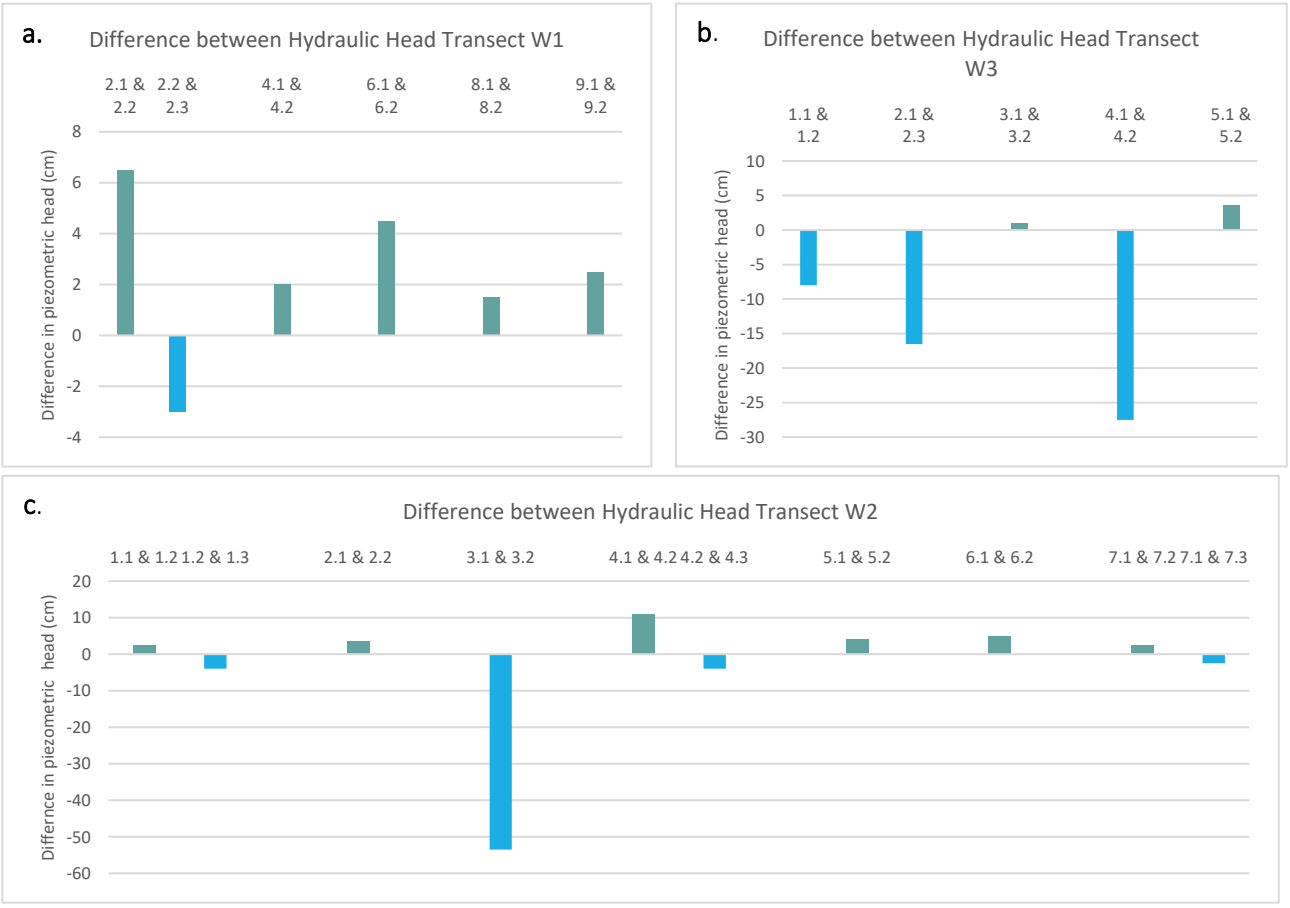

Figure D.9: Difference between the piezometric head of two filters indicating whether infiltration or upward seepage occurs at the well location. The piezometric head was measured on the 30th of September. a. Head differences for transect W1, b. Head differences for transect W3, b. Head differences for transect W2. Negative number (blue) indicates infiltration while a positive number (green) indicates upwards seepage. The hydraulic heads were adjusted using as reference the monitoring well extending the furthest above the surface. The hydraulic head is thus not comparable between locations, only flow direction at each location can be used. The wells filters are located at x.1 = -0.5 m below the surface, x.2 = -1.25 m below the surface and x.3 = -3 m below the surface (in sand).

D.IV: Hydraulic Conductivity

Calculation

At six locations auger hole measurements were taken. Three of these locations were near the placed monitoring wells. The last two measurements (W4-6 and W4-7) were taken on the other side of the proposed location for the future suppletion ditch (next to W4-5). The location of the measurements

The data of these measurements can be found in Table D.2-6. Using the data from these tables and the following formula the hydraulic conductivity at each location was calculated:

$$K_s = \frac{4000r^2}{(H + 20r)\left(2 - \frac{y}{H}\right)y}\frac{\Delta y}{\Delta t}$$

For the calculation of the conductivity it is important to take only the measurements into account until $\Delta y = ¼\ y_0$. For the found data this occurred quite rapidly, within two to three measurements, therefore the aim of a minimum of 5 measurements could not be achieved. For the calculation of the K_s the first three observations were used for all locations to limit the variability in approach taken. The calculated values can be found in Table D.1.

Table D.1: Used parameters for the calculation of the hydraulic conductivity

Location	Measurement	Parameter					
		¼ y0	Yav	Δt	Δy	C	Ks
W4-2	1	0.625	1.75	30	1.5	95.17	4.76
	2	0.5	1.25	20	1.5	132.57	9.94
W4-3	1	1.2	4.1	38	1.4	62.60	2.31
	2	1.25	4	15	2	64.10	8.55
W4-5	1	0.2	0.7	20	0.2	229.0728	2.29
	2	0.25	1	22	0.4	160.81	2.92
W4-6	1	0.5	3	65	-2	49.85	-1.53
	2	0.25	-0.15	41	1.5	-966.61	-35.90
	3	1.375	4.75	50	1.5	31.74	0.95
W4-7	1	0.75	2.5	28	1	60.23	2.15
	2	0.75	2	46	2	74.98	3.26

From the calculations it is visible that during the measurements some errors likely occurred for measurement W4-6 1 and 2 as the hydraulic conductivity is calculated to be negative. These values are there for not further considered.

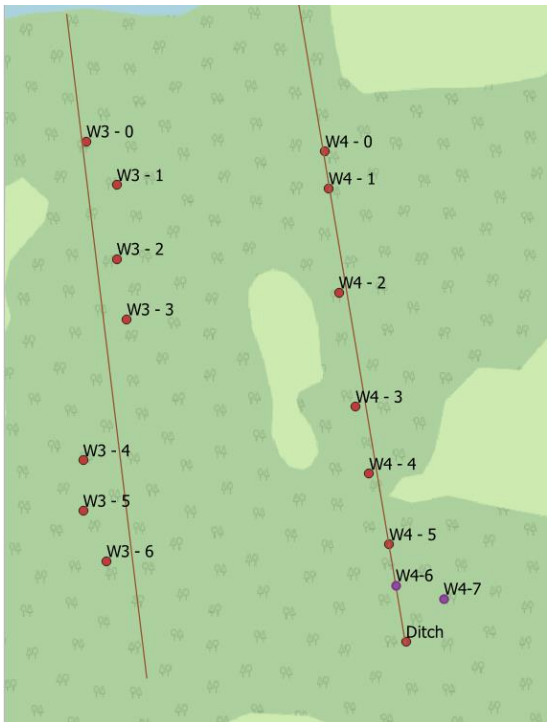

Figure Figure D.10: The location of the Auger-Hole Measurement refers to the position of the monitoring wells along transect W4. At Point W4-6 and W4-7 for the Auger-Hole measurements, indicated by purple dots, monitoring wells do not occur.

Used Data

Table D.2: Measurements W4-2								
Location	*W4-2*							
Measurement			1			*2*		
Data	*D =*	*80*	*t*	*dn*	*yn*	*t*	*dn*	*yn*
	W =	30	10	32.5	2.5	0	?	?
	H =	50	20	31.5	1.5	20	32	2
	r =	3	40	31	1	30	30.7	0.7
			60	31.3	1.3	40	30.5	0.5
			70	31.1	1.1	55	30.3	0.3
			78	30.8	0.8	80	30.3	0.3
			110	30.6	0.6	100	30.2	0.2
			144	30.5	0.5	120	30.2	0.2

Table D.3: **Measurements W4-3**								
Location	*W4-3*							
Measurement			*1*			*2*		
Data	*D =*	*80*	*t*	*dn*	*yn*	*t*	*dn*	*yn*
	W =	30	12	34.8	4.8	15	35	5
	H =	50	25	34.4	4.3	25	34	4
	r =	4	50	33.4	3.4	30	33	3
			70	33	3	55	32.5	2.5
			85	32.8	2.8	67	32	2
			110	32	2	78	31.6	1.6
			135	31.4	1.4	90	31.2	1.2
			165	31	1	106	31	1
			190	30.6	0.6	134	30.8	0.8
			240	30.5	0.5	150	30.5	0.5
			250	30.4	0.4	180	30.4	0.4
			260	30.3	0.3	205	30.3	0.3
			310	30.3	0.3	240	30.25	0.25
						265	30.2	0.2

Table D.4: **Measurements W4-5**								
Location	*W4-5*							
Measurement			*1*			*2*		
Data	*D =*	*70*	*t*	*dn*	*yn*	*t*	*dn*	*yn*
	W =	17	10	17.8	0.8	10	18.2	1.2
	H =	53	20	17.7	0.7	25	18	1
	r =	3	30	17.6	0.6	32	17.8	0.8
			45	17.5	0.5	45	17.3	0.6
			58	17.4	0.4	60	17.4	0.4
			82	17.2	0.2	77	17.35	0.35
			95	17.1	0.1	93	17.3	0.3
			110	17.1	0.1	105	17.3	0.3
			139	17.05	0.05	185	17.15	0.15
			150	17	0	215	17.1	0.1
			200	17	0	175	17.1	0.1

Table D.5: **Measurements W4-6**											
Location	*W4-6*										
Measurement			*1*			*2*			*3*		
Data	*D =*	*80*	*t*	*dn*	*yn*	*t*	*dn*	*yn*	*t*	*dn*	*yn*
	W =	16	0	18	2	17	17	1	10	21.5	5.5
	H =	64	30	18	2	35	16.5	0.5	30	20	4
	r =	3	65	20	4	58	15.5	-0.5	60	20	4
			85	19	3	70	15.2	-0.8	70	19.5	3.5
			100	18.5	2.5	80	14.8	-1.2	90	19.2	3.2
			160	17.5	1.5	110	14.8	-1.2	120	19.1	3.1
			220	16.5	0.5	120	14.8	-2	150	19.1	3.1
			310	16.5	0.5	240	14	-2.5	170	19	3
						290	13.5		200	19	3
									240	19	3

Table D.6: **Measurements W4-7**								
Location	W4-7							
Measurement			1			2		
Data	D =	80	t	dn	yn	t	dn2	yn
	W =	18	5	21	3	10	21	3
	H =	62	21	20.5	2.5	25	20.2	2.2
	r =	3	33	20	2	56	19	1
			52	19.3	1.3	60	19	1
			60	19	1	180	19	1
			87	18.4	0.4	220	18.8	0.8
			115	18.4	0.4	250	18.8	0.8
			125	18.2	0.2			
			168	18.1	0.1			
			220	18	0			
			260	18.3	0.3			

Appendix E: Results Simulation Suppletion Ditch

E.I: Phreatic Level Along the Transect

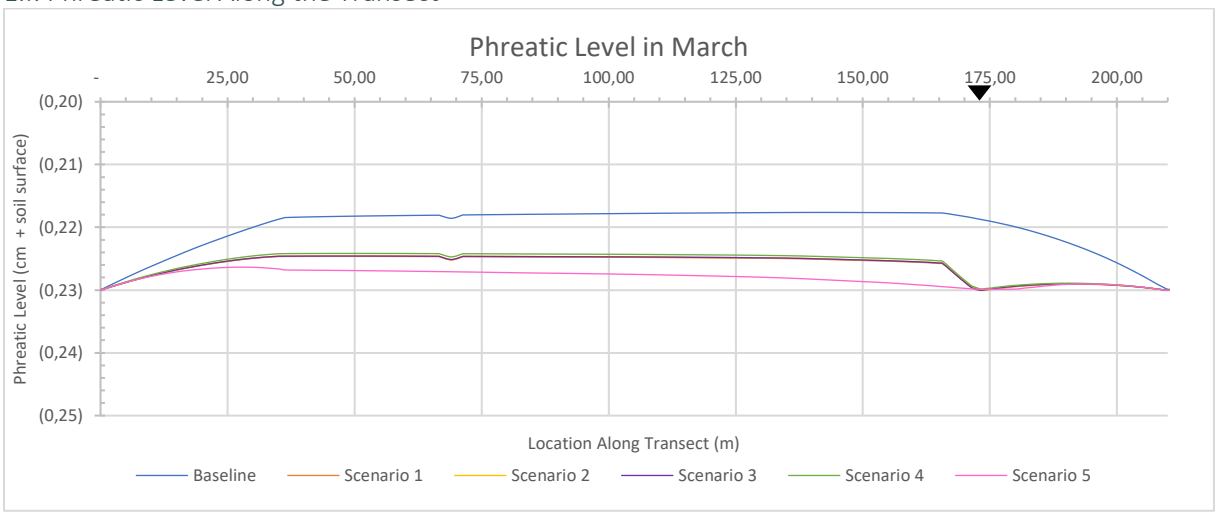

Figure E.1: Phreatic Level along the full length of the transect simulated for March 2019. The Beulakerwijde is located at 0 m while the secondary ditch at the end of the transect is located at 210 m. The location of the suppletion ditch is indicated by a black triangle. The graph shows a small decrease in phreatic level occurs for all suppletion ditch scenarios; this decrease is largest (0.8 cm) for Scenario 5 in which the slurry layer is connected to the suppletion ditch. Notable the decrease is larger on the right of the suppletion ditch for all scenarios.

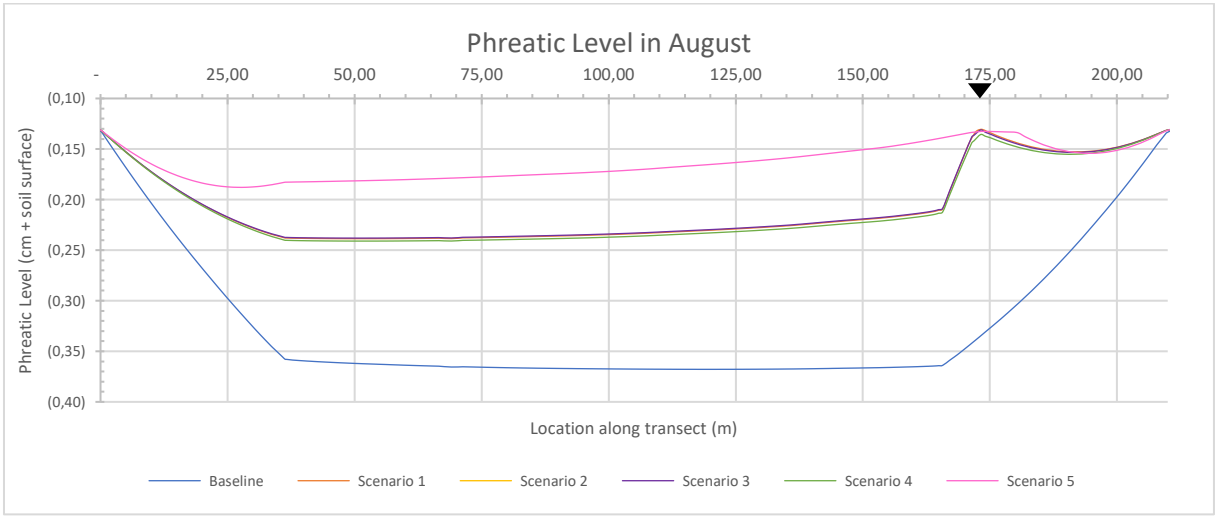

Figure E. 2: Phreatic Level along the full length of the transect simulated for August 2019. De Beulakerwijde is located at 0 m while the secondary ditch at the end of the transect is located at 210 m. The location of the suppletion ditch is indicated by a black triangle. The figure indicates an increase in phreatic level occurs along the full length of the transect for all suppletion ditch scenarios but is most prominent for Scenario 5 (20 cm). On the right side of the suppletion ditch the increase is larger for all scenarios.

E.II: Simulated Electrical Conductivity

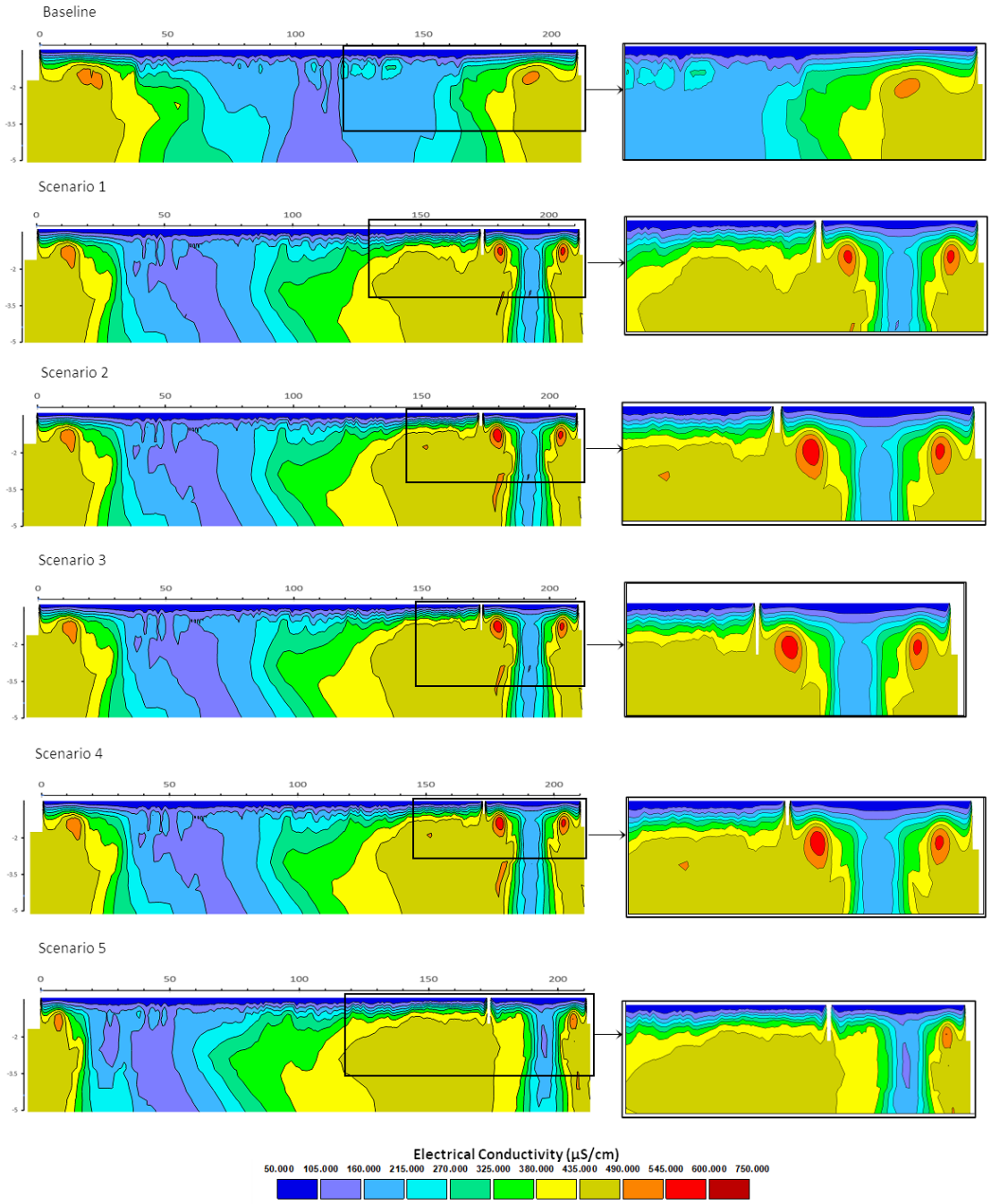

Figure E.3: Simulated Electrical Conductivity along the transect in March 2019 for all scenarios. On the left side the full side is represented. While the right side gives a closer look at the EC patterns in the vicinity of the suppletion ditch.

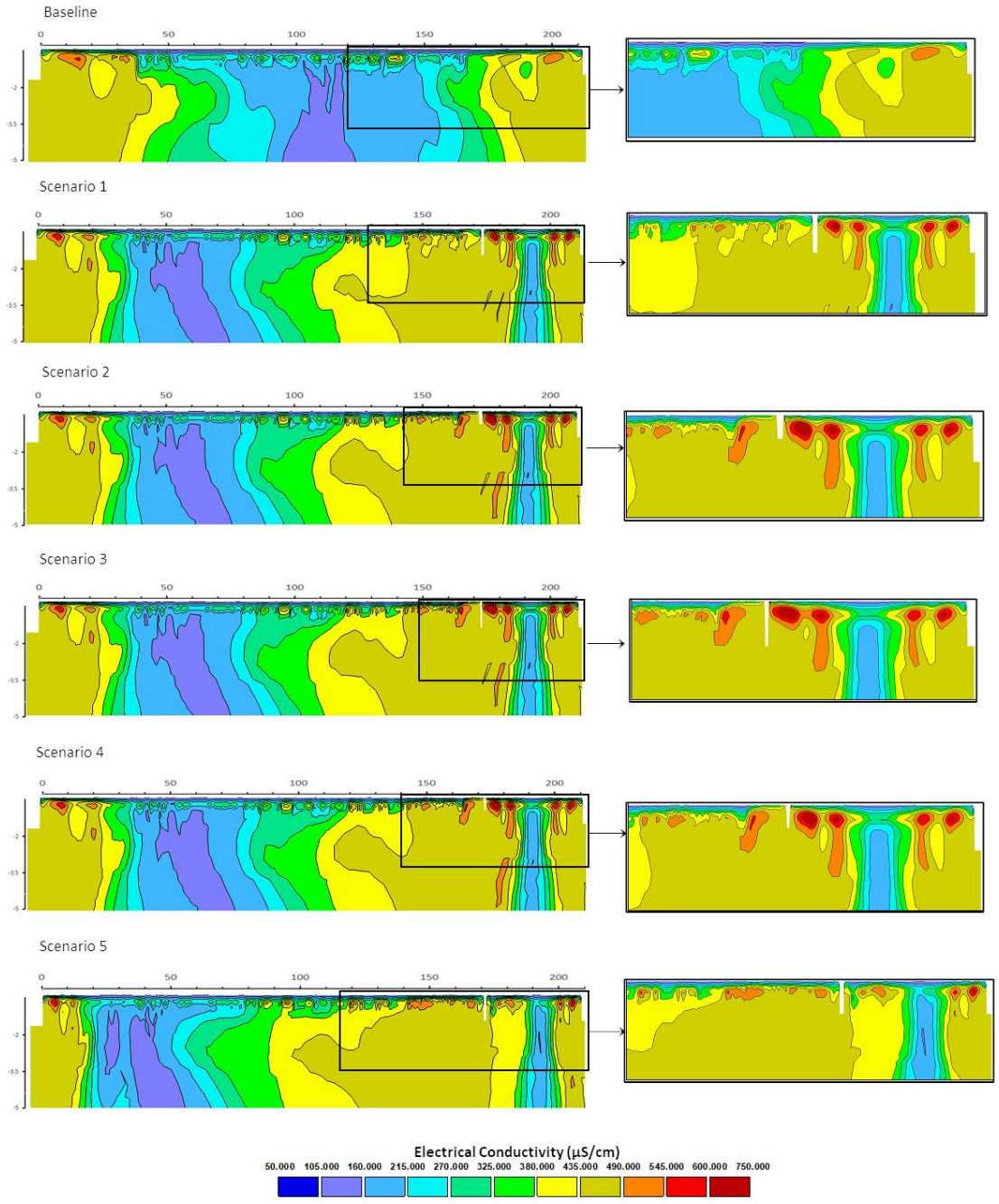

Figure E.4: Simulated Electrical Conductivity along the transect in August 2019 for all scenarios. On the left side the full side is represented. While the right side gives a closer look at the EC patterns in the vicinity of the suppletion ditch.

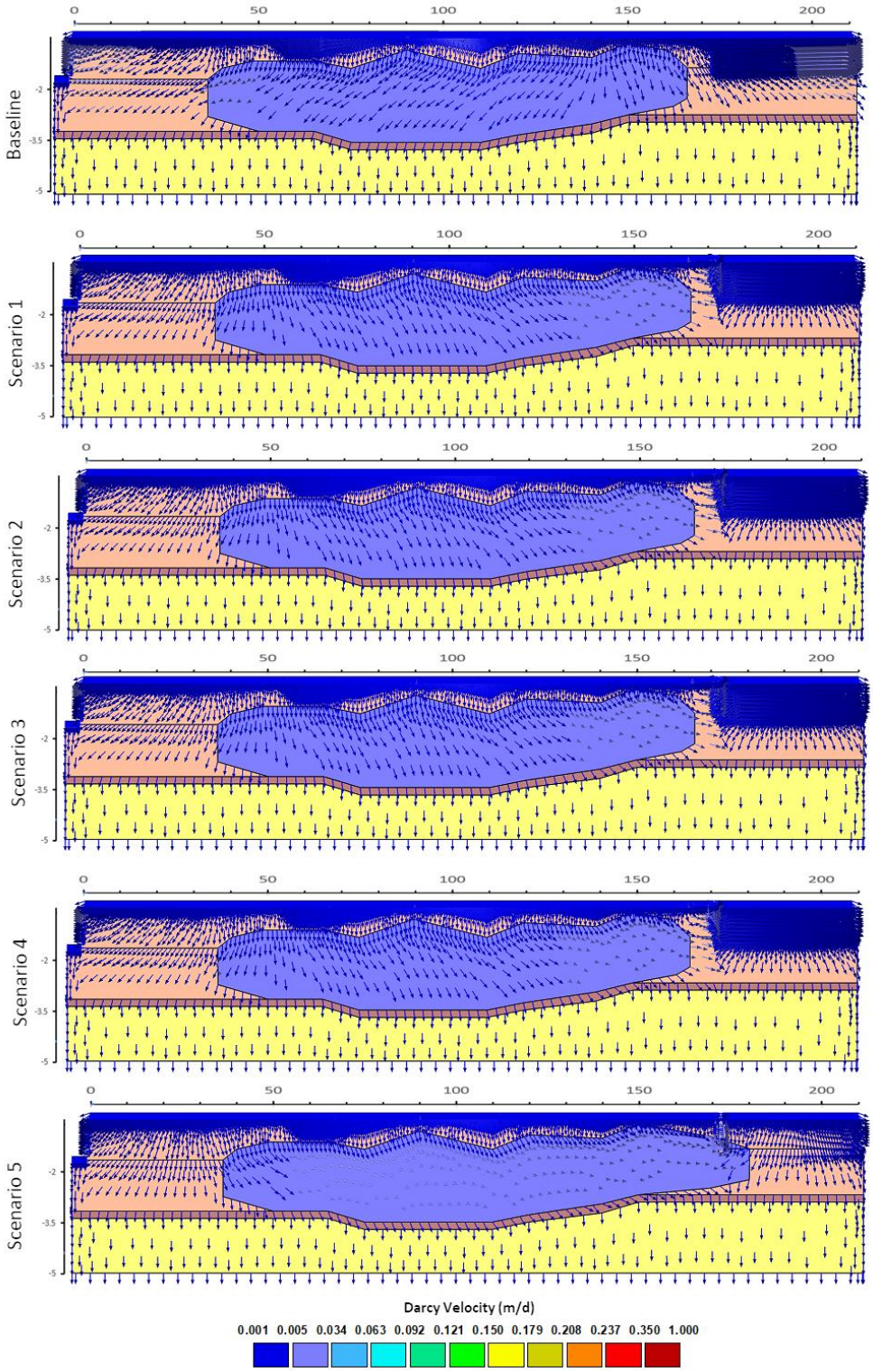

Figure E. 5: Darcian Velocity vectors for the full transect in March 2019 for all scenarios. On the left side the full side is represented.

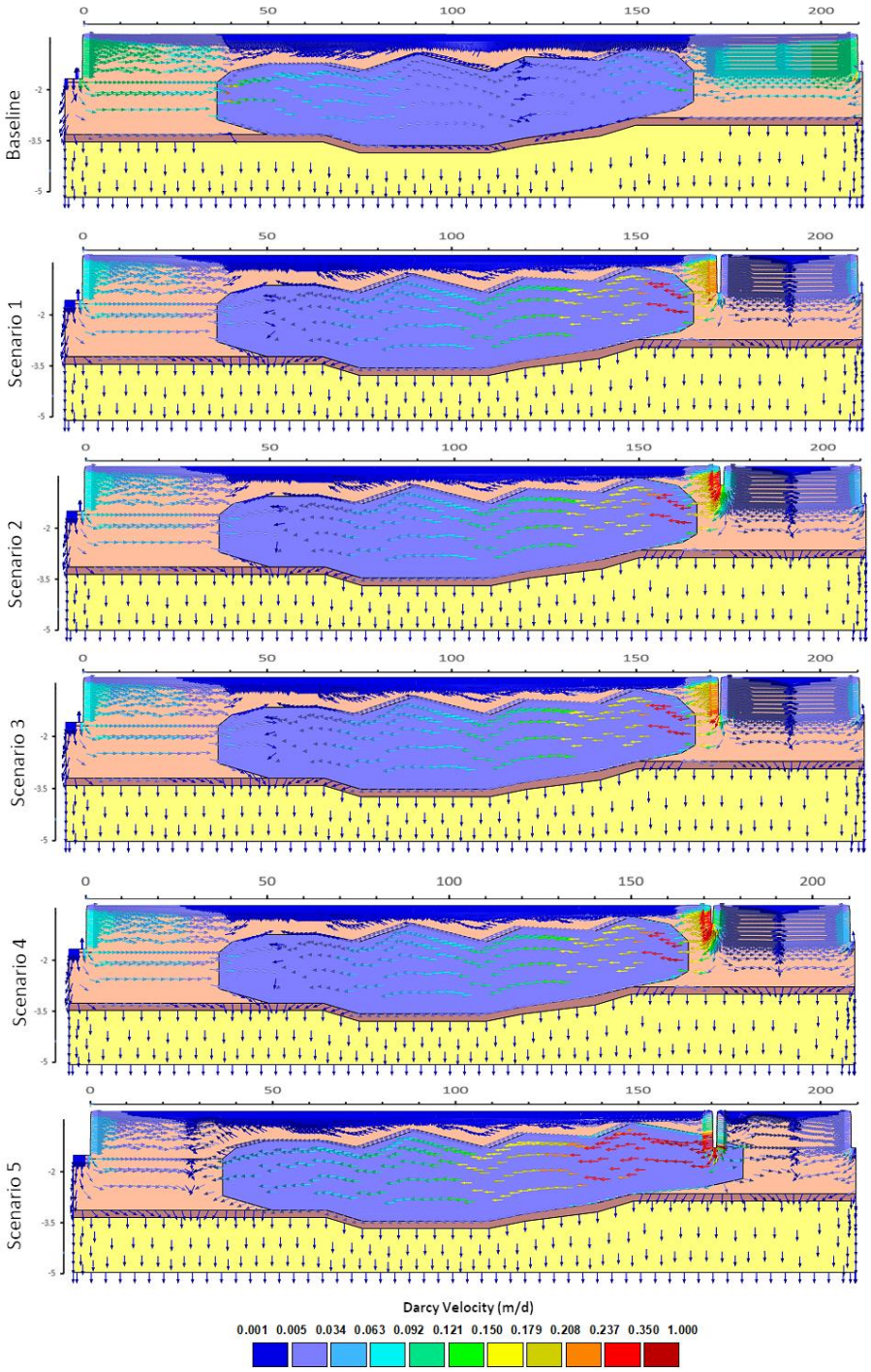

Figure E.6: Darcian Velocity vectors for the full transect in August 2019 for all scenarios. The velocity vectors indicate the main direction of flow at the mesh node. On the left side the full side is represented.

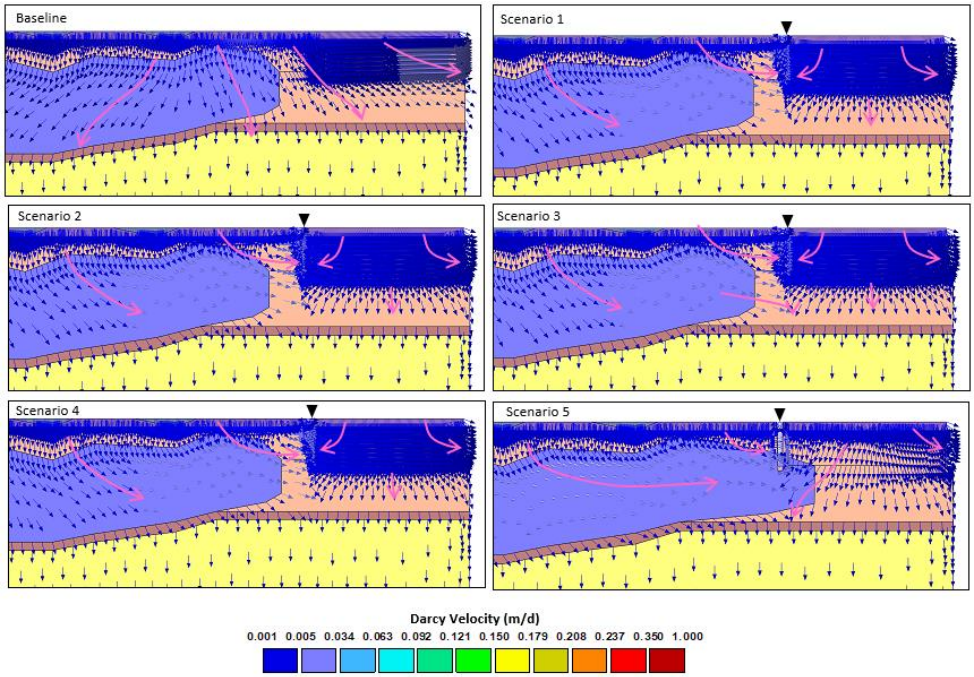

Figure E.7: Close-up of the Darcian Velocity vectors near the suppletion ditch, indicated by the black triangle, for March. The velocity vectors show the main direction of flow is towards the ditches, indicating drainage of water occurs.

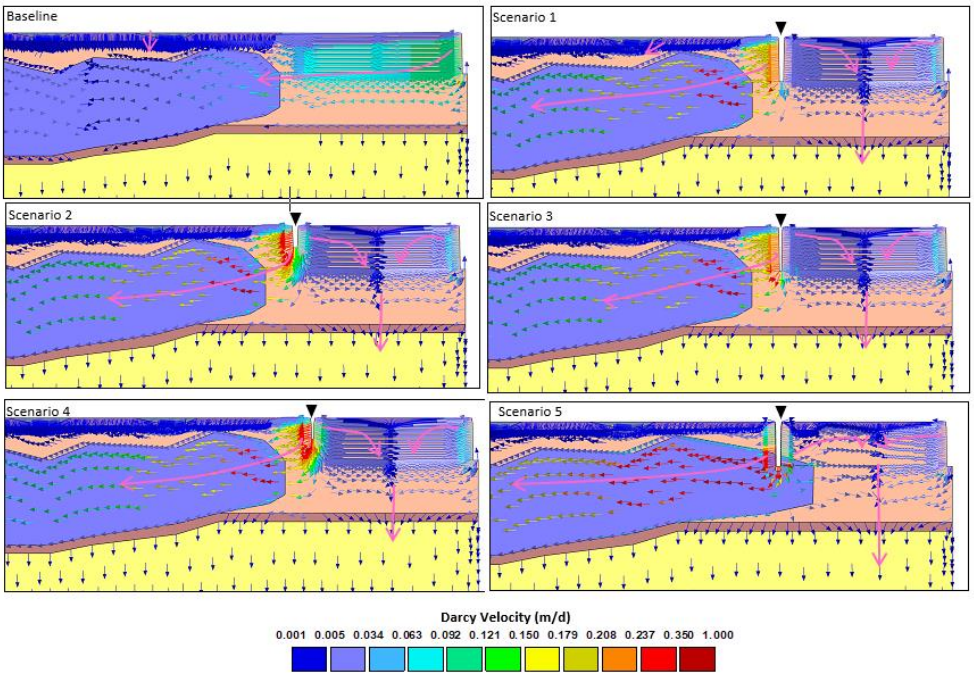

Figure E.8: Close-up of the Darcian Velocity vectors near the suppletion ditch, indicated by the black triangle, for August. The velocity vectors indicate lateral inflow of surface water from the suppletion ditch primarily towards the slurry layer.